

AD-A286 134



Defense Nuclear Agency
Alexandria, VA 22310-3398



94-35047



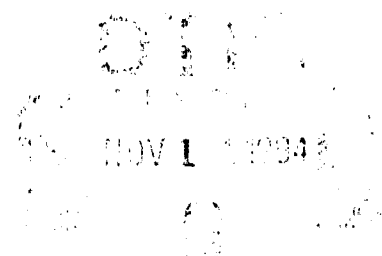
DNA-TR-93-164

Response of the B-1B Air Data Sensor to Simulated Dust Cloud Environments

Robert G. Oeding
PDA Engineering
P.O. Box 11491
Costa Mesa, CA 92627

November 1994

Technical Report



CONTRACT No. DNA 001-91-C-0021

Approved for public release;
distribution is unlimited.

94 1 30 00

Destroy this report when it is no longer needed Do not
return to sender

PLEASE NOTIFY THE DEFENSE NUCLEAR AGENCY,
ATTN: CSTI, 6801 TELEGRAPH ROAD, ALEXANDRIA, VA
22310-3398, IF YOUR ADDRESS IS INCORRECT, IF YOU
WISH IT DELETED FROM THE DISTRIBUTION LIST, OR
IF THE ADDRESSEE IS NO LONGER EMPLOYED BY YOUR
ORGANIZATION



DISTRIBUTION LIST UPDATE

This mailer is provided to enable DNA to maintain current distribution lists for reports (We would appreciate your providing the requested information.)

- Add the individual listed to your distribution list
- Delete the cited organization/individual.
- Change of address.

NOTE:
Please return the mailing label from the document so that any additions, changes, corrections or deletions can be made easily. For distribution cancellation or more information call DNA/IMAS (703) 325-1036.

NAME _____

ORGANIZATION: _____

OLD ADDRESS

CURRENT ADDRESS

TELEPHONE NUMBER: () _____

DNA PUBLICATION NUMBER/TITLE

CHANGES/DELETIONS/ADDITIONS, etc.)
(Attach Sheet if more Space is Required)

DNA OR OTHER GOVERNMENT CONTRACT NUMBER: _____

CERTIFICATION OF NEED-TO-KNOW BY GOVERNMENT SPONSOR (if other than DNA):

SPONSORING ORGANIZATION: _____

CONTRACTING OFFICER OR REPRESENTATIVE: _____

SIGNATURE _____

CUT HERE AND RETURN



REPORT DOCUMENTATION PAGE

Form Approved
OMB No. 0704-0188

Public reporting burden for this collection of information is estimated to average 1 hour per response including the time for reviewing instructions, searching existing data sources, gathering and maintaining the data needed, and completing and reviewing the collection of information. Send comments regarding this burden estimate or any other aspect of this collection of information, including suggestions for reducing this burden, to Washington Headquarters Services, Directorate for Information Operations and Reports, 1215 Jefferson Davis Highway, Suite 1204, Arlington, VA 22202-4302, and to the Office of Management and Budget, Paperwork Reduction Project (0704-0188), Washington, DC 20503.

1. AGENCY USE ONLY (Leave blank)	2. REPORT DATE <p style="text-align: center;">941101</p>	3. REPORT TYPE AND DATES COVERED <p style="text-align: center;">Technical 920917 - 930815</p>	
4. TITLE AND SUBTITLE <p style="text-align: center;">Response of the B-1B Air Data Sensor to Simulated Dust Cloud Environments</p>		5. FUNDING NUMBERS C - DNA 001-91-C-0021 PE - 62715H PR - RA TA - RJ WU - DH309130	
6. AUTHOR(S) <p style="text-align: center;">Robert G. Oeding</p>		8. PERFORMING ORGANIZATION REPORT NUMBER <p style="text-align: center;">PDA-TR-1754-02-01</p>	
7. PERFORMING ORGANIZATION NAME(S) AND ADDRESS(ES) PDA Engineering P.O. Box 11491 Costa Mesa, CA 92627		10. SPONSORING/MONITORING AGENCY REPORT NUMBER <p style="text-align: center;">DNA-TR-93-164</p>	
9. SPONSORING/MONITORING AGENCY NAME(S) AND ADDRESS(ES) Defense Nuclear Agency 6801 Telegraph Road Alexandria, VA 22310-3398 SPWE/DiNova		11. SUPPLEMENTARY NOTES This work was sponsored by the Defense Nuclear Agency under RDT&E RMC Code B4662D RA RJ 00193 SPWE 4400A 25904D.	
12a. DISTRIBUTION/AVAILABILITY STATEMENT <p style="text-align: center;">Approved for public release; distribution is unlimited.</p>		12b. DISTRIBUTION CODE	
13. ABSTRACT (Maximum 200 words) This report describes an experimental evaluation of the effects of dusty flow environments on the performance of the B-1B air data sensor (ADS). The evaluations were conducted in the DNA dust erosion facility which is located at PDA Engineering laboratories in Santa Ana, CA. The dust erosion facility was modified to provide a high speed dusty jet with controlled moisture addition. Full-scale ADS probes were submerged in the dust flow and probe performance was monitored. Performance measurements included total, static and angle-of-attack pressure outputs. Also pre- and post-test weights of the probes and pressure line dust filters were obtained in order to determine ingested particle mass. Both dry and wet flows included two levels of water addition to simulate cloud precipitation/moisture. The test configurations, procedures and results are described.			
14. SUBJECT TERMS Dust Erosion Simulation Testing Air Data System Particle Flow Survivability			15. NUMBER OF PAGES <p style="text-align: center;">104</p>
17. SECURITY CLASSIFICATION OF REPORT <p style="text-align: center;">UNCLASSIFIED</p>			16. PRICE CODE
18. SECURITY CLASSIFICATION OF THIS PAGE <p style="text-align: center;">UNCLASSIFIED</p>	19. SECURITY CLASSIFICATION OF ABSTRACT <p style="text-align: center;">UNCLASSIFIED</p>	20. LIMITATION OF ABSTRACT <p style="text-align: center;">SAR</p>	

UNCLASSIFIED

SECURITY CLASSIFICATION OF THIS PAGE

CLASSIFIED BY:

N/A since Unclassified.

DECLASSIFY ON:

N/A since Unclassified.

SECURITY CLASSIFICATION OF THIS PAGE

UNCLASSIFIED

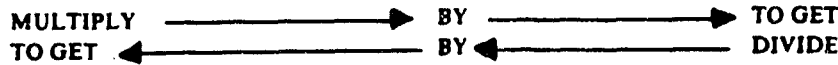
PREFACE

The measurement program described herein was performed by PDA Engineering under support provided by the Defense Nuclear Agency, Contract No. DNA001-91-C-0021. The DNA Contract Technical Monitor was Lt. Col. Gerald Miatech. His contribution to the success of this program is gratefully acknowledged. Thanks are also extended to the PDA Systems Engineering Department staff and especially Mr. Charles Lennon for providing valuable laboratory test support .

APPROVED FOR	
NIES	A
DTIC	
UNCLASSIFIED	
DATE	
BY	
DATE	
DATE	
DATE	
A-1	

CONVERSION TABLE

Conversion factors for U.S. Customary to metric (SI) units of measurement



angstrom	1.000 000 X E -10	meters (m)
atmosphere (normal)	1.013 25 X E +2	kilo pascal (kPa)
bar	1.000 000 X E +2	kilo pascal (kPa)
barn	1.000 000 X E -28	meter ² (m ²)
British thermal unit (thermochemical)	1.054 350 X E +3	joule (J)
calorie (thermochemical)	4.184 000	joule (J)
cal (thermochemical)/cm ²	4.184 000 X E -2	mega joule/m ² (MJ/m ²)
curie	3.700 000 X E +1	giga becquerel (GBq)
degree (angle)	1.745 329 X E -2	radian (rad)
degree Fahrenheit	$t_c = (t_f - 459.67)/1.8$	degree kelvin (K)
electron volt	1.602 10 X E -19	joule (J)
erg	1.000 000 X E -7	joule (J)
erg/second	1.000 000 X E -7	watt (W)
foot	3.048 000 X E -1	meter (m)
foot-pound-force	1.355 818	joule (J)
gallon (U.S. liquid)	3.785 412 X E -3	meter ³ (m ³)
inch	2.540 000 X E -2	meter (m)
jerk	1.000 000 X E +9	joule (J)
joule/kilogram (J/kg) (radiation dose absorbed)	1.000 000	Gray (Gy)
kilotons	4 183	tera(joule)
kip (1000 lbf)	4 448 222 X E +3	newton (N)
kip/inch ² (ksi)	6 894 757 X E +3	kilo pascal (kPa)
ktop	1.000 000 X E +2	newton-second/m ² (N-s/m ²)
micron	1.000 000 X E -6	meter (m)
mil	2.540 000 X E -5	meter (m)
mile (international)	1.609 344 X E +3	meter (m)
ounce	2.834 952 X E -2	kilogram (kg)
pound-force (lbf or oldpoids)	4 448 222	newton (N)
pound-force inch	1 129 848 X E -1	newton-meter (N·m)
pound-force/inch	1 751 268 X E +2	newton/meter (N/m)
pound-force/foot ²	4 788 026 X E -2	kilo pascal (kPa)
pound-force/inch ² (psi)	6 894 757	kilo pascal (kPa)
pound-mass (lbm or oldpoids)	4 535 924 X E -1	kilogram (kg)
pound-mass-foot ² (moment of inertia)	4 214 011 X E -2	kilogram-meter ² (kg·m ²)
pound-mass/foot ³	1 601 846 X E -1	kilogram/meter ³ (kg/m ³)
rad (radiation dose absorbed)	1.000 000 X E -2	*Gray (Gy)
roentgen	2 579 760 X E -4	coulomb/kilogram (C/kg)
shake	1.000 000 X E -8	second (s)
slug	1 458 330 X E +1	kilogram (kg)
torr (mm Hg, 0° C)	1 333 22 X E -1	kilo pascal (kPa)

*The becquerel (Bq) is the SI unit of radioactivity; 1 Bq = 1 event/s
 **The Gray (Gy) is the SI unit of absorbed radiation

TABLE OF CONTENTS

Section		Page
	PREFACE.....	iii
	CONVERSION TABLE.....	iv
	FIGURES.....	vii
	TABLES.....	ix
1	INTRODUCTION	1
	1.1 Background.....	1
	1.2 Objectives	2
2	TEST DESCRIPTION.....	3
	2.1 Overview	3
	2.2 Test Facility and Experimental Apparatus	6
	2.2.1 DNA Dust Erosion Test Facility.....	6
	2.2.2 Particle Injection System	9
	2.2.3 Water Injection System	12
	2.2.4 Large Nozzle Characteristics.....	15
	2.3 Test Item Description	26
	2.3.1 Air Data Sensor.....	26
	2.3.2 Pressure Transducer Interface	28
	2.3.3 Sensor Heater Interface.....	30
	2.3.4 Description of Particle Blends	31
	2.4 Instrumentation	33
	2.4.1 Hardware Description.....	33
	2.4.2 Data Acquisition System.....	36
	2.5 Test Procedure.....	37
	2.5.1 General Description	37
	2.5.2 Basic Test Procedure.....	38
3	TEST RESULTS	40
	3.1 Test Parameters.....	40
	3.1.1 Particle Size	40
	3.1.2 Particle Flow Velocity	41
	3.1.3 Particle Loading	41
	3.1.4 Moisture	42
	3.1.5 Probe Heating.....	42
	3.2 Test Matrix	44
	3.2.1 Test Plan.....	44
	3.2.2 Completed Test Matrix.....	46

TABLE OF CONTENTS (Continued)

Section		Page
3.3	Baseline ADS Performance	46
3.4	Dry Particle Flow Results	56
	3.4.1 Pressure Response Data	56
	3.4.2 Dust Ingestion Data	63
3.5	Wet Particle Flow Results	67
	3.5.1 Pressure Response Data	69
	3.5.2 Dust Ingestion Data	76
	3.5.3 Post-Test Observations	84
4	SUMMARY AND RECOMMENDATIONS	87
	4.1 Summary	87
	4.2 Recommendations	89
5	REFERENCES	91

FIGURES

Figure		Page
2-1	B-1B ADS Test Configuration.....	4
2-2	DNA Dust Erosion Test Facility.....	8
2-3	Particle Feed System.....	10
2-4	Screw Feeder Calibration Curves for Particle Mass Flow Rate.....	11
2-5	Water Injection System schematic.....	13
2-6	Photograph of Metering Pump Used with Water Injection System.....	13
2-7	Water Injection Calibration Curves for Liquid Flow Rate.....	14
2-8	Nozzle Configuration for ADS Evaluations.....	16
2-9	Photograph of Gas/Particle Nozzle Used for ADS Evaluations.....	16
2-10	Photograph of Small Pitot-Static Probe Mounted in Gas Jet.....	17
2-11	Jet Coordinate Definition for Pressure Scans.....	17
2-12	Total and Static Pressure Response vs Nozzle Inlet Pressure.....	19
2-13	Total Pressure Scans as a Function of Vertical Position - $P_n = 40$ psig ..	20
2-14	Total Pressure Scans as a Function of Vertical Position - $P_n = 70$ psig ..	21
2-15	Total Pressure Scans as a Function of Vertical Position - $P_n = 80$ psig ..	22
2-16	Temperature Scans as Function of Vertical Position.....	23
2-17	Particle Velocity Profiles Measured with LDV System.....	25
2-18	B-1B Air Data Sensor Specification Drawing.....	27
2-19	Sensor Fittings and Connections.....	29
2-20	Pressure Transmission Lines and Particle Filters.....	29
2-21	ADS Heater Schematic.....	30
2-22	Photomicrographs of Test Particles.....	32
2-23	Data Acquisition System.....	36
3-1	Effect of Flow Diameter on Equivalent Cloud Concentration.....	43
3-2	Effect of Particle Velocity on Equivalent Cloud Concentration.....	43
3-3	Axial Pressure Scan with B-1B ADS Probe - $P_n = 70$ psig.....	50
3-4	Horizontal Pressure Scans with B-1B ADS Probe - $P_n = 70$ psig.....	51
3-5	Axial Pressure Scan with B-1B ADS Probe - $P_n = 80$ psig.....	52
3-6	Horizontal Pressure Scans with B-1B ADS Probe - $P_n = 80$ psig.....	53
3-7	B-1B ADS Probe Baseline Pressure Response - Low Water Flow.....	55
3-8	B-1B ADS Probe Baseline Pressure Response - High Water Flow.....	57
3-9	B-1B ADS Pressure Response with Dry Flow - Blend #15.....	59

FIGURES (Continued)

Figure		Page
3-10	B-1B ADS Pressure Response with Dry Flow - Crushed Silica (<38 microns).....	60
3-11	B-1B ADS Pressure Response with Dry Flow - Crushed Silica (53-74 microns).....	61
3-12	B-1B ADS Pressure Response with Low Velocity - Crushed Silica (<38 microns).....	62
3-13	Inline Filter Used for Particle Collection	63
3-14	Total Ingested Dust Mass Correlations - Dry Flow	66
3-15	Effect of Particle Velocity on Dust Ingestion.....	66
3-16	Wet Flow Test Configuration.....	68
3-17	B-1B ADS Pressure Response with Wet Particle Flow - Blend #15.....	70
3-18	B-1B ADS Pressure Response with Wet Particle Flow - <38 micron Crushed Silica	71
3-19	B-1B ADS Pressure Response with Wet Particle Flow - 53-74 micron Crushed Silica	72
3-20	Exposure Time Required for Total Pressure Output Loss.....	74
3-21	Expended Particle Mass Required for Total Pressure Output Loss.....	75
3-22	B-1B ADS Pressure Response with High Water Flow - 53-74 Silica	77
3-23	B-1B ADS Pressure Response with High Water Flow - Blend #15	78
3-24	Ingested Mass vs Total Dust Mass Expended - Blend #15.....	82
3-25	Ingested Mass vs Total Dust Mass Expended - <38 μ m Silica	82
3-26	Ingested Mass vs Total Dust Mass Expended - 53-74 μ m Silica	83
3-27	Ingested Mass vs Total Dust Mass Expended - High Water Flow	83
3-28	Post-Test Photo of Probe Following Exposure to Blend #15.....	85
3-29	Post-Test Photo of Probe Following Exposure to <38 micron Crushed Silica	86
3-30	Post-Test Photo of Probe Following Exposure to 53-74 micron Crushed Silica	86

TABLES

Tables		Page
2-1	Air Data Sensor Label Information.....	26
2-2	Particle Size Data	31
2-3	Test Instrumentation	34
3-1	B-1B ADS Test Plan.....	45
3-2	B-1B ADS Completed Test Matrix.....	47
3-3	B-1B ADS Particle Collection Data - Dry Particle Flow.....	64
3-4	Total Pressure Failure Reponse Characteristics.....	73
3-5	B-1B ADS Particle Collection Data - Wet Particle Flow.....	80

SECTION 1 INTRODUCTION

1.1 BACKGROUND.

Both strategic and tactical aircraft may be forced to operate in environments which contain significant loadings of dust and debris. These environments may be generated by a nuclear strike, by conventional weapons laydown or by naturally occurring conditions such as those encountered in Desert Shield/Storm operations. Small and well-distributed dust particulates can remain airborne in post-burst and natural environments for significant periods. Detection and avoidance of such dust environments by operational aircraft may not be feasible within mission constraints. Thus, the ability of critical aircraft components to survive flight through extended dust environments is an important vulnerability issue.

The significant hazard to aircraft operations posed by airborne dust environments has been well established through a number of commercial aircraft encounters with volcano-generated ash clouds (Reference 1 and 2). These encounters have resulted in the loss of all engines (for a significant period of time), severe hazing of forward windscreens and landing light lens, plugging of air data sensors (pitot-static probes) and removal of paint on leading edges and forward-facing surfaces.

In order to address aircraft erosion issues, PDA Engineering, in 1983, developed a laboratory-scale facility to evaluate the effects of particle erosion on surface materials and key aircraft components. Since 1986, when DNA assumed sponsorship, this facility has been known as the DNA Dust Erosion Test Facility and has been located in PDA Engineering's laboratory facilities in Santa Ana, California. It was designed to meet a wide range of flight environments and provided precise control over the key physical impact parameters. The approach taken in the facility design was to sweep a small particle jet over a 6-in by 6-in test area in a controlled and uniform manner. Compared to a dusty wind tunnel design this approach requires lower air flow rates and provides better control over particle impact parameters. The facility has been used extensively to evaluate particle impact effects on aircraft transparencies (windscreens and canopy materials), composite materials (leading edge, control surface and radome materials) and sensor windows (IR transmitting materials). These tests complemented other DNA sponsored efforts to evaluate dust ingestion effects on aircraft engines. Data generated in this facility have demonstrated that aircraft transparencies and sensor windows are highly vulnerable to particle impact effects.

A key component of commercial aircraft that has proven vulnerable to volcanic ash encounters is the air data sensor (ADS) or pitot-static probes which are subject to plugging from ingested particles leading to a loss in air speed data. Boeing 747 aircraft have experienced loss of air data in volcanic encounters in Java (Mt. Galunggung) in 1982 and Alaska (Mt. Redoubt) in 1989. For strategic aircraft such as the B-1B, which must be able to perform low altitude penetration missions in post-strike nuclear environments, the ingestion of dust and debris is a vulnerability issue. This is particularly true for the B-1B since the ADS system provides vital inputs to the flight control and weapons delivery systems.

In order to conduct an initial evaluation of the vulnerability of the B-1B ADS to dusty flows, the DNA Dust Erosion Test Facility was modified to provide a suitable simulation of flight through a dusty environment. The principal modifications to the facility included the design and development of larger nozzles (exit diameters of 0.5 and 0.635-inches), the installation of a precision screw feeder system for improved particle metering, development of a water injection system to simulate cloud moisture, and the installation of a computer based data acquisition system for recording, analyzing and displaying facility data and ADS pressure/temperature outputs.

1.2 OBJECTIVES.

The DNA dust erosion test facility (Reference 3) was used to evaluate the effects of dust laden flows on B-1B ADS probe performance. The primary objective of this test program was to determine dust exposure conditions sufficient to degrade the performance of the ADS probe. Particle type, size, velocity and total mass loading were simulated in order to assess the effects of the key flight parameters. Performance was evaluated based on ADS pressure outputs and ingested particle mass as measured with laboratory instrumentation.

SECTION 2 TEST DESCRIPTION

2.1 OVERVIEW.

The basic approach used to evaluate the response of the B-1B ADS (pitot-static) probe consisted of mounting the probe in a high speed dust laden jet and monitoring its performance with pressure transducers. The gas/particle speed, mass flow rate and water content of the jet were controlled in order to simulate flight through a late-time nuclear dust environment. This test configuration is shown schematically in Figure 2-1. The gas jet consisting of dry nitrogen (GN_2) was formed in a specially designed converging-diverging nozzle having a constant diameter extension. Particles were metered into the flow upstream of the nozzle via a precision screw feeder system mounted in a pressure plenum. An external control unit allowed the feed rate to be adjusted and the on/off functions to be controlled remotely with the flip of a switch.

The nominal nozzle exit diameter for the B-1B ADS evaluations was 0.5 inches. Jet conditions were achieved by controlling the nozzle inlet pressure. For a given particle size, the particle velocity in the jet becomes a function of nozzle inlet pressure and axial position. Thus, nozzle inlet pressure and axial distance of the probe from the nozzle exit were selected to provide a specified particle velocity at the ADS total pressure port. A nominal separation distance of 1-inch between the probe and the nozzle exit was used. A small high precision laboratory pitot-static probe was used to obtain pressure distribution measurements within the jet in order to characterize gas flow conditions at the ADS total pressure port and to compare with the ADS pressure readings.

In order to simulate cloud moisture, a very fine stream of water was injected into the nozzle (along the centerline) at high pressure via hypodermic tubing. This stream, which disintegrated in the nozzle, formed a spray of vapor and a very fine mist which was carried in the jet along with the dust particles. The liquid flow was controlled via a positive displacement metering pump with the flow rates being selected via prior calibration so as to simulate two different cloud liquid water content conditions.

Also, an AC power source was connected to the heater in the B-1B pitot-static probe to simulate operation of the probe in the anti-icing mode which is a common operating condition. A surface thermocouple was mounted on the probe (aft of the static pressure ports) in order to monitor probe surface temperature. Since the probe was tested at approximately room temperature, power to the probe was adjusted so as to simulate the probe inflight temperature.

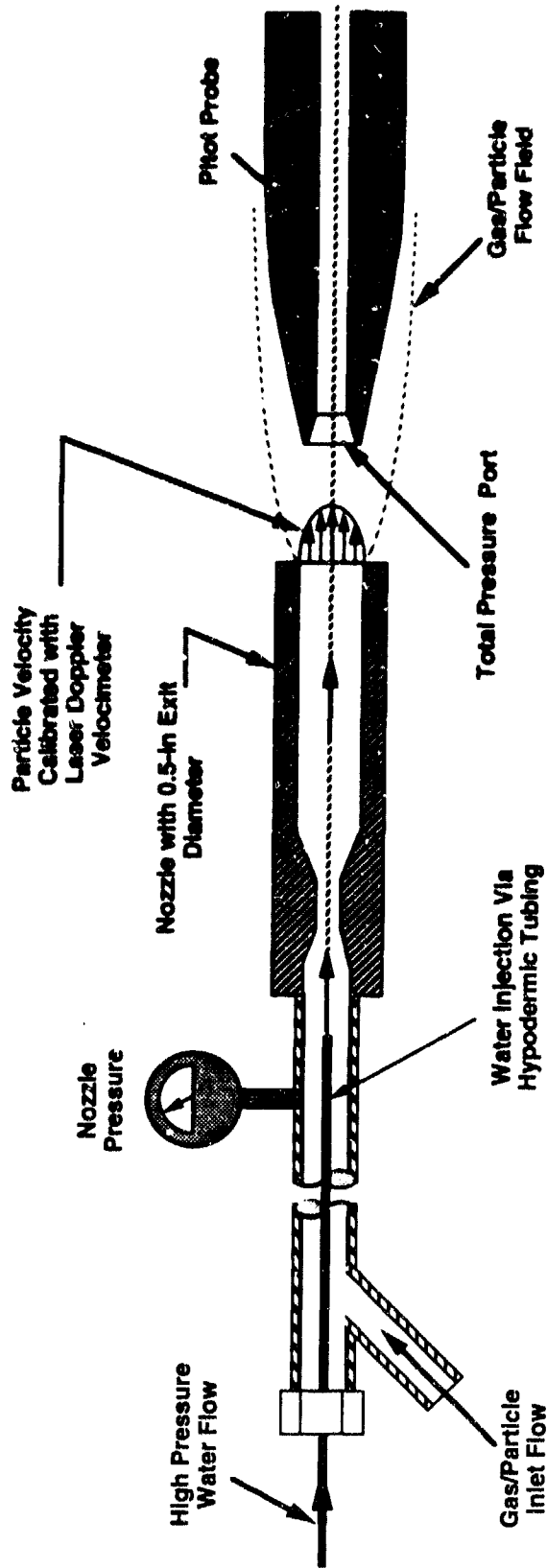


Figure 2-1. B-1B ADS test configuration.

The pressure outputs from the ADS were connected to pressure transducers. Dust filters were placed inline ahead of the transducers to trap any particles that passed through the probe. Probe temperature was measured on some tests with a surface mounted thermocouple. Pressure and temperature outputs were routed to a computer-based Data Acquisition System (DAS) along with the facility diagnostics such as plenum and nozzle inlet pressure and temperature. The DAS displayed the time histories of each output and logged the data to disk for later analysis and display. The DAS handles up to 16 analog input channels.

The actual test consisted of mounting the B-1B probe, setting test conditions, initiating the clear gas flow for a period of time to allow flow conditions and temperatures to stabilize, initiating particle flow for a specified period and finally shutting down the jet. During the test, pressure and temperature measurements were recorded and displayed. Following the test, the probe was removed and weighed to determine the mass of particles trapped within the probe. Also the dust filters on each pressure output line were weighed to determine dust mass which passed through the probe and which could be transported to the ADS transducer.

The primary objective of these evaluations was to determine the exposure threshold where dust ingestion affects the ADS pressure outputs and to determine the mass of particles trapped by the probe and the inline filters. The test's primary approach was to expose a clean pitot-static probe to a specified dust flow environment for a specific period of time in order to establish particle ingestion data for the probe (and the inline filters) and observe any degradation in pressure measurements. Preliminary data indicated that the amount of particle ingestion was a function of the total particle loading. This appeared to be true for a range of particle flow rates and exposure times. Preliminary data also indicated, that for some conditions, long exposure times (on the order of an hour) would be required to fill the probe with dust and to degrade the output pressure readings.

A second approach was also examined. This involved filling the total pressure port of the pitot-static probe with particles to determine the maximum particle mass that could be collected. This filled or partially filled probe was then exposed to the particle flow while the total pressure was monitored. This provided information on the pressure performance of a filled probe and its subsequent response to continued exposure to the dust flow environment. By carefully monitoring the response of the "filled" probe, it was hoped that information could be obtained to help determine damage thresholds for various test environments. However, several attempts to fill and expose the probes failed to provide useful damage threshold data. The probe filled with dry dust did not show any significant degradation in pressure response and quickly cleared when exposed

to the high speed jet. Most of the "fill" particles were forced into the pressure line leading to the transducer.

2.2 TEST FACILITY AND EXPERIMENTAL APPARATUS.

A valid experimental simulation of solid particle impact effects on aircraft surfaces/components requires a unique facility which can provide a match to the key physical parameters associated with the impact phenomenology. These parameters include particle type/size, mass concentration, impact velocity, impact angle and gas dynamic pressure. Since aircraft operation is predominantly at subsonic cruise speeds, a supersonic particle velocity test capability is not a primary requirement. However, highly accurate measurements of impacted particle mass and velocity are required over a broad range of subsonic velocities (e.g. 100 to 1000 fps) in order to determine the erosion characteristics of critical materials.

In order to meet these simulation requirements, PDA Engineering developed what is currently known as the DNA Dust Erosion Test Facility which is located at PDA Engineering's laboratory facilities in Santa Ana, California.. This facility, which has been in operation since 1984, was designed to meet a wide range of particle environments and provides precise control over the key physical parameters in a laboratory test environment. The test facility and key features of the experimental apparatus including particle injection system, water injection system and gas/particle flow characteristics are described below.

2.2.1 DNA Dust Erosion Test Facility.

In order to accomplish simulation requirements, dust particles are accelerated in a high speed gas jet and caused to impinge on a test specimen. The transport gas stream is provided by either compressed air or pure nitrogen (GN_2) with regulators and pressure transducers to measure and control the pressure at the nozzle inlet. Dust particles are metered into the transport gas stream from a pressurized screw feeder system. With this system both screw type, diameter and RPM can be controlled to provide a wide range of flow rates with particle sizes from a few microns to millimeters. Particle flows are uniform and stable. The dust mass flow rate is established by prior calibration for each particle size range or special blend. The total particle mass delivered to the specimen is then determined from the measured exposure time and the calibrated particle feed rate.

Dust velocity is determined as a function of the nozzle inlet pressure and the particle size by pre and post-test calibration. A laser doppler based velocimeter (LDV) is used to rapidly obtain accurate velocity distributions for large particle sample sizes. Thus, for a given test with a specified particle size, a specific test velocity is selected from this velocity versus pressure

calibration. Once the pressure condition is established, particle velocity is verified via both pre- and post-test measurements using the LDV system.

Particle size, velocity, impact angle and loading can be controlled independently. This provides an excellent capability to parametrically evaluate the response of critical aircraft materials to solid particle impact effects. Materials from such components as leading edges, windscreens, radomes, paints and any special coatings can be evaluated in a well controlled laboratory environment under realistic particle impact conditions. Details of this facility are described in Reference 3. A photograph of the primary test hardware at the beginning of the ADS evaluations is presented in Figure 2-2. This figure shows the gas flow control panel, an earlier (fluidized bed type) particle feed system, the test chamber, switching box for diagnostic instrumentation and a strip chart recorder. Separate areas for specimen preparation, physical examination/measurement and optical evaluation are located adjacent to the test cell and are a key part of the laboratory facility, although they are not shown in the photograph.

For tests involving flat coupons or coupon arrays up to 6-inches square, a small diameter nozzle is used to produce approximately a 0.25-inch diameter jet. Since the diameter of this dust jet is smaller than the test specimen area, the specimen holder and jet are articulated so that the test specimen is moved through the dust jet in a uniform manner. This articulation provides a uniform particle loading (dust mass intercepted per unit surface area) over an approximately square area of 310 cm^2 (i.e. 6.9-inch square). This is the primary mode of testing used for evaluation of aircraft surfaces including windscreens, canopies, paints/coatings and sensor windows.

The evaluation of ADS sensor response in dusty flows required capabilities that were not available in the the DNA Dust Erosion Test Facility at the beginning of this program in 1991. Specifically, the ADS probe must be submerged in a steady two-phase (gas/particle) flow with the capability of adding a third phase (liquid water) in the form of a fine spray or mist. Also, since the ADS probe response was based on the measurement of various probe output pressures, a computerized data acquisition system was required to collect and store the various diagnostic and probe performance measurements.

In order to achieve the required test capabilities for evaluating pitot-static probes in dusty flow environments, upgrades to the DNA test facility were required. These included (1) changing the particle feed system from a fluidized bed system to a precision screw feeder system, (2) developing a large (≥ 0.5 -inch) diameter nozzle, (3) developing a water injection system which was compatible with the dust flow and large nozzle and (4) acquiring necessary data acquisition capability. Each of these areas of upgrade are described in the following subsections.

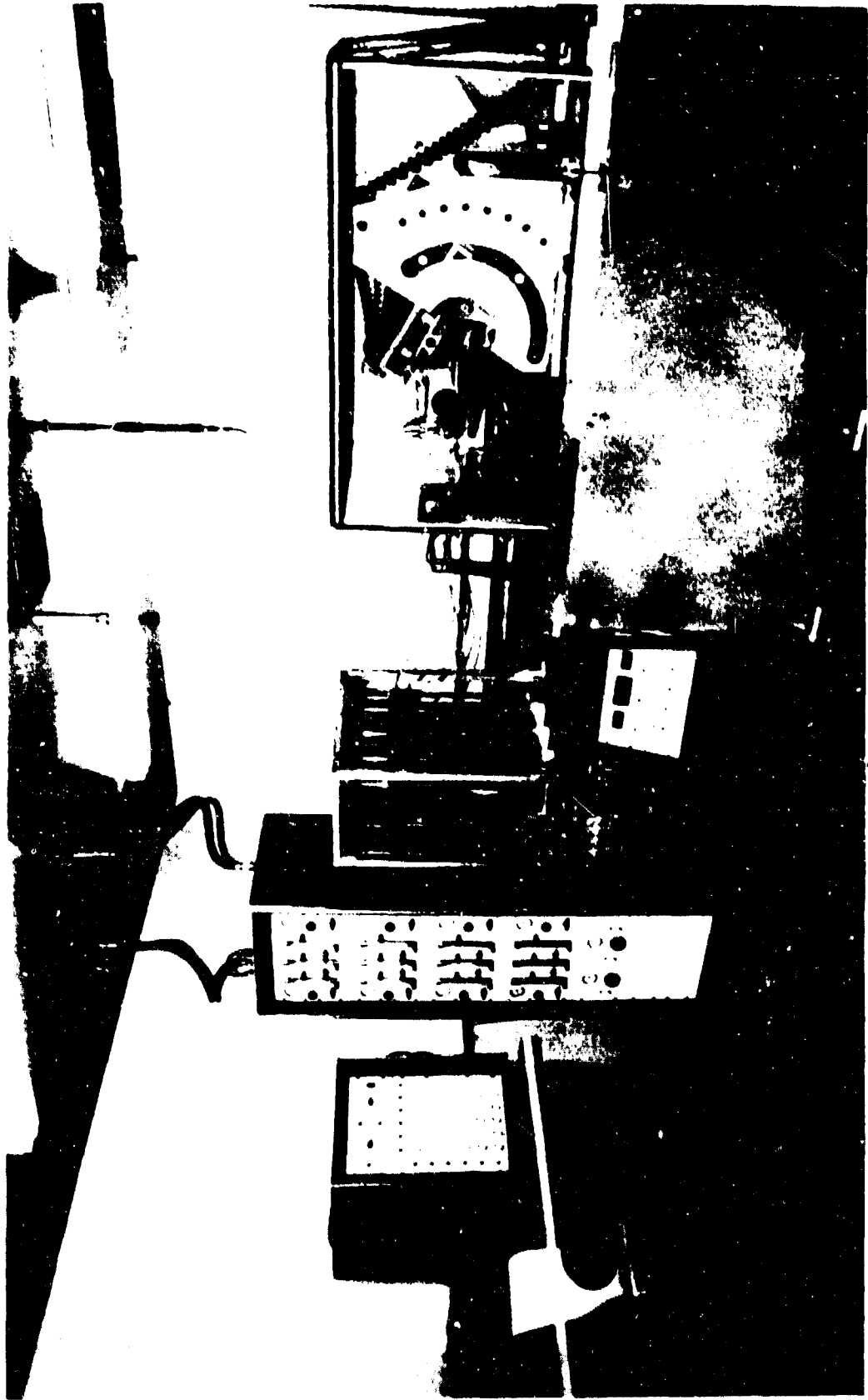


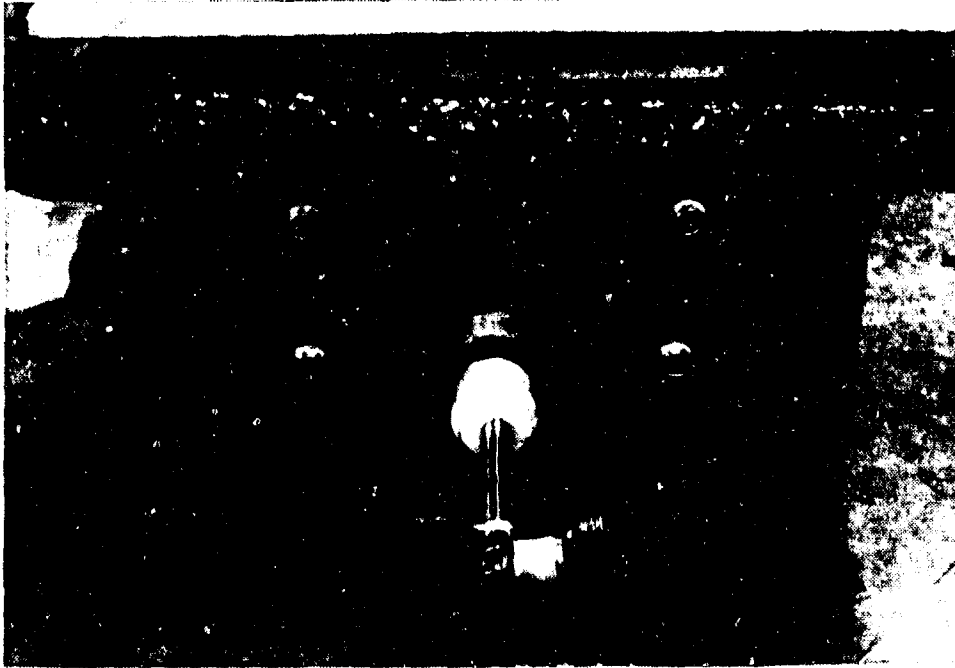
Figure 2-2. DNA dust erosion test facility.

2.2.2 Particle Injection System.

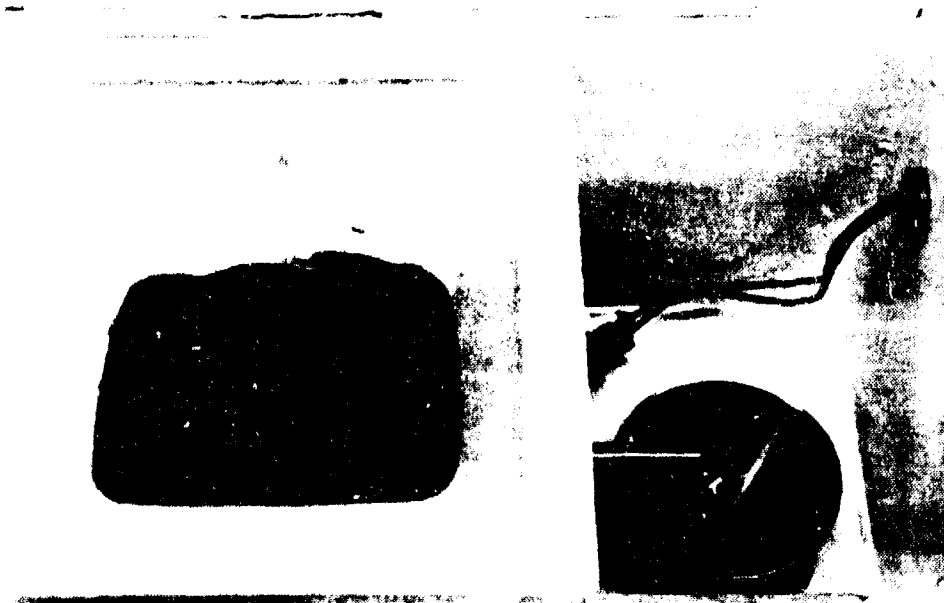
A fluidized bed system was originally developed to provide a steady, low mass flow rate particle source for dust erosion testing. Although this system was successfully employed for over eight years, it had significant limitations. These included a high level of required maintenance, a limited range of flow rates, complex adjustment procedures and difficulties in maintaining steady flow for long test exposures. In order to eliminate most of these restrictions, a precision screw feeder system (Accu-Rate Series 300) was obtained and installed. Adapting the feeder to the test facility required the design and fabrication of a pressure vessel to hold the feeder. Since the particles must be metered into the transport gas stream at high pressure prior to expansion through the nozzle, the entire screw feeder was enclosed in a pressurized plenum chamber capable of operating pressures to 100 psig.

A funnel was used to collect the material as it was discharged from the screw feeder nozzle. Since the transport gas also flows through the plenum and funnel, it entrains the particles and transports them through the nozzle to form the particle jet. Photographs of (1) the screw feeder showing the discharge nozzle and (2) the plenum chamber showing the collection funnel are presented in Figure 2-3. As seen in the photograph, a vibrator was attached to the discharge nozzle to improve flow uniformity for the smaller particle sizes. Available screw sizes included 0.25, 0.375 and 0.50-inch diameter. For the ADS evaluations, the two larger diameter screws were used.

Three particle type/size ranges were considered in the ADS evaluations. These were a particle blend (identified as Blend #15) which was used for B-1B engine testing, $< 38 \mu\text{m}$ crushed silica and a $53\text{-}74 \mu\text{m}$ crushed silica. Each of these particle mixes is discussed in more detail in Section 2.3.4. In order to know how much particle mass has been expended at any time during the test, it is necessary to obtain a particle mass flow rate by prior calibration. Therefore, the screw feeder system was calibrated over a range of flow rates (i.e. screw speeds) for each particle type/size and screw diameter used in the testing. The calibration consisted of measuring the mass of material discharged from the feeder over various prescribed time intervals. The calibration results for all three particle mixes are presented in Figure 2-4. For the larger particles shown in Figure 2-4 (a), the 3/8-inch diameter screw was used and the measured mass flow rate was a linear function of screw speed setting. The flow rates for these two larger particle sizes were very close. The small particle mixture, Blend #15, showed a linear relationship with screw speed at the lower speeds (e.g. 80 to 500) which were used for the testing. However, above a screw speed setting of approximately 500, the flow rate was increasing at a significantly lower rate which is indicative of poor screw filling. Typical feed rates used in the tests were 2.5, 5 and 10 gm/min.

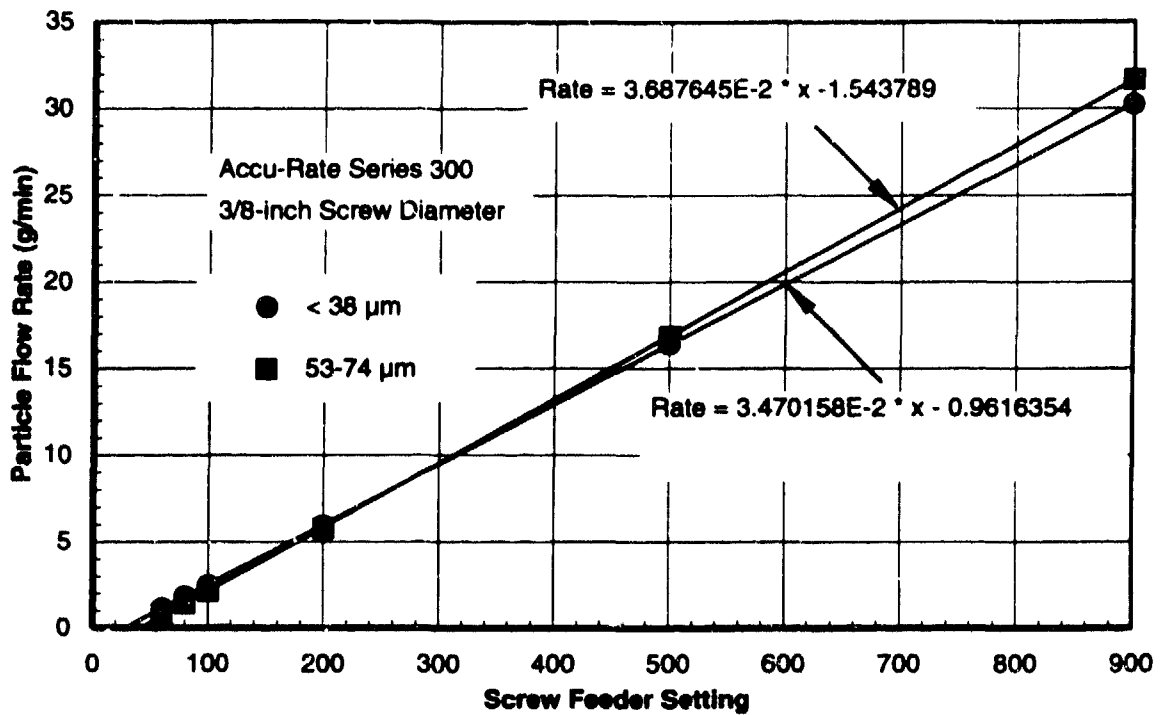


(a) Screw feeder with vibrator.

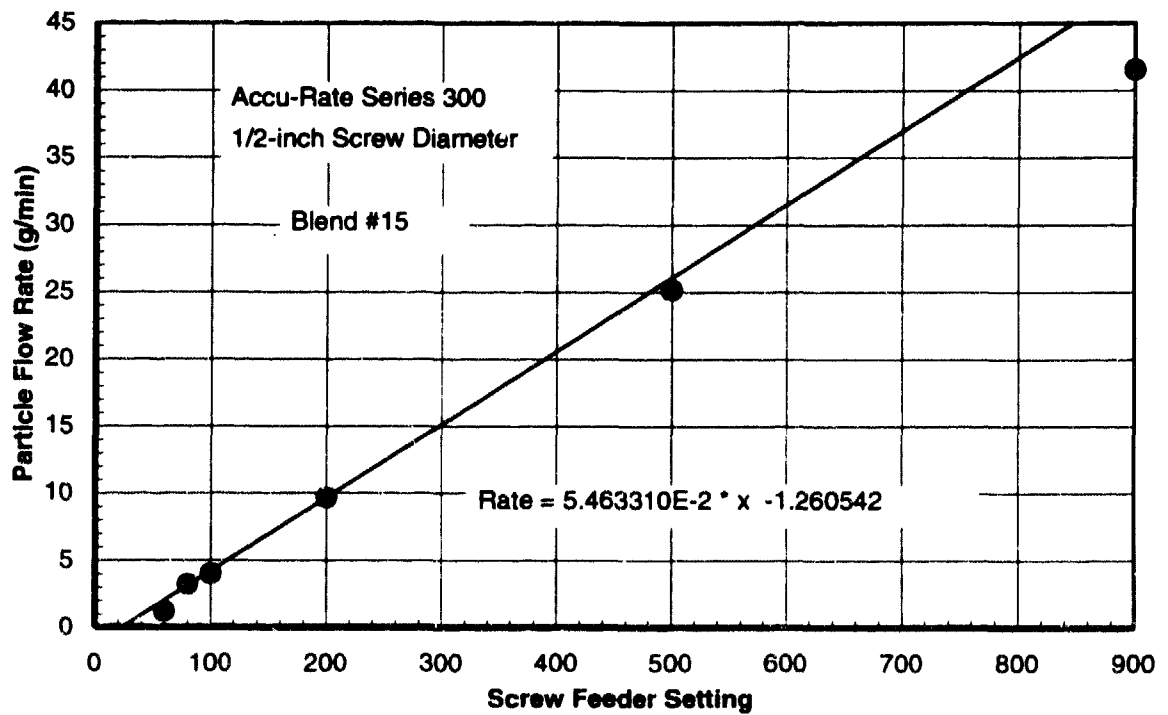


(b) Pressure plenum with collecting funnel.

Figure 2-3. Particle feed system.



(a) Calibration Data for 3/8-inch Diameter Screw



(b) Calibration Data for 1/2-inch Diameter Screw

Figure 2-4. Screw feeder calibration curves for particle mass flow rate.

2.2.3 Water Injection System.

A key parameter that was addressed in the ADS sensor evaluations is the water content of the gas/particle flow. Since the dust cloud environments also contain water, it was important to be able to simulate dusty flows with moisture. Cloud liquid water can be in the form of fog or small droplets or for higher water contents as rain or ice. For simulation purposes, the approach taken was to inject liquid water into the gas/particle flow to form a fine spray or mist. A liquid metering pump was used to provide a controlled high pressure water flow. This flow was injected along the axis of the gas/particle flow/nozzle through a length of hypodermic tubing to form a very small diameter liquid jet. This water jet disintegrated in the nozzle forming a spray of vapor and very fine mist which is carried along in the dusty jet. The gas/particle flow and water injection configuration is illustrated in Figure 2-1.

A schematic of the water injection system is shown in Figure 2-5. Water flow rate was controlled by the pump configuration/parameters (i.e. piston size and stroke length) and the diameter of the injection tube. The pump system which consisted of a Chem-Tech Series 400 reciprocating, positive displacement, piston type metering pump manufactured by Pulsafeeder, Inc is shown in Figure 2-6. The pump is driven by an attached 1/4 hp, 60 Hz gear motor. Piston diameters from 0.25 to 1.0-inch are available for this pump. The piston stroke length is increased or decreased using a micrometer type adjustment thereby accurately controlling output of the pump. Two different flow rates (low and high) were used for the ADS sensor evaluations. The low flow condition, having a nominal 8 ml/min flow rate, utilized a 0.25-inch pump piston and a 0.010-inch diameter injection tube. The high flow condition with a nominal 185 ml/min flow rate used a 0.625-inch diameter piston and a 0.0275-inch diameter injection tube. As is shown in Figure 2-5, the water injection pressure was monitored with a dial gage in order to detect any significant changes in the operation of the injection system.

The water flow rate was determined by pre and post-test calibration. For the two specific configuration and pump settings, the water injection system was calibrated by measuring the volume of water exiting the injection tube over various selected time intervals. Calibration curves for both the high and low flow conditions are presented in Figure 2-7. These are plots of the actual volume of water collected over each specific time period. Thus, the slope of the linear curve fit represents the volumetric flow rate as indicated on each plot.

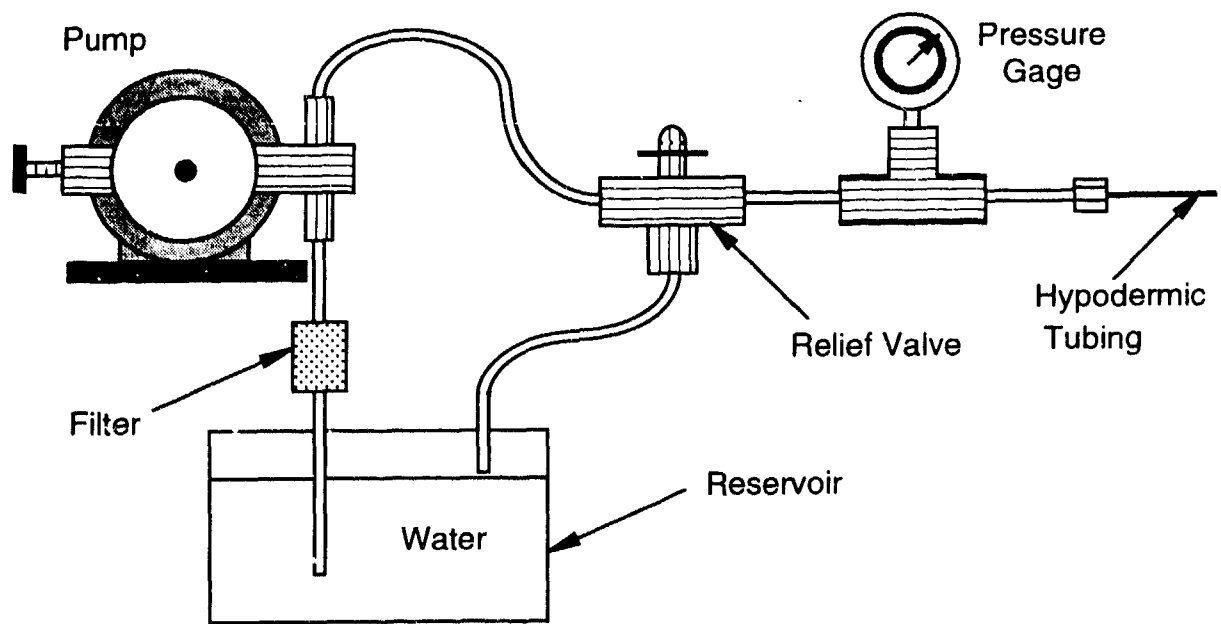


Figure 2-5. Water injection system schematic.

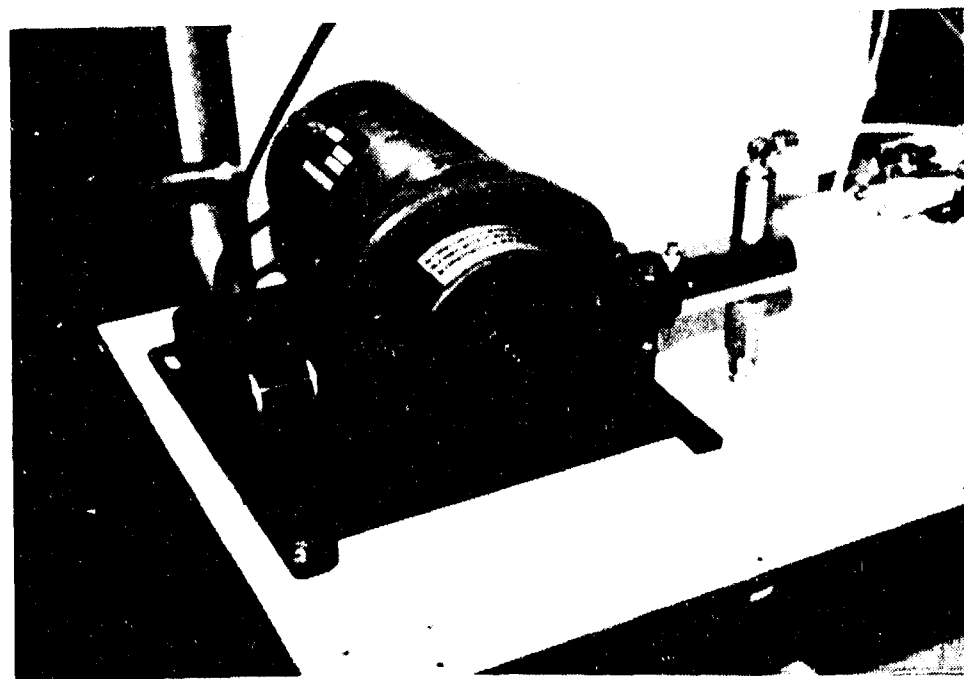


Figure 2-6. Photograph of metering pump used with water injection system.

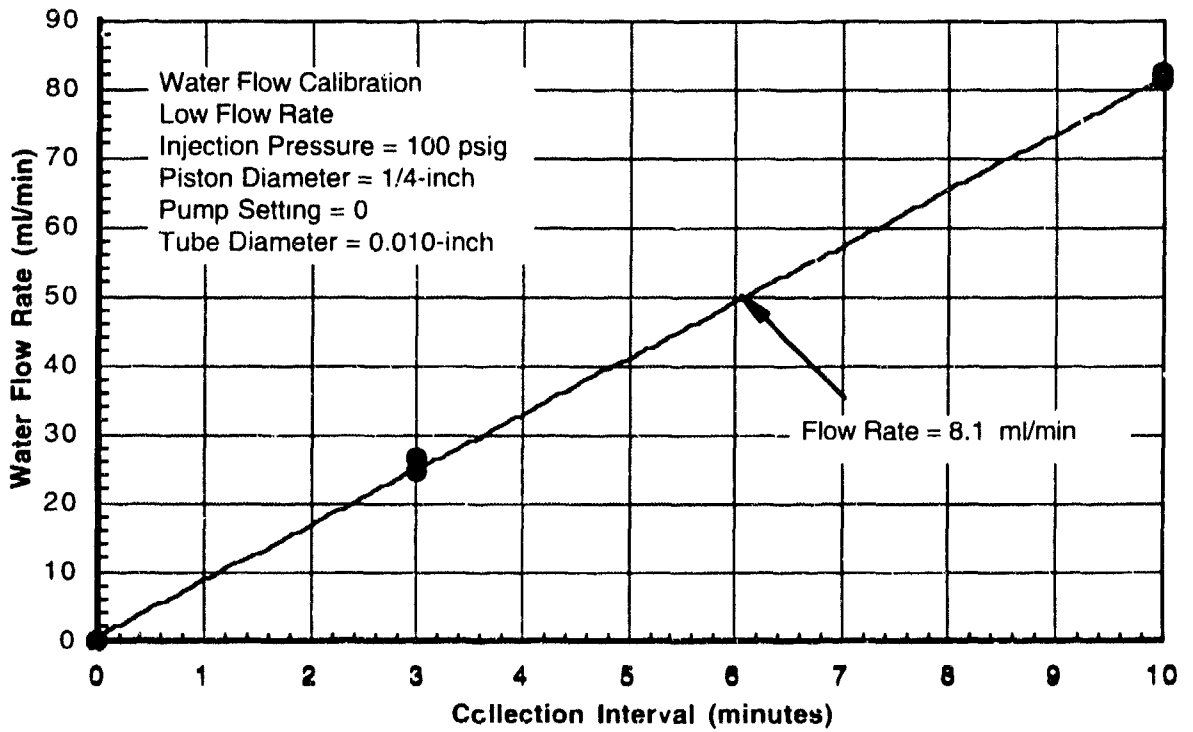
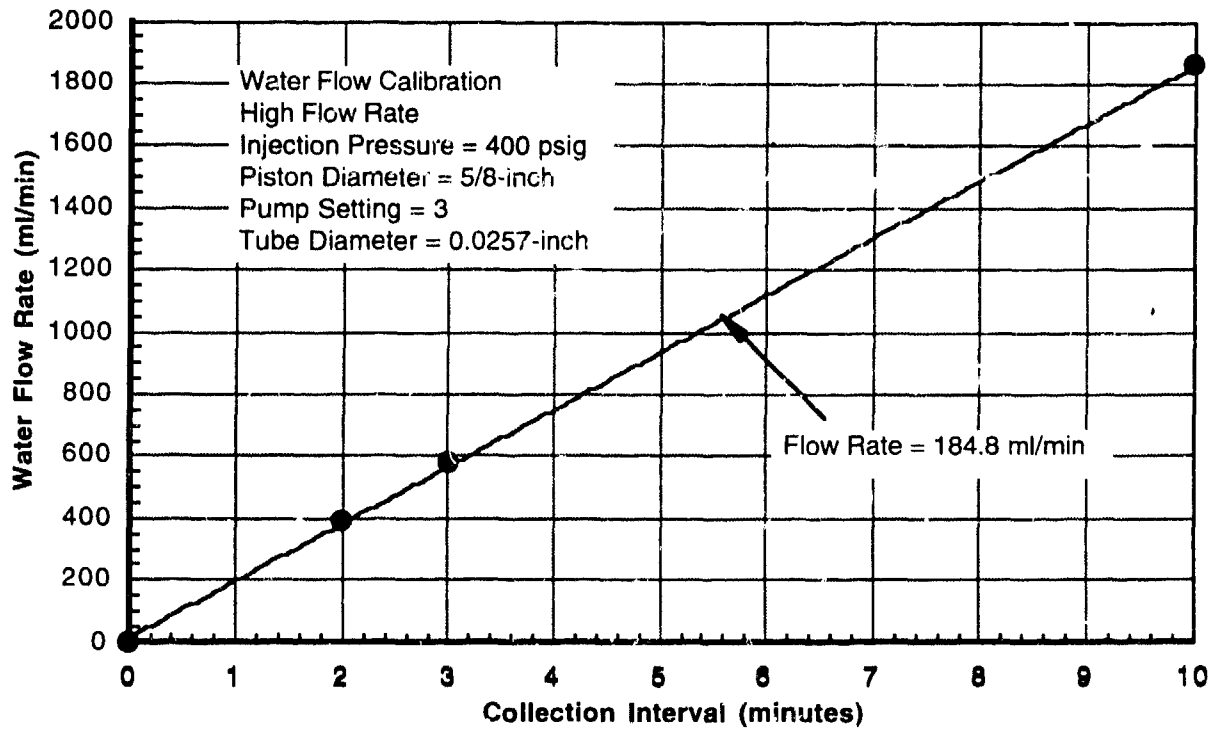


Figure 2-7. Water injection calibration curves for liquid flow rate.

2.2.4 Large Nozzle Flow Characteristics.

A key element in simulating dusty flow conditions on the B-1B ADS pitot probe was the generation of a high speed gas/particle flow surrounding the forward portion of the probe. Specifically, the design and calibration of a large (0.5-inch exit diameter) nozzle for expanding the gas/particle flow to high subsonic Mach numbers was a critical issue. The primary criterion used in sizing the nozzle was that the dusty jet formed by the nozzle must provide a relatively uniform flow environment over the total pressure port on the ADS probe. This port located in the front of the probe is approximately 0.3-inches in diameter.

The nozzle design utilized in the ADS evaluations was based on a scaled-up version of the standard nozzle used in the DNA test facility. A sketch of the nozzle geometry is shown in Figure 2-8 with a photograph of the nozzle included in Figure 2-9. As seen in Figure 2-8, the nozzle is a converging/diverging design with a constant diameter extension. The converging/diverging section accelerates the gas to high speeds while the constant diameter extension provides residence time for the gas flow to accelerate the particles. With the sharp breaks in the nozzle throat contour, the gas flow is quite complex at transonic and supersonic operating conditions (i.e. at nozzle inlet pressures greater than approximately 30 psig).

In order to characterize the the gas/particle jet formed by the nozzle, several different diagnostic measurements were made. These included the use of a small pitot-static probe to measure flowfield pressures (total and static pressure), a thermocouple probe to measure temperatures, and a laser doppler velocimeter (LDV) to measure particle velocities. Initially, measurements were made as a function of nozzle inlet pressure at one location in the jet in order to investigate the response of the jet. Once specific operating conditions were selected scans were made along all three jet coordinates.

Flowfield pressures were measured with a small precision pitot-static probe obtained from Davis Instrumentation Mfg. Co. in Baltimore, Maryland. The probe which has a 0.091-inch diameter head and a 0.157-inch diameter tube utilizes a modified ellipsoidal nose which does not require calibration and is less susceptible to directional errors than other designs. A photograph of the small pitot-static probe mounted on the jet axis is presented in Figure 2-10. The various optical components/mounts located just to the right of the probe in the photograph are part of the LDV optics. The coordinate system used to define positions within the jet is shown in Figure 2-11 and includes scan lines above and below the horizontal plane through the jet axis. These scan lines were used to measure jet pressure and temperature in a plane normal to the jet axis at a distance of one inch from the nozzle. This corresponds to the B-1B probe position used during the ADS tests.

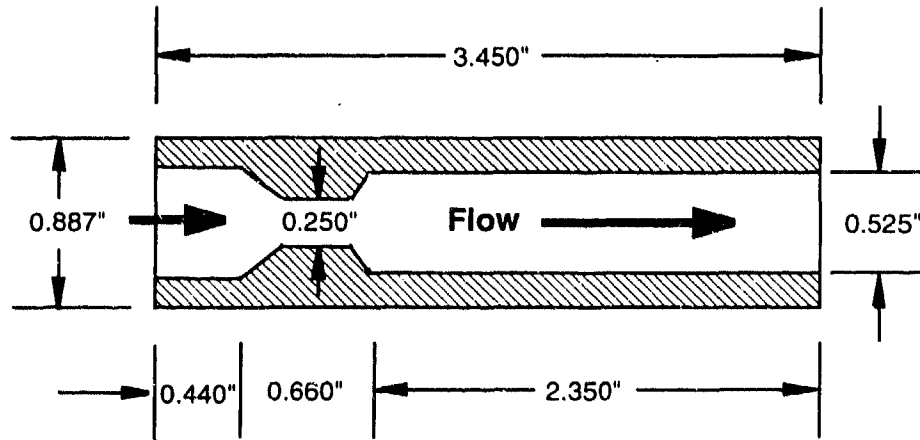


Figure 2-8. Nozzle configuration for ADS evaluations.

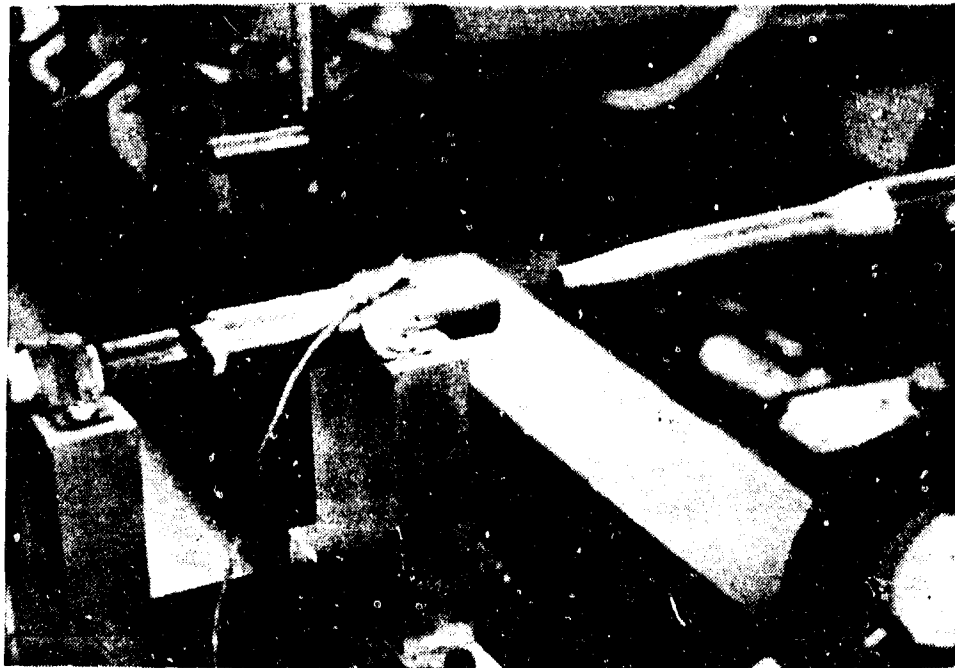


Figure 2-9. Photograph of gas/particle nozzle used for ADS evaluations.

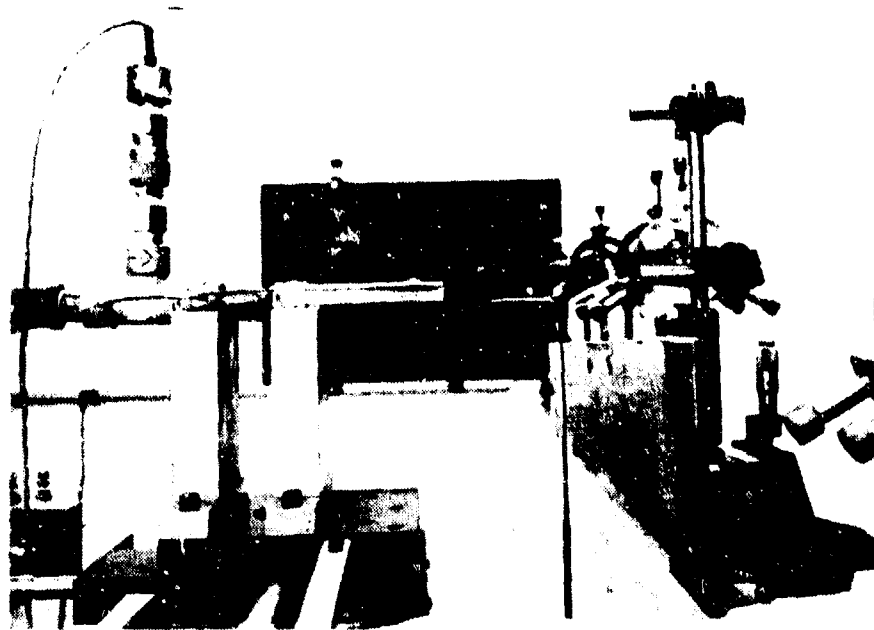


Figure 2-10. Photograph of small pitot-static probe mounted in gas jet.

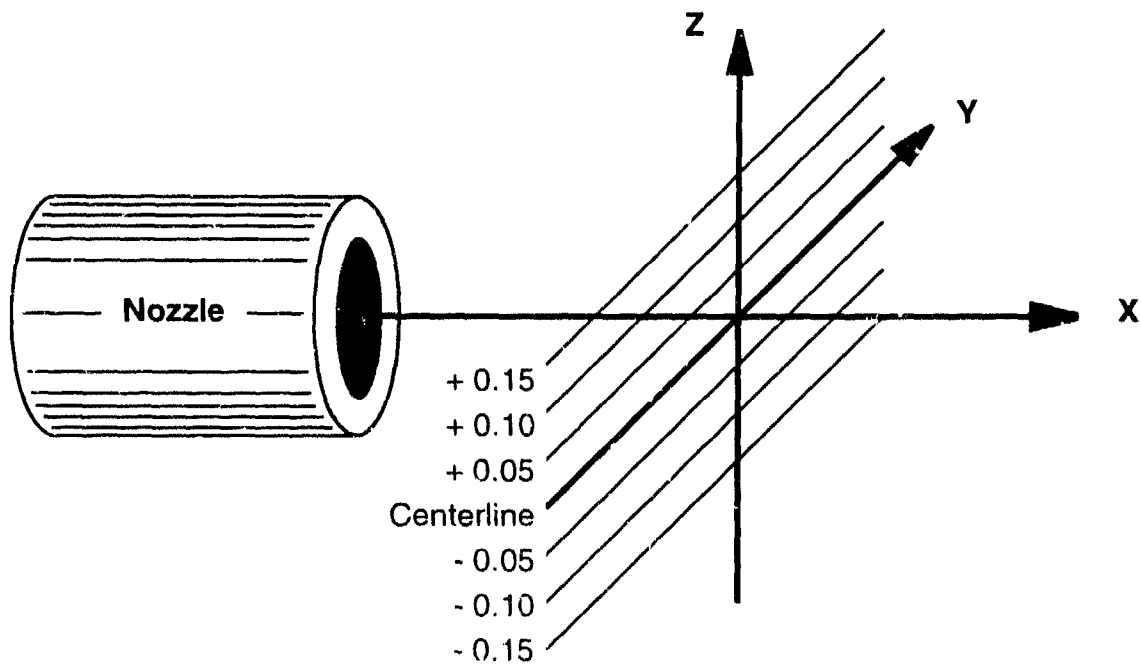


Figure 2-11. Jet coordinate definition for pressure scans.

Pressures measured on the jet axis at a axial distance of one inch using the small pitot-static probe are presented in Figure 2-12 for nozzle inlet pressures (P_n) up to 80 psig. The flow generated at nozzle inlet pressures greater than 30 psig is complex with sonic and supersonic conditions developing in the nozzle and jet. The measured total pressure actually declines slightly between nozzle pressures of 30 and 50 psig while the static pressure increases over this same region. A total pressure of approximately 10 psig is obtained at the maximum nozzle pressure of 80 psig. Static pressures, as expected, are quite small.

Three operating conditions were used for the ADS evaluations. These corresponded to nozzle pressures of 40, 70 and 80 psig. The primary testing, however, was done at 70 and 80 psig with the low pressure condition corresponded to a low particle velocity environment. Horizontal scans with the small pitot-static probe were conducted along the scan lines shown in Figure 2-11 for the three nozzle inlet pressures used in the ADS evaluations. Plots of the total pressure variation across the jet at each of seven vertical locations are presented in Figures 2-13 through 2-15 for nozzle inlet pressures of 40, 70 and 80 psig, respectively. The centerline scans indicate that the pressure is relatively uniform over a width of approximately 0.25 to 0.3-inches depending on nozzle pressure. The pressure distributions become more peaked further from the centerline as would be expected for an axisymmetric jet. For a nozzle pressure of 40 psig, the total pressure along the vertical axis between -0.15 to +0.15-inches varies only about $\pm 6\%$. For a nozzle pressure of 70 psig, the total pressure variation over the same distance is about $\pm 10\%$ and for the 80 psig nozzle pressure this variation is closer to $\pm 18\%$. For all of these conditions, the total pressure in the vertical direction tends to be near minimum on axis and increases above and below the axis to a maximum at a distance of approximate 0.12 to 0.13-inches from the axis.

Temperature scans were also conducted at nozzle inlet pressures of 70 and 80 psig using a thermocouple probe. The probe consisted of a bare type K thermocouple bead with insulated wires mounted parallel to the flow. Figure 2-16 presents temperature scans at three vertical locations. The temperatures appear to vary approximately linearly between the center and the edges of the jet. Also, temperatures above and below the centerline scan appear to be lower than those measured on the centerline. The temperature measured by the thermocouple probe is neither the total nor the static temperature at the probe location. For high speed flows, where viscous dissipation is important, the thermocouple should read the local recovery temperature (in the absence of heat conduction in the thermocouple leads). Thus, the temperatures in Figure 2-16 should be close to the recovery temperature. Temperatures on the jet axis one-inch from the nozzle were between 40 and 45 °F for nozzle inlet pressures of 70 and 80 psig. Based on these temperatures and calculated flow Mach numbers, the total temperature for all three conditions is approximately 51 °F.

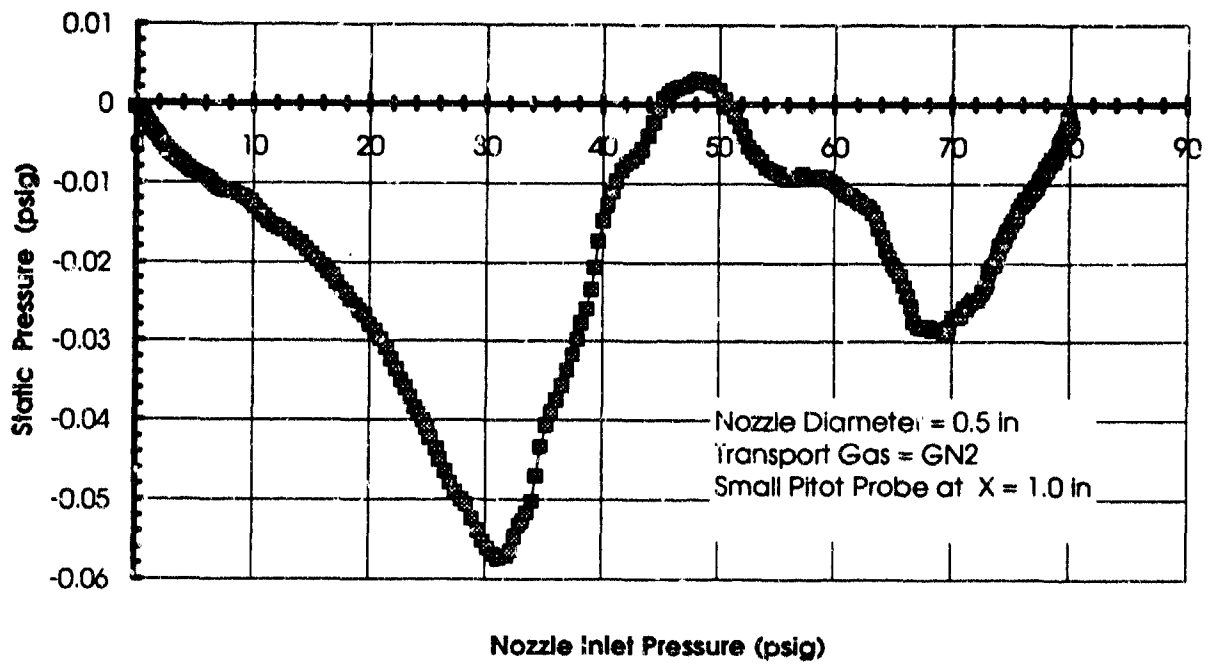
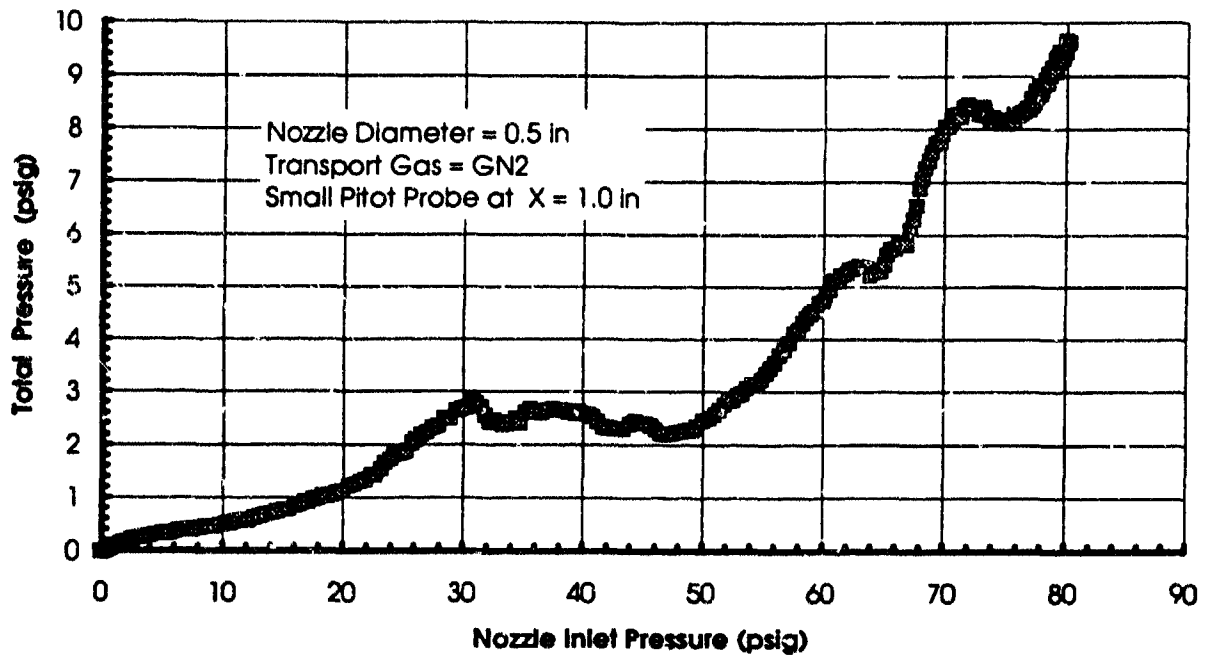


Figure 2-12. Total and static pressure response vs nozzle inlet pressure.

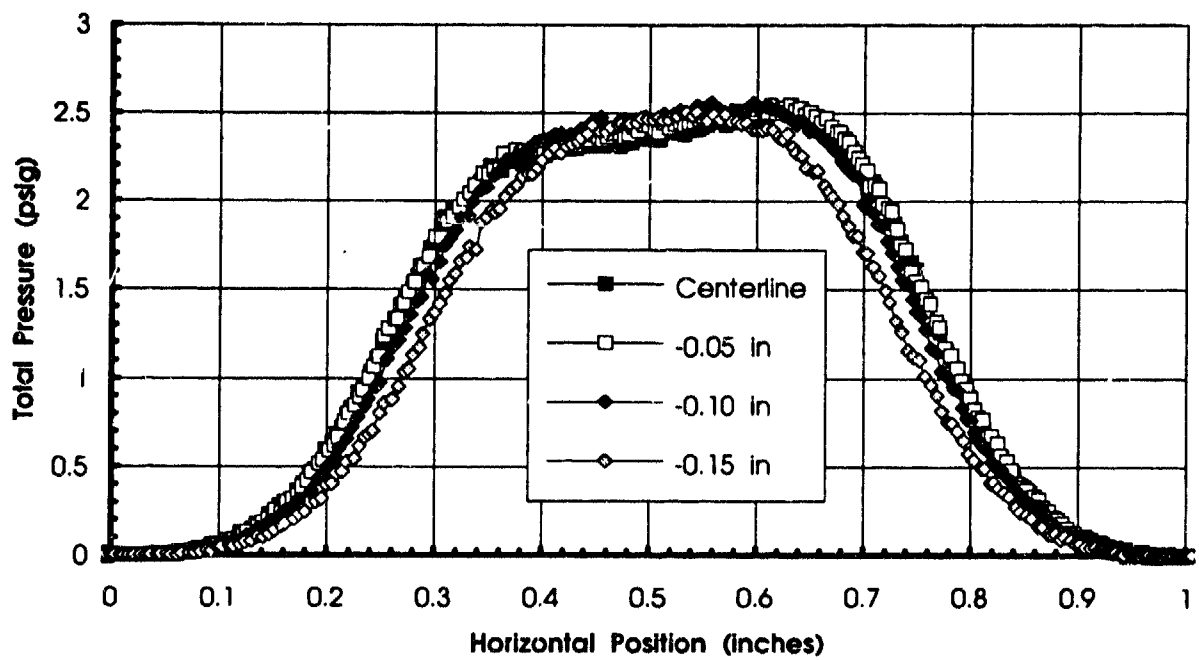
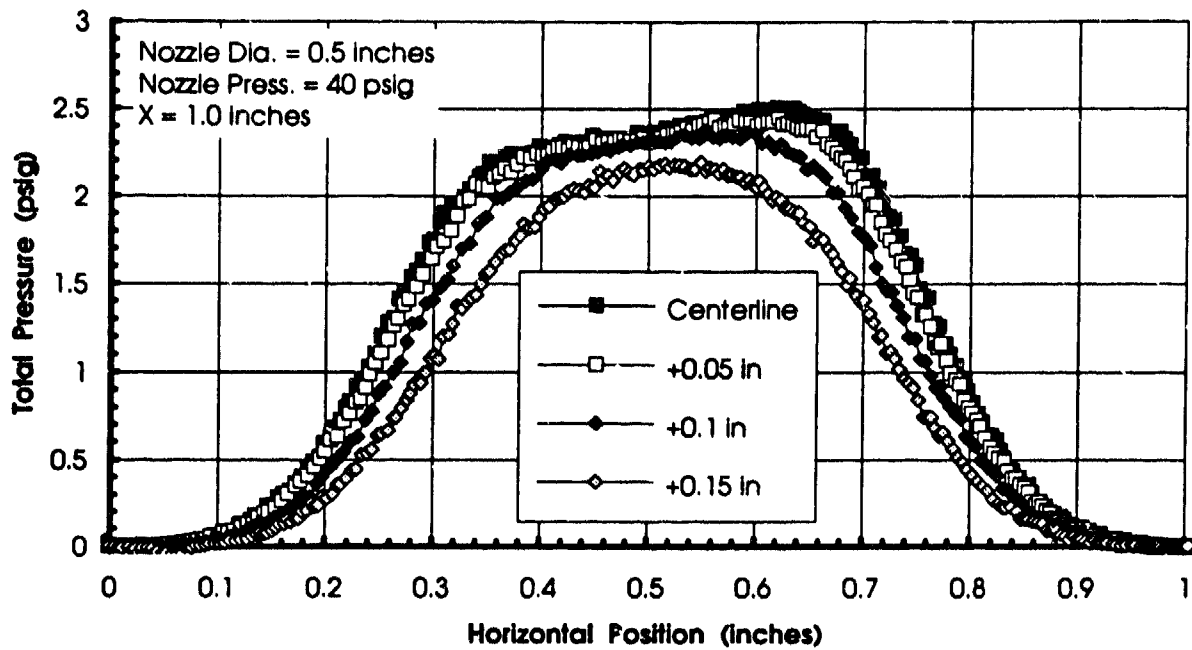


Figure 2-13. Total pressure scans as a function of vertical position - $P_n = 40$ psig.

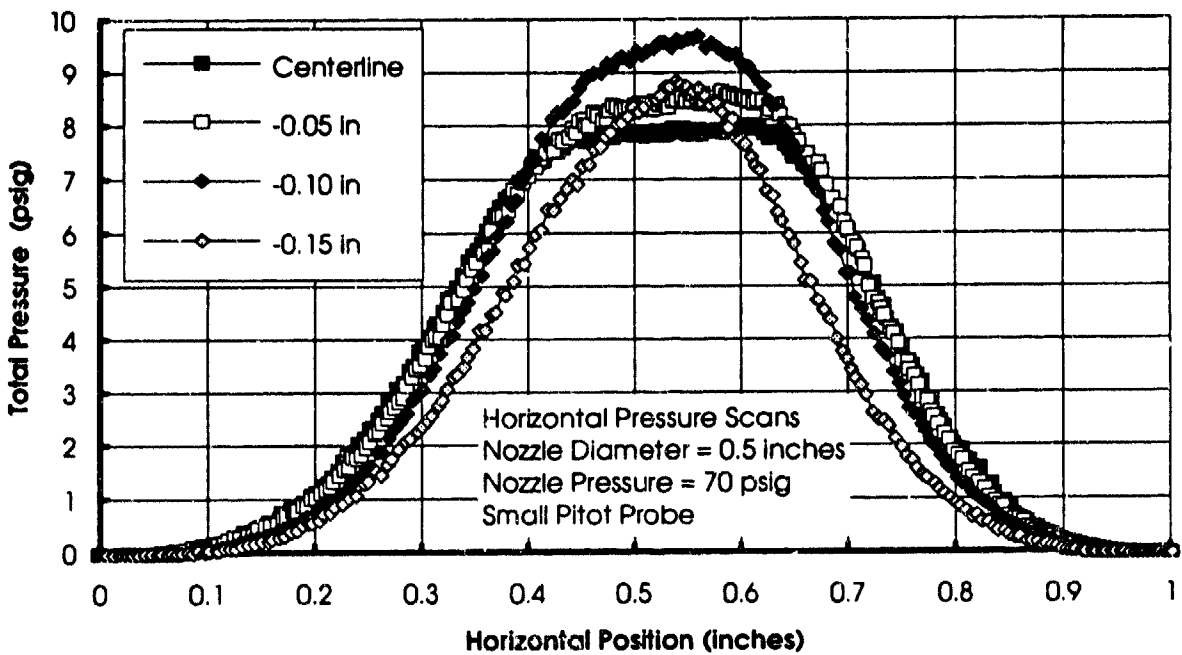
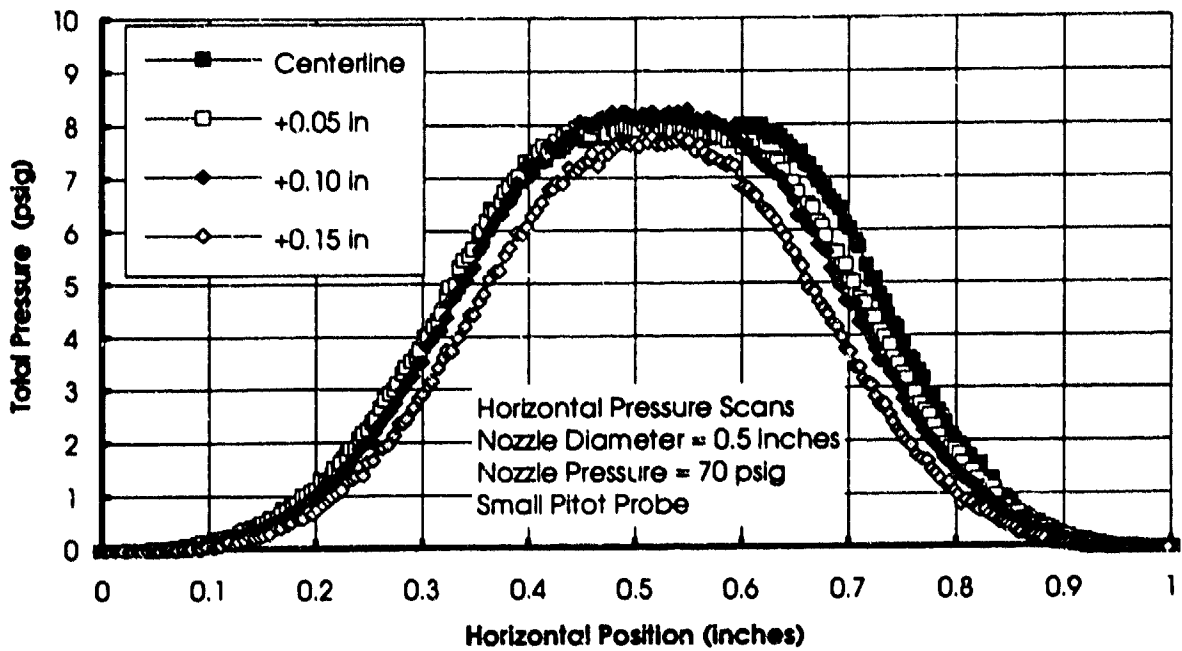


Figure 2-14. Total pressure scans as a function of vertical position - $P_n = 70$ psig.

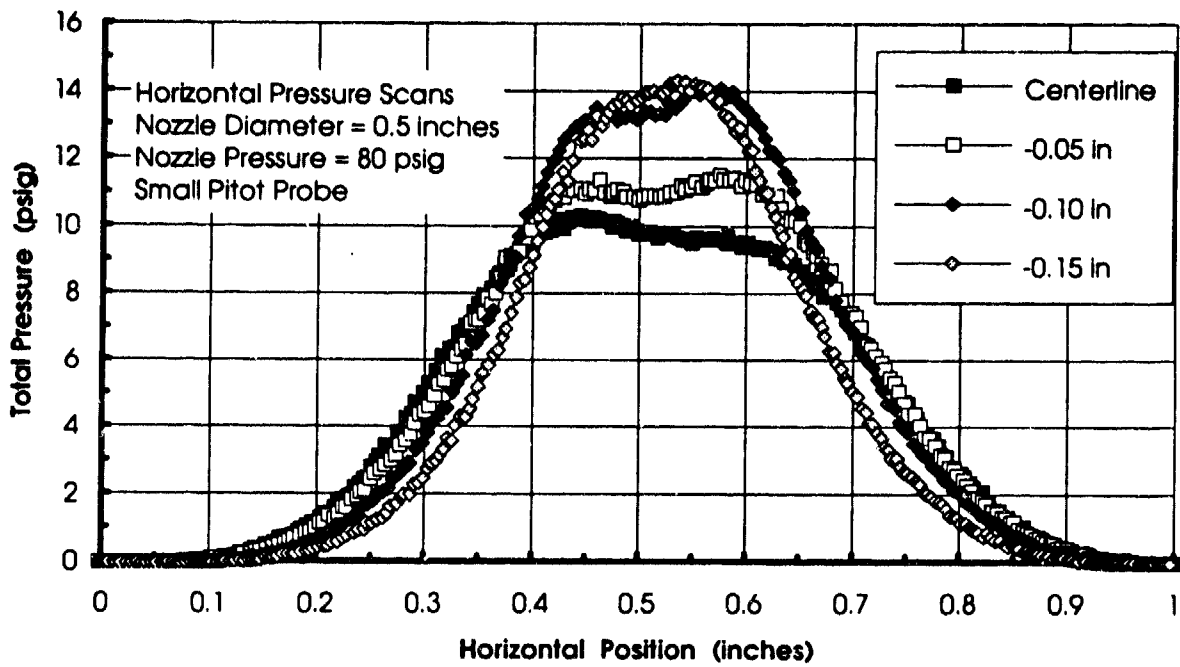
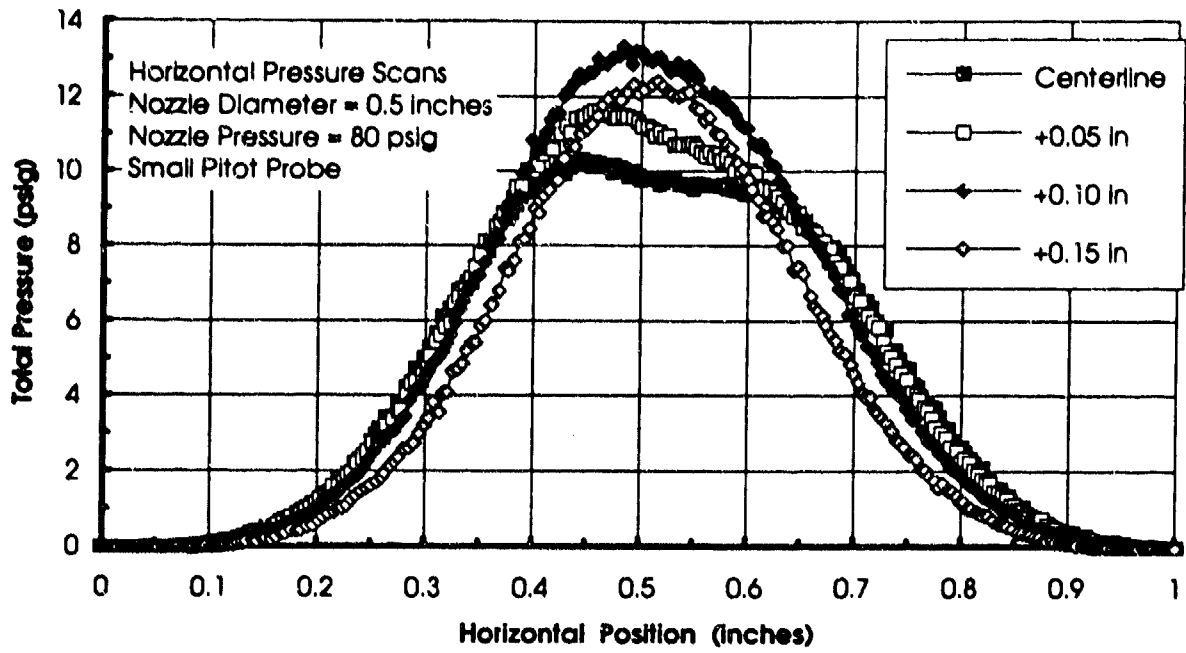


Figure 2-15. Total pressure scans as a function of vertical position - $P_n = 80$ psig.

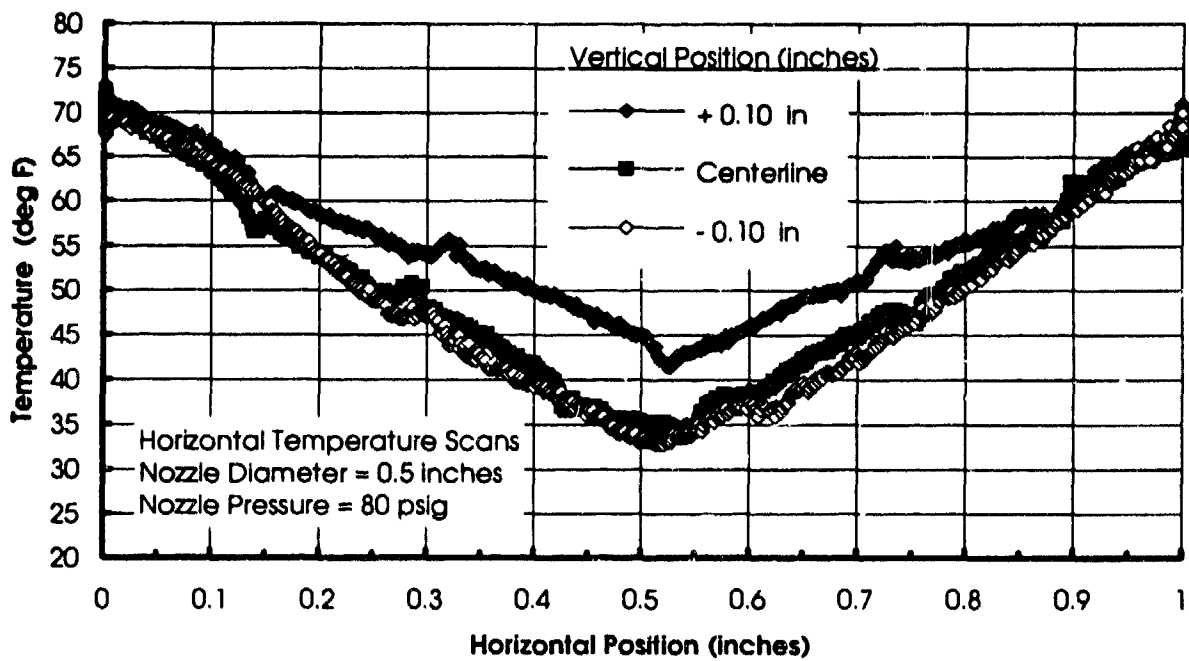
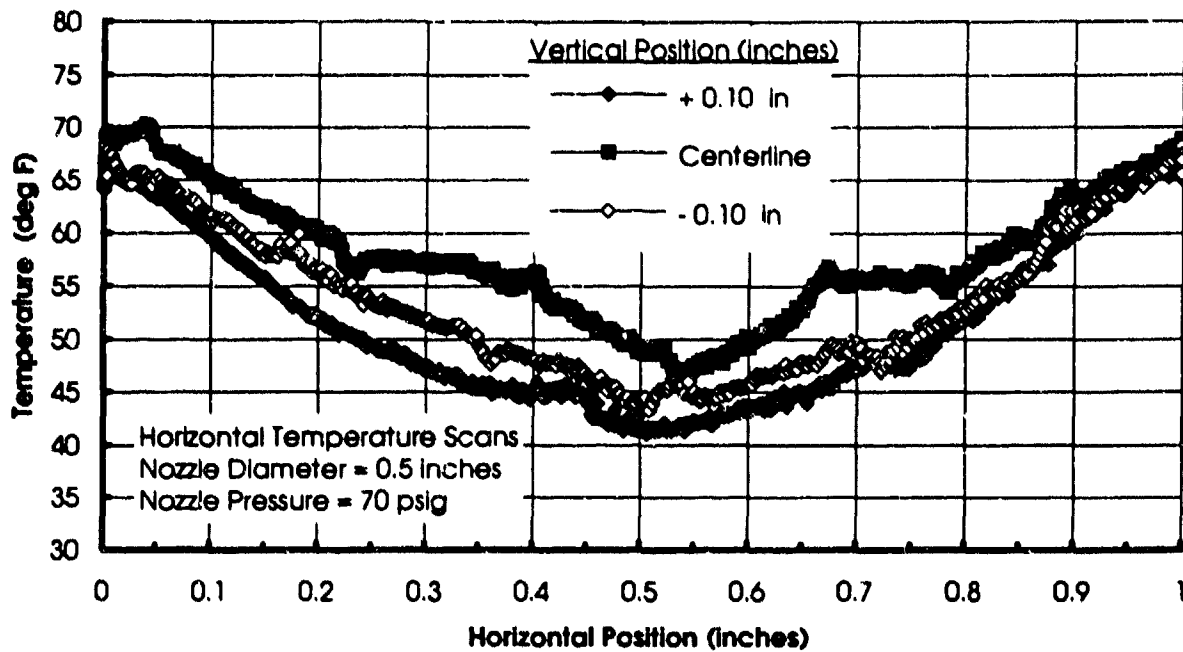


Figure 2-16. Temperature scans as a function of vertical position.

Particle velocity measurements were made with a Laser Doppler Velocimeter (LDV) system developed for the DNA Dust Erosion Test Facility. This system which is described in Reference 3 utilizes a non-intrusive technique which provides accurate and rapid measurement of the velocity of individual particles. The optical probe volume is small compared to the jet diameter allowing the velocity distribution across the jet to be determined. At any position within the jet, a nominal particle sample size of 2000 is used to determine mean velocity. Since the system utilizes a computer to store and process data, velocity measurements for a sample of 2000 particles can be completed in a matter of a few seconds.

Velocity distributions across the jet (i.e. the "Y" axis in Figure 2-11) at an axial position of one inch from the nozzle exit are presented in Figure 2-17. This Figure 2-contains two plots, one for a nominal test velocity of 288 m/s and the second for a lower velocity of 186 m/s. All three particle sizes were evaluated at the nominal velocity while only the $<38 \mu\text{m}$ crushed silica particles were evaluated at the lower velocity. The velocity distributions are relatively constant across the center of the jet which includes a diameter equivalent to the total pressure aperture of the B-1B pitot-static probe (approximately 0.3-inches). In fact, this constant velocity region appears to grow as particle size increases. For the nominal velocity, which corresponds to flight at Mach 0.85 at an altitude of 1,000 feet, all of the particles in the core of the jet are within $\pm 10\%$ of the target velocity of 288 m/s. For the lower velocity, which corresponds to flight at Mach 0.55 at an altitude of 1,000 feet, the uniformity across the jet is even better with particle velocity within approximately $\pm 2\%$ over a diameter of 0.55-inches.

Flow properties on the axis of the jet at one-inch from the nozzle exit were computed based on pitot-static and temperature probe measurements. Mach numbers at the nominal velocity condition were 0.82 and 0.89 corresponding to nozzle inlet pressures of 70 and 80 psig, respectively. This was close to the desired Mach number of 0.85 noted above. At the lower speed, the computed Mach number was 0.48 compared to the target of 0.55. The gas velocities for the nominal condition (266 and 285 m/s) were in the same range as the particle velocities shown in Figure 2-17. For the lower speed, the computed gas velocity was 160 m/s which was approximately 14% below the particle velocity.

Thus, based on results of pitot-static, thermocouple and particle velocity measurements in the gas/particle jet, it appears that the nozzle design and operating conditions provide a reasonable simulation of the selected flight environments. It should be noted that these conditions, however, exist only in a region of the flow corresponding to the position of the total pressure port on the B-1B pitot-static probe. Conditions, at other locations on the B-1B probe will not be as well simulated.

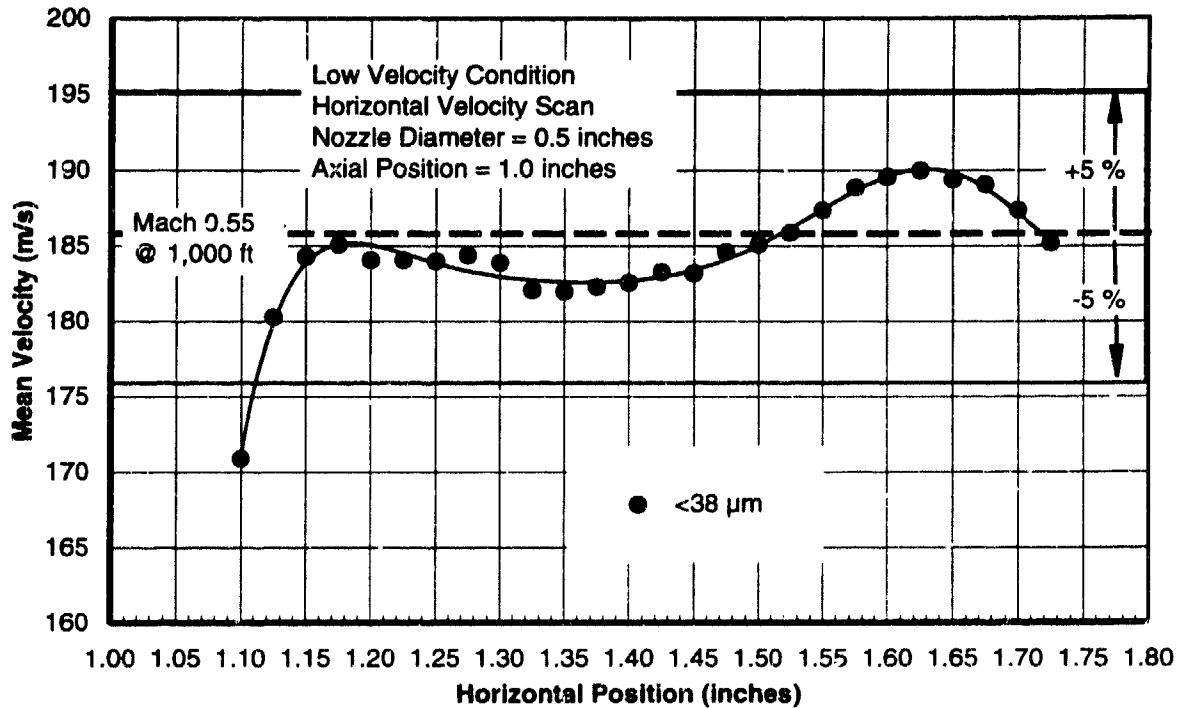
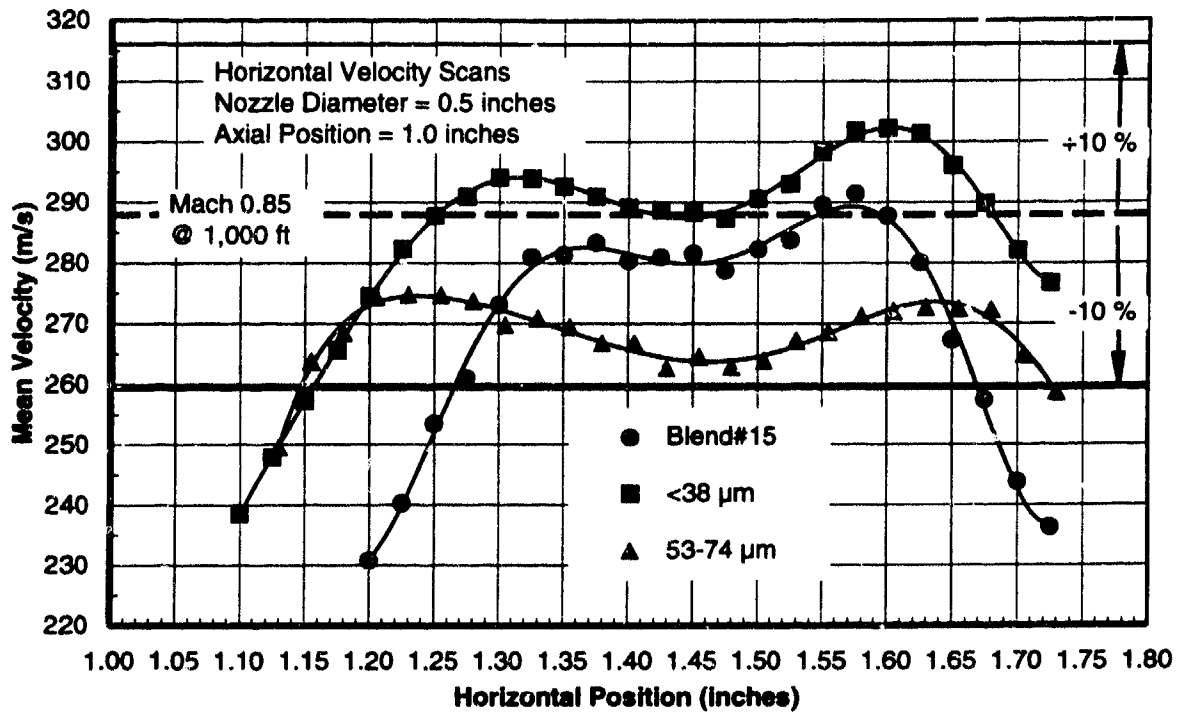


Figure 2-17. Particle velocity profiles measured with LDV system.

2.3 TEST ITEM DESCRIPTION.

The test item consisted of a B-1B air data sensor (ADS) Model 857AC manufactured by Rosemount Inc. This is an aerodynamically compensated pitot-static and angle-of-attack (AOA) probe which is mounted on the forward fuselage surface. A total of six probes (three on each side) are used on the aircraft. The probe provides total, static and AOA pressure outputs. Two operational probes were available for testing and one rejected probe was utilized for procedural checkout and calibration. The rejected ADS unit had a defective angle of attack output but was operational in all other respects. The ADS unit has both pressure and electrical interfaces. These include four pressure output ports and one (five-pin) electrical connector. The characteristics of the pitot-static probe and associated subsystems for pressure measurements and electrical power are identified in this section.

2.3.1 Air Data Sensor.

A specification drawing of the B-1B air data sensor is presented in Figure 2-18. In the test configuration, the probe was mounted horizontally utilizing the mounting flange and fastener holes on the ADS unit. The probes consisted of right side and left side mounting configurations. The only difference in the two configurations was the position of the drain hole on the bottom surface. The two fully operational test items consisted of one right side and one left side probe. Test item label information for the right side probe is presented in Table 2-1.

Table 2-1. Air data sensor label information.

AIR DATA SENSOR AERODYNAMICALLY COMPENSATED FUSELAGE MOUNTED, RIGHT SIDE ELECTRICALLY HEATED, 230 VOLT, 400 HZ RMT MODEL 857AC2-FT1, S/N 1813 ROSEMOUNT INC., FSCM NO. 59885 BURNSVILLE, MINNESOTA MFG DATE 06/88 R.I. SPEC. NO. L431C2026-1, REV D NSN 6610-01-204-7281 CONTRACT NO. F34601-88-C-6608-0002 U.S.A.

The probe has four sensing ports. These are (1) the total pressure port which forms the 0.28-inch diameter opening at the tip of the probe, (2) two small static pressure ports (0.070-in dia.) on top and bottom of the barrel of the probe approximately 1.9-inches aft of the total pressure port, (3) two small (0.070-in dia.) ports which are approximately 2.4-inches aft of the static ports and located on opposite sides of the flared section of the probe and (4) a single small (approximately 0.030-in) diameter moisture drain hole for the total pressure duct. The moisture drain hole is approximately 6.2-inches aft of the tip of the probe. When the probe is mounted on the aircraft, the moisture drain hole is positioned on the bottom surface of the probe barrel.

2.3.2 Pressure Transducer Interface.

The four output pressure lines emerge from the base of the pitot-static probe and terminate with threaded fittings as shown on the drawing in Figure 2-18 and in the photograph presented in Figure 2-19. When installed on the aircraft, these fittings provide the connections for the pressure transmission lines which attach to the B-1B air data transducer (Rosemount Model 1581C3). Initial attempts to utilize an actual B-1B transducer and provide a more complete simulation of the ADS system response were unsuccessful. The ADS transducer digital output required a specialized and proprietary transponder which could not be provided by the Air Force, Rockwell International or Rosemount. Thus, for the dusty flow evaluations, separate commercial pressure transducers were connected via flexible pressure line to each of the output pressure fittings for the measurement of total, static and angle of attack pressures.

For these ADS evaluations, the primary probe output was the total pressure since that was the only port likely to ingest dust particles during an exposure to the high speed particle flow. Also, since the flowfield in the laboratory tests was an expanding jet, a significant axial decay in pressure was experienced. Thus, the static and angle-of-attack pressure readings were not expected to correspond to flow conditions at the total pressure port location at the tip of the probe. However, the pressure outputs from the static and AOA ports were monitored with pressure transducers in order to detect degradation or change in pressure which may indicate dust ingestion in those ports.

The pressure transducers and their characteristics are listed below in Section 2.4. A transducer with a 0-15 psig range was used on the total pressure line while more sensitive 0-1 psig and 0-2" H₂O transducers were used on the static and AOA pressure lines. Also, in order to collect any solid particles that may be transmitted by the pitot-static probe to the pressure transducers, particle filters were installed in-line just ahead of the transducers. A photograph of the pressure transmission lines and particle filters attached to the probe is shown in Figure 2-20.

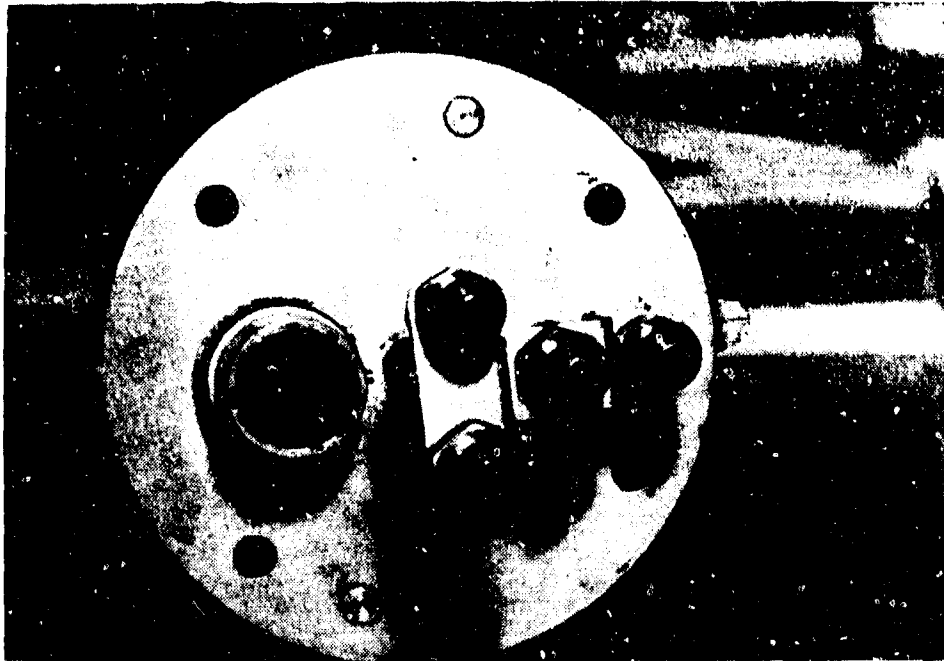


Figure 2-19. Sensor fittings and connections.

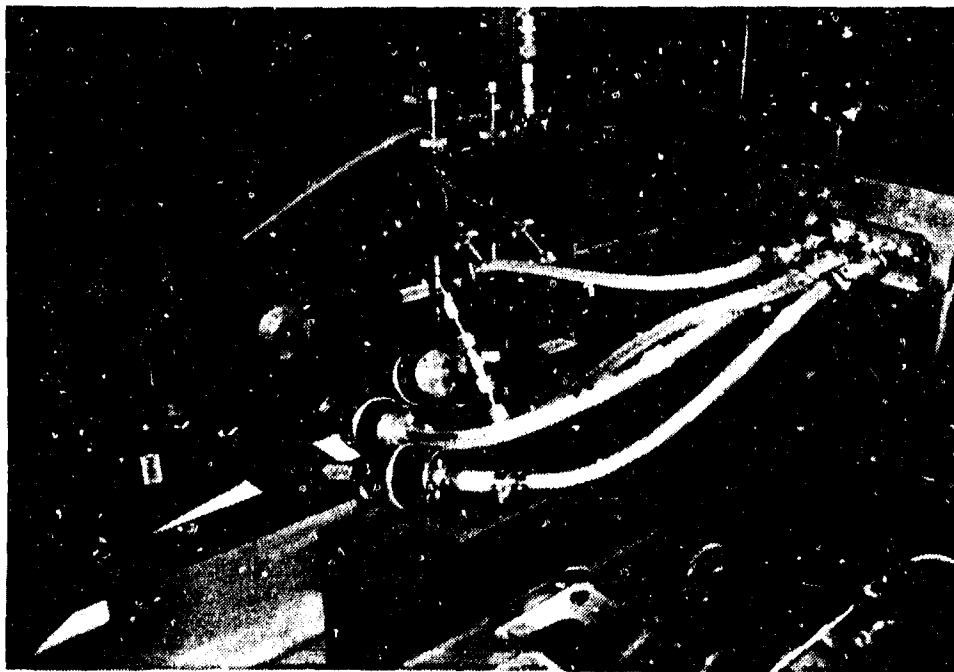


Figure 2-20. Pressure transmission lines and particle filters.

2.3.3 Sensor Heater Interface.

The electrical connection on the base of the ADS probe, which is shown in Figure 2-19, provides power to internal heaters. The pitot-static probe has resistance heaters located in the head of the tube and in the mast. The two heaters are electrically isolated from each other but are connected together by external wiring to operate in series as shown in Figure 2-21. The electrical power requirements are 230 VAC, 400 HZ, single phase with a maximum output after 5 minutes of operation of 395 watts in still air at ambient temperatures of 68° to 86°F. The heaters are self-regulated in such a manner that the power dissipated through the heaters is an inverse function of the heater-element temperature.

For the dusty flow evaluations, the heaters when in use were supplied with 208 VAC, 60 HZ, single phase electrical power. Since the heater elements are essentially resistors, they are insensitive to the AC frequency and the readily available 60 HZ laboratory power was utilized. During testing the supply voltage and current flow to the probe were measured to insure that the room temperature power limits were not exceeded. Nominal heater voltage used was 208 VAC and the current was 1.8 A which provided approximately 375 watts.

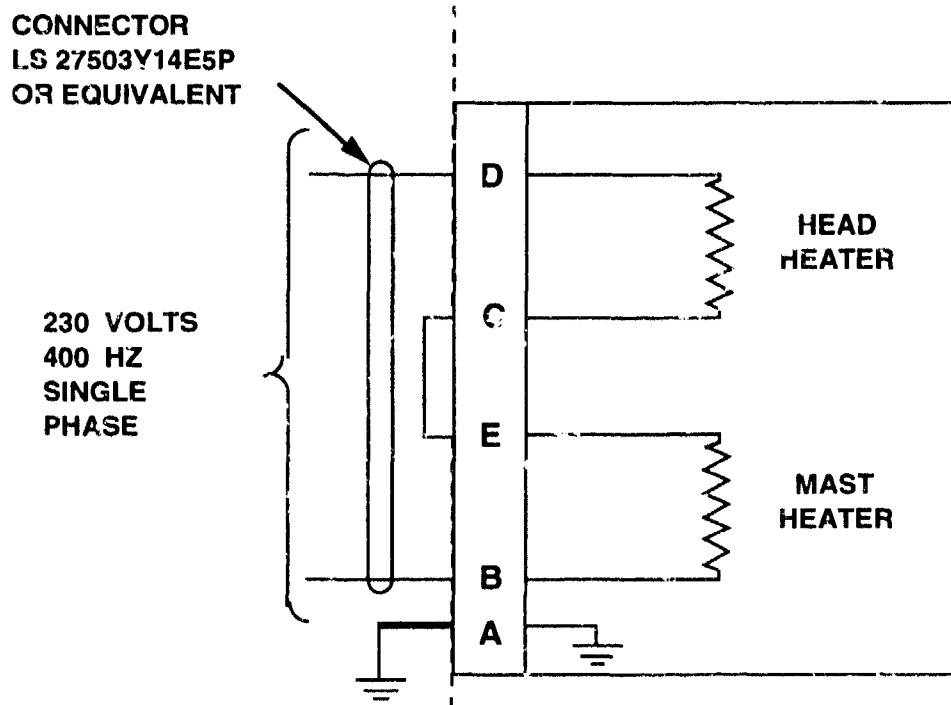


Figure 2-21. ADS heater schematic.

2.3.4 Description of Particle Blends.

The B-1B air data sensors were subjected to three dust particle blends. The first dust blend used in these evaluations was Blend #15, a particle mixture used in B-1B engine tests and provided by Calspan Corporation. This blend, which is intended to represent soil from a particular region of the earth, was constructed from four constituents in the following proportions:

Blend #15: 25% Ottawa Quartz, 25% Red Clay, 25% Feldspar and 25% synthetic glass.

The remaining two blends used in these evaluations were obtained from a different bulk material. Referred to as brown foundry sand, this material consists of crushed silica with approximately 4% impurities. It was purchased from Whitehead Brothers Company in Leesburg, N.J. and sieved on site at PDA to obtain two different size distributions. The two sizes were <38 μm which included all material passing through a screen with 38 μm hole size and 53- 74 μm material which was collected between the 53 and 74 μm screens.

Particle size distributions were obtained for the two crushed silica particle ranges and for all of the components of the Blend #15 except the synthetic glass. The synthetic glass was not available as a separate component but appears to be in the same general size ranges as the other Blend #15 components. Particle sizing was conducted by Horiba Instruments, Inc. in Irvine, California using laser diffraction analysis. Table 2-2 summarized the particle size results in terms of the median diameter and the 90% under diameter. Blend #15 is significantly smaller than the crushed silica particles as is also shown by the photomicrographs of the three particle blends presented in Figure 2-22.

Table 2-2. Particle size data.

PARTICLE SAMPLE	MEDIAN DIA. (μm)	90% UNDER DIA. (μm)
BLEND #15 COMPONENTS		
Quartz	5.16	11.56
Red Clay	7.28	14.38
Feldspar	12.16	26.98
CRUSHED SILICA		
<38 μm	35.83	55.12
53-74 μm	78.12	114.36

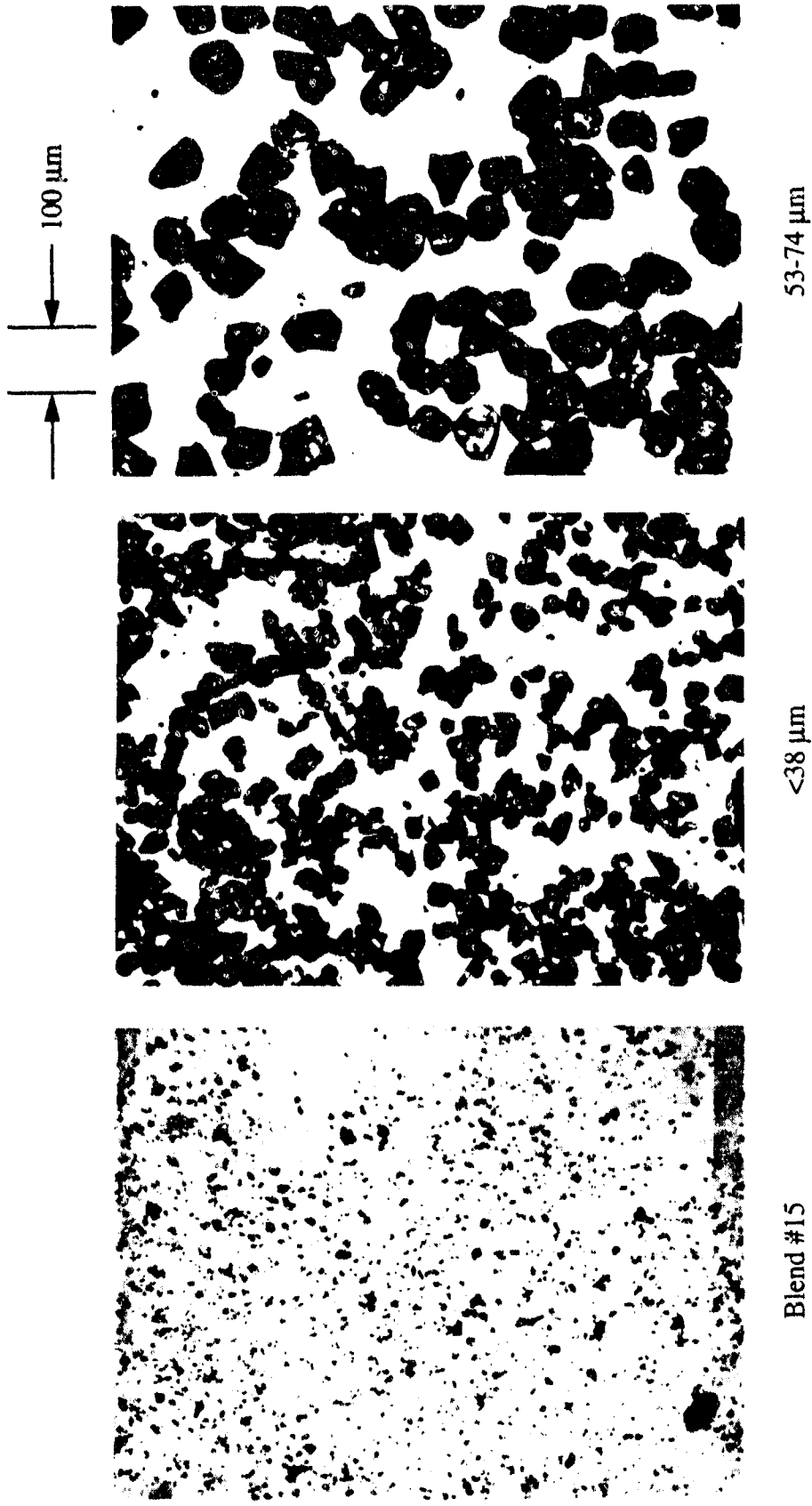


Figure 2-22. Photomicrographs of test particles.

2.4 INSTRUMENTATION.

Instrumentation was required to support primary measurement functions: (1) facility diagnostics, (2) ADS probe response and (3) pre/post-test characterization and calibration. A list of the test instrumentation including function, make/model, range and accuracies is presented in Table 2-3. The run-time facility diagnostics consisted primarily of gas pressure measurements. The key diagnostic parameter was the nozzle inlet pressure which (in conjunction with the particle size distribution) determined the gas/particle jet characteristics. The pressure and temperature in the particle feeder plenum as well as the nozzle inlet temperature were monitored to verify flow stability. Also, the injection of water to simulate cloud moisture effects introduced an additional system. Since the water flow rate was a function of the injector tube size and metering pump settings, it was determined by prior calibration as discussed in Section 2.2.3. These diagnostics were integrated into the computerized data acquisition system and were recorded during each test.

2.4.1 Hardware Description.

The primary ADS response measurements were the pitot-static pressure outputs. Probe surface temperature was also monitored with a surface thermocouple mounted aft of the angle-of-attack ports during certain tests when the probe was being heated. The probe pressure measurements included the total pressure, static pressure and average pressure at the two angle-of-attack ports. These probe pressures and temperature were recorded along with the facility diagnostic measurements using the computerized data acquisition system.

Pre- and post-test measurements included probe and filter weight measurements. The weight measurements were made using the electronic balance for the dust filters or other small items. Since the pitot-static probe weighs over a kilogram, a larger scale was required to measure probe weight changes. Also, the probe was cleaned by a backflow of compressed air. Particles flushed from the probe were collected in a filter and weighed. This procedure provided a check on the particle mass as determined from the difference in pre- and post-test probe weight.

The jet flowfield diagnostics included the particle velocity, gas flow pressures (total and static) and gas temperature distributions across the jet at the location of the B-1B ADS total pressure port, which was located 1-inch aft of the nozzle exit plane. The particle velocity measurements were conducted using a Laser Doppler Velocimeter (LDV) as discussed in Section 2.2.4. The gas flow diagnostic were obtained using a small precision pitot-static probe to measure total and static pressure distributions and a custom designed thermocouple probe to measure temperature distributions within the jet.

Table 2-3. Test instrumentation.

MEASUREMENT	INSTRUMENT	MAKE	MODEL	TYPE/ RANGE	COMMENTS
<u>Pressure</u>					
Plenum/Nozzle Pressure	Transducer	Barksdale	302H1-05CG-04-J	0 - 150 psig	Accuracy: $\pm 0.5\%$ FS
Pitot Total Pressure	Transducer	Data Instruments	SA (Part #9301201)	0 - 15 psig	Accuracy: $\pm 1\%$ FS
Pitot Static Pressure	Transducer	AutoTran	600D1P12D5	0 - 1 psig	Accuracy: $\pm 1\%$ FS
Angle-of-Attack Pressure	Transducer	AutoTran	600D2*1204	0 - 0.072 psig	Accuracy: $\pm 1\%$ FS
<u>Temperature</u>					
Plenum Temperature	Thermocouple	Omega	CXSS-18(U)-12	Type T	1/8-in Dia. Probe
Probe/Total Temperature	Thermocouple	Omega	GG-K-20	Type K	Bead/Insulated Wire
<u>Weight</u>					
Particle/Filter Weight	Electronic Balance	Sartorius	R160D (Dual Range)	0 - 30 gm 0 - 160 gm	Accuracy: $\pm .00001$ gm Accuracy: $\pm .0001$ gm
Probe Weight	Scale(Digital Display)	Mettler	PJ4000	0 - 4000 gm	Accuracy: ± 0.1 gm
<u>Electrical</u>					
Voltage & Current	Digital Multimeter	Fluke	8062A	4-1/2 Digits	

Table 2-3. Test instrumentation. (Continued)

MEASUREMENT	INSTRUMENT	MAKE	MODEL	TYPE/ RANGE	COMMENTS
<u>Particle Velocity</u>	LDV Processor	Aerometrics	PDP-3100 Processor	LDV-Signal	w/ Data Acq. Software
Velocimeter Hardware	PC Computer	AMT	286AT	PC/AT Clone	EGA Monitor/Printer
Processing Hardware	PC Computer	Royal	486DX33	32-Bit Bus	130 MB HD & SVGA
<u>Data Acquisition</u>	A-to-D Board	Strawberry Tree	ACPC-12	12-Bit A-to-D	16-Channels
Digital Processing/Storage	Software	LabTech	Notebook		Plots with Log to Disk
Data Acquisition Hardware	Optical Microscope	Olympus	BHT	50X - 500X	Auto Exp. Photography
Data Acquisition Software	35mm Camera	Nikon	F-3HP with Lens	50mm/104mm	Motor Drive, etc.
<u>Observations</u>	VHS Video Camera	Panasonic	WV-F2	CCD Color	With AG-2400 VCR
High Resolution					
Documentation (Still)					
Documentation (Video)					

2.4.2 Data Acquisition System.

To support the automated data acquisition and analysis requirements, a PC computer system with capable data acquisition/analysis hardware and software was utilized. The computer used was a 486/33 PC clone having a 32-bit local bus architecture and a 130 MB hard drive. A Strawberry Tree 12-bit, 16-channel AD board and LabTech Notebook data acquisition software provided data acquisition rates of over 10 Hz and adequate disk storage space. Figure 2-23 presents a photograph of the data acquisition system including computer, SVGA monitor and terminal box for analog/digital connections. The nominal acquisition rate used was 5 Hz (data point every 0.2 seconds). For a 10-min run, this data rate produced a data file having 3000 time points. The LabTech data files were fully compatible with Microsoft Excel 4.0 which was used for data analysis and display.

In addition to the specific pressure and temperature measurements, observational instrumentation was also used for documentation. These systems included a high quality optical microscope with photographic capabilities, a 35-mm still camera system and a video camera system.



Figure 2-23. Data acquisition system.

2.5 TEST PROCEDURE.

Prior to formal evaluation of the air data sensors, calibration measurements were performed on the particle feed system, the water injection system and the gas/particle jet. These calibration results are discussed above in Sections 2.2.2 through 2.2.4. The gas/particle jet measurements were used to establish facility operating conditions and provided both axial and radial distributions of particle velocity, total gas pressure, static pressure and temperature within the high speed gas/particle jet. Measurements were made using the facility Laser Doppler Velocimeter (LDV) system (particle velocity), a small high accuracy pitot-static probe (flowfield pressures) and a small thermocouple probe (temperature). Also, flow rate calibrations were conducted for the screw feeder based particle metering system and the positive displacement (water) metering pump system, used for moisture injection. These calibration measurements were conducted for each test condition prior to and following formal testing.

Except for a few test runs to investigate special effects, the same basic procedure was used for all of the dust exposure runs associated with the ADS evaluations. A description of the general procedure used as well as a detailed list of specific steps including both moisture injection and probe heating options are included in this section.

2.5.1 General Description.

An overview of the primary test method was presented in Section 2.1 and illustrated in Figure 2-1. It involves the exposure of a clean B-1B ADS probe to a calibrated dust jet. The exposure was initiated with a clear gas flow (no particles or water) for a stabilization period of approximately 1 to 2 minutes. This initial period was utilized in order to (1) allow the jet and probe flow conditions to stabilize and (2) obtain baseline ADS pressure data which are essential for determining performance deviations. Once stable conditions were established, a steady particle flow was initiated and continued for a planned exposure period.

Typically, data acquisition was initiated just prior to opening the GN₂ valve so that diagnostic data were available during the initial stabilization period. Data were acquired throughout the exposure until GN₂ valve closure. A nominal sampling rate of 5 Hz was chosen to provide good temporal resolution without exceeding storage array-size limits for a normal 10 to 15-min exposure. During the exposure, ADS probe output pressures and surface temperature (if specified) were recorded along with key facility diagnostics. The LDV system was utilized to make particle velocity measurements at the entrance to the total pressure port for a selected dry particle exposure. The LDV could not be operated with water injection due to contamination of the exposed optics.

One modification that was required for flows with water injection was the addition of heat to the nozzle. Specifically, with the initial wet flow runs, ice buildup was observed on the lip of the total pressure port. This was apparently caused by the low gas temperature in the nozzle and jet which promoted freezing of the water mist. The problem appeared to be most severe on the interior surface of the constant diameter section of the nozzle near the exit. Moisture appeared to collect, freeze and break off to produce relatively large ice particles that impacted the probe. Fear that these ice particles may be contributing to plugging of the total pressure port, led to the addition of a heater to maintain the nozzle at a temperature above the freezing point of water. This was accomplished using a propane torch to heat the bottom of the nozzle. A thermocouple was installed on the top exterior surface of the nozzle to monitor the nozzle temperature and control the heating rate.

After each run, the probe was carefully removed from the mounting fixture, the pressure transducers disconnected and the pressure lines disconnected from the probe. Before the particle filters were removed, compressed air was used to force particles from the lines into the filters. The ADS probe and individual particle filters were weighed in order to determine the amount of dust collected in the probe and the amount deposited in the lines leading to the transducers. In the case of moisture addition, the exterior to the probe usually was coated with moist particles (i.e. mud). Thus, the exterior surface of the probe was cleaned, in this case, prior to taking a post-test weight measurement.

In addition to the nominal dust exposure runs, test runs were also conducted with water injection only (no dust particles) in order to determine the baseline response of the ADS probe in the moisture environments. In addition, two runs were conducted to explore the response of an ADS probe in a gas flow environment after it had been filled with dust particles.

2.5.2 Basic Test Procedure.

The specific procedure that was employed to evaluate the response of a clean B-1B pitot-static probe to a dusty flow environment including moisture injection and probe heating was as follows:

- (1) Weigh test article (ADS probe) and filters separately without pressure lines.
(*Moisture injection*) Prime metering pump and verify water flow.
- (2) Mount and align the ADS probe in the test facility so that the tip (total pressure port) is at an axial distance of one inch from the facility nozzle exit plane and the axis of the probe is align with the nozzle axis. The nominal probe orientation is such that the moisture drain hole is pointing vertically downward.

- (3) Connect the pressure transducers to the probe's pressure output ports via flexible tubing with dust filters mounted inline just ahead of each transducer.

(*Probe heating*) Attach the electrical connector from the heater power supply to the probe.
- (4) Check type and quantity of particles in the screw feeder. Verify feeder mass flow rate settings and make sure feeder switch is in the off position.
- (5) Initialize computer-based data acquisition system. Initiate data acquisition and verify operation of active data channels.

(*Probe heating*) Turn on probe heater power supply, verify current flow and monitor probe surface temperature.
- (6) Initiate test by opening GN2 supply valve and adjusting pressure regulator to achieve specified nozzle pressure. Operate facility at test conditions for approximately one minute to allow temperatures and pressures to stabilize while verifying data outputs.

(*Moisture injection*) Initiate liquid metering pump, open valve and verify water spray in the jet.
- (7) Initiate dust flow by switching on screw feeder. Note data acquisition system time and start stop watch with feeder initiation in order to time dust exposure.
- (8) Record particle velocity data using LDV system at specified time intervals during test if LDV measurements are included.
- (9) Terminate screw feeder operation at specified exposure time or if GN2 supply can no longer support operating pressure. Close GN2 pressure regulator to shut down nozzle flow and terminate data acquisition.

(*Moisture injection*) Close water flow valve and turn off metering pump

(*Probe heating*) Turn off probe heater power supply.
- (10) Cover ADS total pressure port with tape, disconnect pressure transducers (and probe heater plug), and remove test item from mounting fixture.
- (11) Weigh ADS probe after carefully removing tape from pressure port. Remove and weight each dust filter. Document weight data, exposure time and test observations.
- (12) Clean ADS probe by back flowing compressed air through each pressure port. Place flexible tubing with attached filter over each probe surface port and collect purged dust particles in the same dust filter. Weigh probe and filter. Compare probe weight with initial weight to verify that probe is clean.
- (13) Examine recorded data files and plot key pressure/temperature outputs.

SECTION 3 TEST RESULTS

The purpose of this experimental program was to evaluate the effects of gas/particle flows on the B-1B air data sensor (pitot-static probe) performance. The primary goal was to determine dust exposure conditions sufficient to degrade the performance of the probe. The key test parameters were simulated and performance was evaluated based on pressure outputs and dust mass collected by the probe and associated pressure feed lines. This section of the report presents the results of these evaluations. It includes a review of the key test parameters, a discussion of the test matrix, the results of the test runs and a discussion of the data/observations. A detailed description of the original test plan is presented in Reference 4.

3.1 TEST PARAMETERS.

The primary parameters considered in evaluating ADS response to dust particles were (1) particle type/size distribution, (2) flow velocity and (3) integrated particle loading. Secondary parameters which were also considered to be important in the ADS response included (4) the moisture content of the gas-particle flow and (5) the temperature of the probe. These five parameters were considered in the development of the test matrix and in the conduct of the test program. They are discussed in this subsection.

3.1.1 Particle Size.

Particle size was identified as a potentially key parameter. Bridging or plugging of internal passages such as the moisture drain hole could be sensitive to particle size. Since very fine particles are better able to follow the gas flow, they may not easily deposit within the probe. Thus, it was important to consider a range of particle sizes in the ADS response evaluations. A minimum of three particle sizes were considered in this test program. Particle size selection was guided by cloud environment analyses and available materials. Particle sources included crushed silica from $< 38 \mu\text{m}$ to $250 \mu\text{m}$ and the fine particle blends ($\leq 10 \mu\text{m}$) being used for engine ingestion tests. One of the fine particle blends identified as Blend #15 was used in B-1B engine evaluations.

A sample of Blend #15 was provided by Calspan for use in the ADS testing. This material was formulated to represent a "most likely" dust mixture based on specific B-1B missions. The other two particle sizes included in these evaluations were significantly larger than the Blend #15 and were identified as $< 38 \mu\text{m}$ and $53\text{-}74 \mu\text{m}$ crushed silica. These sizes represent sieve screen sizes which produced that particular particle range. As discussed in Section 2.3.4, the median particle sizes are approximately $36 \mu\text{m}$ and $78 \mu\text{m}$ for these two crushed silica samples. These

larger particle sizes were selected in order to explore particle size effects and since larger particles may be present in the real environments. For example, a sample of volcanic ash was recovered from a plugged pitot-static probe on a commercial Boeing 747-400 airliner. This aircraft had encountered an ash cloud from Mt Redoubt (Alaska) in December 1989. An analysis of the particles recovered from the probe yielded sizes from a few microns to over 100 μm . Thus, it was believed to be important that a full range of particle sizes be included in these ADS evaluations.

3.1.2 Particle Flow Velocity.

Although particle velocity is an important parameter in evaluating ADS response to dusty flows, the range of air speeds are limited for the B-1B during penetration where particle environments are likely to be encountered. Depending on fuel load, the B-1B cruise speed will range from Mach 0.79 to 0.88 (approximately 520 to 580 knots at 1,000 ft altitude). Since the variation in particle speed across the dust jet (in the laboratory testing) will be in this same range, one nominal particle velocity corresponding to Mach 0.85 was selected for the primary testing. Limited evaluations at a lower particle speed (i.e. Mach 0.55) corresponding to a minimum aircraft flight speed was also included. The measured particle velocities obtained in the post-test calibrations are presented above in Figure 2-17.

3.1.3 Particle Loading.

The total amount of particle mass encountered by the ADS probe per unit area (normal to the flow) is a primary test variable. If cloud particle concentrations are very low and/or exposure duration is short, the amount of dust encountered by the probe may be insufficient to cause plugging or bridging within the probe. Thus, the evaluations of probe response were conducted based on particle loading as an independent test variable. For the laboratory test environment, particle mass loading is related to particle flow rate, nozzle size and exposure duration: however, in the flight environment, the particle mass loading is related to cloud concentration, flight speed and exposure duration. These relationships can be represented as follows:

$$\text{Particle Loading (gm/cm}^2\text{)} = \frac{\dot{m} \Delta t}{A} = 0.006 C_c V \Delta t,$$

where \dot{m} = particle mass flow rate (gm/min)

Δt = exposure duration (min)

A = flow cross sectional area (cm^2)

C_c = cloud mass concentration (gm/m^3)

V = velocity (m/s)

Thus, for a specific laboratory test condition, an equivalent cloud concentration can be determined using the above relationship and solving for C_c . Figures 3-1 and 3-2 present equivalent concentrations as a function of particle flow rate with flow diameter (Figure 3-1) and with particle velocity (Figure 3-2) as parameters. A range of flow diameters is shown in Figure 3-1 since the effective diameter of the particle jet is difficult to specify. If the jet did not spread and the particle concentration and velocity were constant across the jet, the flow diameter would correspond to the 0.5-inch diameter nozzle. However, with the jet spreading and the drop in concentration and velocity near the outer edges the effective flow diameter may be 0.625-inches or larger. For the particle flow rates selected for these evaluations, the corresponding range of equivalent cloud concentrations was between 1×10^{-6} and 5×10^{-6} gm/cm³. While these values are at the upper end of the predicted ambient cloud concentration ranges, they are reasonable for a laboratory simulation where exposure time drives the test conditions. Also, preliminary particle-flowfield interaction analyses for the forward B-1B fuselage indicate that the effective particle concentration in the vicinity of the pitot-static probes may be higher than the ambient concentration due to flow deflection effects over the nose of the aircraft.

3.1.4 Moisture.

Another important parameter in the ADS response was the moisture content of the gas-particle flow. A mixture of water and dust particles forms a slurry that may bridge or plug probe passages. Thus, evaluations were conducted with both wet and dry particle flows. Since only two fully operational B-1B pitot-static probes were available, cleaning the probes following exposure was an important issue. Experience had shown that dry particles can be easily flushed from the probe with air flow. However, mud formed by fine particles and water could be more difficult to remove. Therefore, tests with water injection were performed after the dry particle testing. Also, a water backflow technique was developed which provided an effective cleaning method. Two water flow rates were utilized in the evaluations as discussed in Section 2.2.3.

3.1.5 Probe Heating.

Heating of the ADS probe in the anti-icing mode is a common operating condition. The effects of elevated temperature on probe response to gas/particle flows was examined as part of the evaluation matrix. Heating of the pitot-static probe was not expected to affect the response to dry particles. However, in the presence of moisture, it was postulated that an elevated probe temperature may promote caking and bridging of internal passages as the wet particle mixture dries and solidifies. Thus, heating effects were considered in conjunction with moisture testing as discussed in Section 2.3.3.

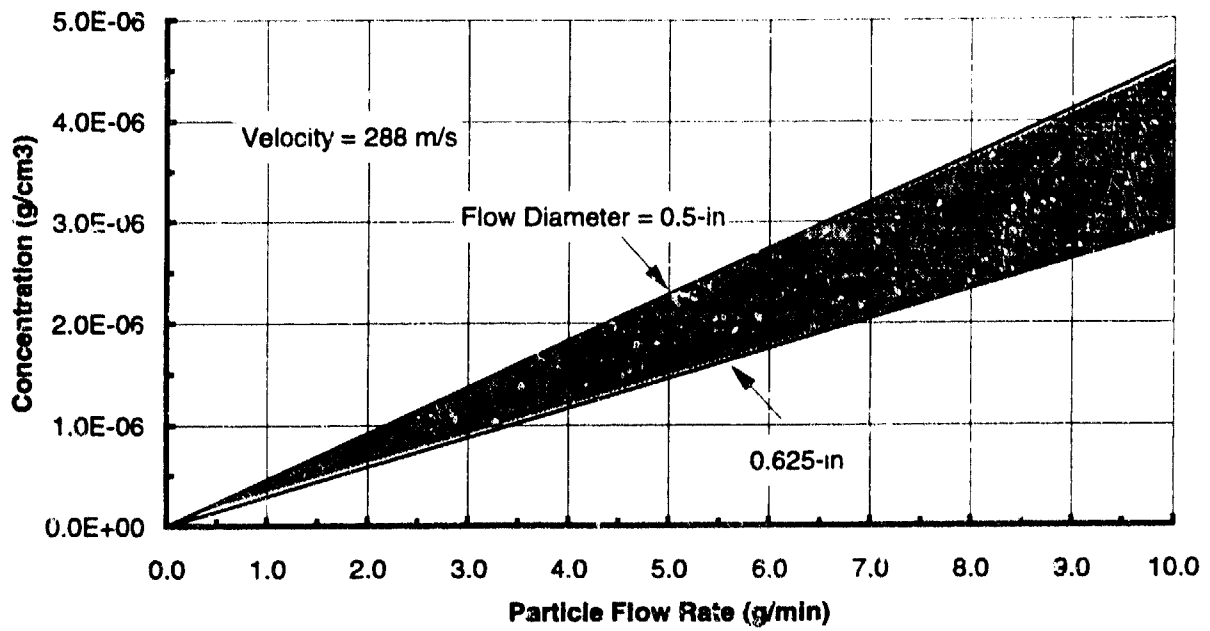


Figure 3-1. Effect of flow diameter on equivalent cloud concentration.

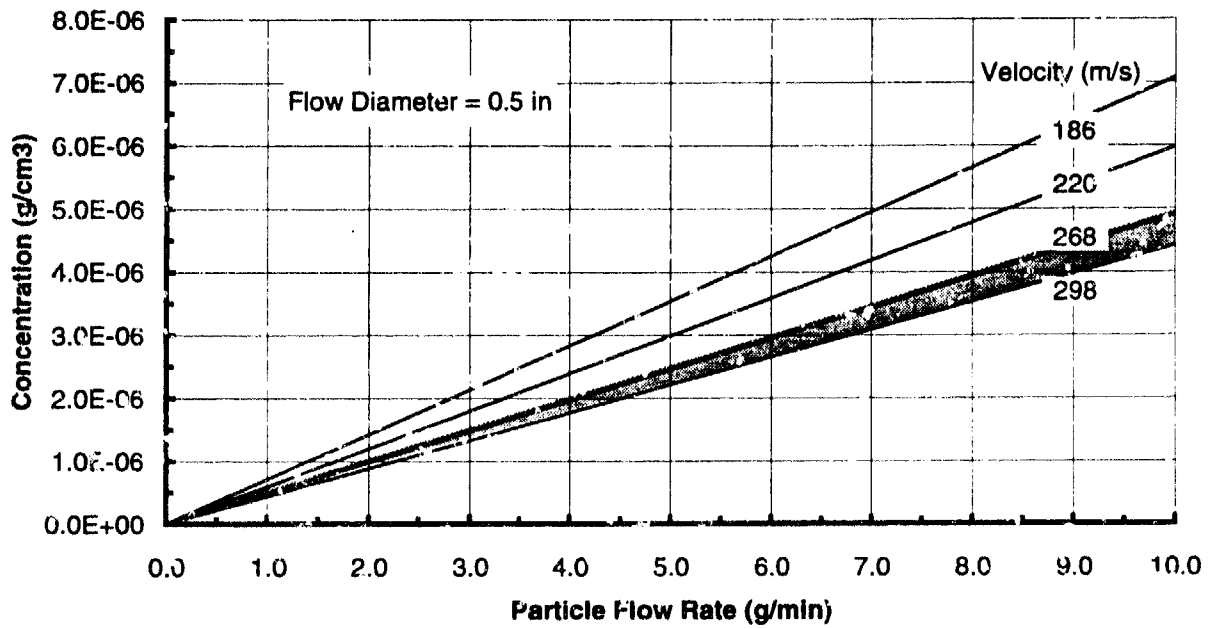


Figure 3-2. Effect of particle velocity on equivalent cloud concentration.

3.2 TEST MATRIX.

The original test plan and rationale are reviewed and the completed test matrix including modifications and additions is presented and discussed in this section.

3.2.1 Test Plan.

A recommended test sequence for evaluating the effects of dusty flows on the B-1B ADS probe was constructed well in advance of the actual data runs and was presented in Reference 4. This plan, shown in Table 3-1, consisted of 24 test conditions defining particle type/size, flow velocity, particle flow rate, exposure duration and the presence of water flow and/or probe heating. The test series was organized so as to address dry gas/particle flows first, then flows with low moisture content, followed by heavier water flows and finally the lower velocity condition. The specific particle environments specified in this original plan were estimated based on preliminary test data and were modified as required during the evaluations to best characterize ADS response.

Except for the last three runs listed in Table 3-1, which utilized a planned particle velocity of 186 m/s (Mach 0.55), all tests were run at a nominal velocity of 288 m/s (Mach 0.85). All test were conducted with the probe aligned with the dust jet centerline (zero degrees angle-of-attack). The primary limitation associated with the specified test conditions was exposure duration. Since bottled GN₂ was used as the gas source, the relatively high flow required by the nozzle for these test conditions limited continuous run times to approximately 15 minutes or less. Thus, the particle flow rates were selected to provide the maximum particle loading for the available exposure time. While these flow rates result in equivalent cloud concentrations that are slightly greater than 10⁻⁶ gm/cm³, the particle mass flow rates are still less than one percent of gas flow rate. Preliminary tests with <38 μm crushed silica particles showed that the amount of particle mass collected in the pitot-static probe was a linear function of the total particle loading and (for a constant particle flow rate) a linear function of exposure time.

For each particle size, one run was allocated to evaluating the response of an ADS probe that is filled with particles. The particle flow rates and exposures for these runs were to be determined (TBD). Additional runs were also anticipated in order to successfully identify probe degradation thresholds for the various particle types and size ranges. Probe heating was limited to runs with moisture in order to conserve resources for higher priority tests and since temperature was not expected to significantly affect dry dust flow within the probe. The lower moisture flow rate shown in Table 3-1 was selected to be consistent with the dust flow rates, so that the solid particle-to-water weight ratio will be representative of predicted cloud environments.

Table 3-1. Original B-1B ADS test plan.

RUN NO.	PARTICLE TYPE	PART. SIZE (µm)	PART. VEL. (m/S)	PART. FLOW (gm/min)	RUN TIME (min)	PARTICLE LOADING (gm/cm2)	WATER FLOW (gic/min)	PROBE HEATER	COMMENTS
1	Blend #15	<20	288	5	10	40	None	Off	Pre-fill Probe with Dust
2				10	5	40			
3				10	10	80			
4				TBD	TBD	TBD			
5	Crushed Silica	<38		5	10	40			
6				10	5	40			
7				10	10	80			
8				TBD	TBD	TBD			
9	Crushed Silica	53 - 74		5	10	40			
10				10	5	40			
11				10	10	80			
12				TBD	TBD	TBD			
13	Blend #15	<20	288	5	10	40	10	Off	Moisture Effects
14							200	Off	
15							TBD	On	
16	Crushed Silica	<38					10	Off	
17							200	Off	
18	Crushed Silica	53 - 74					TBD	On	
19							200	Off	
20							10	Off	
21							TBD	On	
22	Crushed Silica	<38	186	5	10	40	None	Off	Particle Velocity Effects
23				10	10	80			
24				TBD	TBD	TBD			

3.2.2 Completed Test Matrix.

The completed test matrix is summarized in Table 3-2. The table lists all of the exposures of the B-1B ADS probe conducted during the formal test phase of the program between 4 March and 19 May 1993. Results are listed in chronological order by facility run number. The table does not include preliminary runs conducted with the damaged pitot-static probe. Those runs were used to refine test procedures and acquire preliminary response data. Also, exposures to define baseline ADS performance using gas flow only were conducted as part of the pre and post-test calibrations and were not included in Table 3-2. However, the flows with GN₂ plus water (no particles) were conducted as part of the formal testing per the basic procedure outlined in Section 2.5 and are included in Table 3-2.

The completed test matrix consisted of 78 runs which was slightly over three times the number of specified test conditions presented in Table 3-1. The large number of runs consisted of additional runs to (1) duplicate observed effects, (2) expand the parameter range and (3) explore important observations. The initial set of exposures were conducted with dry particle flows and consisted of 19 runs of which five runs were clear air runs to explore the response of pre-filled probes. These dry exposures included the 12 planned test conditions plus seven duplicate runs which were used to verify results. Results of these exposures plus the three lower velocity exposures are presented below in Section 3.4.

The bulk of the testing was conducted with wet flow conditions. A total of 55 exposures were completed involving the two water flow rates and probe heating. The major variation from the original test plan was the addition of several runs covering a range of dust flow rates. Thus, a series of exposures similar to the dry particle runs were conducted with all three particle sizes for each of the two water flow rates. As noted on Section 2.5.1, it was necessary to heat the nozzle during water injection runs in order to prevent ice buildup. This icing problem was discovered after several of the initial wet flow runs were completed. Thus, reruns of these several test conditions with nozzle heating were conducted to eliminate uncertainties associated with nozzle ice buildup. All of the planned test conditions were accomplished. Results of the wet flow exposures are presented in Section 3.5.

3.3 BASELINE ADS PERFORMANCE.

In order to identify any performance degradation to the B-1B air data sensors due to solid particle flow effects, it was necessary to establish the baseline performance of the probe for each of the three gas flow conditions. Since the primary testing was conducted at nozzle pressures of 70

Table 3-2. B-1B ADS completed test matrix.

RUN NO.	PARTICLE TYPE	PART. SIZE (µm)	PART. FLOW (gm/min)	RUN TIME (min)	PART. MASS (gm)	WATER FLOW (gm/min)	PROBE		COMMENTS
							HEAT	ID	
1226	Blend #15	<20	5.0	10.0	50.0	None	Off	2	Pre-filled Probe Pre-filled Probe Pre-filled Probe Data File Lost Data File Lost Data File Lost Pre-filled Probe Pre-filled Probe
1227	↓	↓	10.0	5.0	50.0	↓	↓	↓	
1228	↓	↓	10.0	10.0	100.0	↓	↓	↓	
1229	↓	↓	---	---	---	↓	↓	↓	
1230	↓	↓	---	---	---	↓	↓	↓	
1231	Crushed Silica	<38	5.0	10.0	50.0	↓	↓	↓	
1232	↓	↓	10.0	5.0	50.0	↓	↓	↓	
1233	↓	↓	10.0	10.0	100.0	↓	↓	↓	
1234	↓	↓	---	---	---	↓	↓	↓	
1235	Crushed Silica	53 - 74	5.0	3.2	15.9	↓	↓	↓	
1236	↓	↓	5.0	10.0	50.0	↓	↓	↓	
1237	↓	↓	10.0	5.0	50.0	↓	↓	↓	
1238	↓	↓	10.0	5.0	50.0	↓	↓	↓	
1239	↓	↓	10.0	5.0	50.0	↓	↓	↓	
1240	↓	↓	10.0	10.0	100.0	↓	↓	↓	
1241	↓	↓	---	---	---	↓	↓	↓	
1242	↓	↓	---	---	---	↓	↓	↓	
1255	Blend #15	<20	10.0	5.0	50.0	↓	↓	↓	
1256	↓	↓	10.0	5.0	50.0	↓	↓	↓	
1257	Blend #15	<20	5.0	10.0	50.0	8.1	Off	2	Moisture Only Nozzle Heating
1259	↓	↓	---	---	---	8.1	↓	↓	
1260	↓	↓	10.0	5.0	50.0	8.1	↓	↓	
1261	↓	↓	2.5	6.0	15.0	8.1	↓	↓	
1262	↓	↓	2.5	20.0	50.0	8.1	↓	↓	
1263	↓	↓	3.8	12.0	45.0	8.1	↓	↓	
1264	↓	↓	5.0	10.0	50.0	8.1	On	↓	
1265	↓	↓	5.0	10.0	50.0	8.1	Off	↓	
1266	↓	↓	5.0	10.0	50.0	8.1	On	↓	
1267	↓	↓	5.0	10.0	50.0	8.1	On	↓	
1268	↓	↓	5.0	8.0	40.0	8.1	Off	↓	
1269	↓	↓	5.0	5.0	25.0	8.1	Off	↓	
1270	↓	↓	5.0	8.0	40.0	8.1	On	↓	
1272	↓	↓	5.0	5.0	25.0	8.1	Off	3	
1273	↓	↓	5.0	5.0	25.0	8.1	On	↓	
1274	↓	↓	2.5	5.0	12.5	8.1	On	↓	
1275	↓	↓	2.5	10.0	25.0	8.1	Off	↓	
1276	↓	↓	1.3	10.0	13.0	8.1	On	↓	
1277	Crushed Silica	<38	5.0	5.0	25.0	8.1	Off	↓	
1278	↓	↓	2.5	14.0	35.0	8.1	Off	↓	
1279	↓	↓	5.0	4.0	20.0	8.1	On	↓	
1280	↓	↓	2.5	10.0	25.0	8.1	On	↓	

Table 3-2. B-1B ADS completed test matrix (Continued).

RUN NO.	PARTICLE TYPE	PART. SIZE (μm)	PART. FLOW (gm/min)	RUN TIME (min)	PART. MASS (gm)	WATER FLOW (gm/min)	PROBE		COMMENTS
							HEAT	ID	
1281	Crushed Silica	<38	2.5	10.0	25.0	8.1	Off	3	Nozzle Heating
1282	↓	↓	5.0	14.0	70.0	8.1	On	↓	↓
1283	↓	↓	2.5	12.0	30.0	8.1	On	↓	↓
1284	↓	↓	10.0	5.0	50.0	8.1	Off	↓	↓
1285	↓	↓	10.0	5.0	50.0	8.1	On	↓	↓
1286	↓	↓	2.5	15.0	37.5	8.1	↓	↓	↓
1287	↓	↓	10.0	3.0	30.0	8.1	↓	↓	↓
1288	Crushed Silica	53 - 74	10.0	4.0	40.0	8.1	Off	↓	↓
1289	↓	↓	5.0	15.0	75.0	8.1	↓	↓	↓
1290	↓	↓	5.0	10.0	50.0	8.1	↓	↓	↓
1291	↓	↓	2.5	8.0	20.0	8.1	↓	↓	↓
1292	↓	↓	10.0	3.0	30.0	8.1	On	↓	↓
1293	↓	↓	5.0	10.0	50.0	8.1	↓	↓	↓
1294	↓	↓	2.5	18.0	45.0	8.1	↓	↓	↓
1295	↓	↓	---	---	---	184.8	Off	↓	Water Only
1296	↓	↓	---	---	---	184.8	On	↓	Water Only
1297	↓	↓	10.0	11.0	110.0	184.8	Off	↓	Nozzle Heating
1298	↓	↓	5.0	10.0	50.0	184.8	↓	↓	↓
1299	↓	↓	2.5	10.0	25.0	184.8	↓	↓	↓
1300	↓	↓	10.0	10.0	100.0	184.8	On	↓	↓
1301	↓	↓	5.0	10.0	50.0	184.8	↓	↓	↓
1302	↓	↓	2.5	8.0	20.0	184.8	↓	↓	↓
1303	Crushed Silica	<38	10.0	13.0	130.0	184.8	Off	↓	↓
1304	↓	↓	5.0	10.0	50.0	184.8	↓	↓	↓
1305	↓	↓	2.5	10.0	25.0	184.8	↓	↓	↓
1306	↓	↓	10.0	10.0	100.0	184.8	On	↓	↓
1307	↓	↓	5.0	10.0	50.0	184.8	↓	↓	↓
1308	↓	↓	2.5	7.0	17.5	184.8	↓	↓	↓
1309	Blend #15	<20	10.0	11.0	110.0	184.8	Off	↓	↓
1310	↓	↓	5.0	10.0	50.0	184.8	↓	↓	↓
1311	↓	↓	2.5	10.0	25.0	184.8	↓	↓	↓
1312	↓	↓	10.0	10.0	100.0	184.8	On	↓	↓
1313	↓	↓	5.0	10.0	50.0	184.8	↓	↓	↓
1314	↓	↓	2.5	10.0	25.0	184.8	↓	↓	↓
1315	Crushed Silica	<38	5.0	10.0	50.0	None	Off	3	Velocity = 186 m/s
1316	↓	↓	10.0	5.0	50.0	None	↓	↓	↓
1317	↓	↓	10.0	10.0	100.0	None	↓	↓	↓

and 80 psig, both axial and radial pressure scans were conducted using the B-1B probe at these flow conditions. In addition to establishing the baseline pressure response, the scans also provide data on the positional sensitivity of the probe. Axial scans were conducted from distances of approximately 0.05 to 1.35-inches from the nozzle exit plane. Horizontal scans were conducted over a one inch span through the jet centerline at an axial position of one inch.

Figure 3-3 presents the axial scan results for the B-1B probe at a nozzle inlet pressure of 70 psig. Measured total and static pressures are shown as a function of axial position. Since the probe tip diameter is nearly 60% of the nozzle exit diameter, flow blockage effects appear to occur when the probe is near the nozzle. However, at axial distances greater than 0.4-inches, the total pressure is nearly constant at a value of approximate 8 psig. This value is in good agreement with the small probe centerline measurements shown in Figures 2-12 and 2-14. The static pressure measured with the B-1B probe shows a continuous decrease beyond approximate 0.4-inches. The static pressure, however, does not agree closely with the small probe measurements since the B-1B ADS static pressure ports are approximately 1.875 inches aft of the total pressure port at the probe tip. Although the static pressure values are not consistent with the total pressure measurements, they do provide a basis for assessing the effects of dusty flow on probe pressure response.

Horizontal pressure scans obtained with the B-1B probe at a nozzle pressure of 70 psig and at axial positions of 0.75, 1.0 and 1.25-inch are presented in Figure 3-4. Although the diameter of the total pressure port is approximately 0.3-inches, the B-1B probe measures nearly a constant pressure over a 0.35-inch span centered on the jet axis. The static pressure profiles show a similar span of approximately 0.3-inches where pressure values are relatively constant. The axial variation in static pressure profiles are consistent with the axial scan data shown in Figure 3-3. Thus, the total pressure response of the B-1B probe is relatively insensitive to positioning errors at a nozzle pressure of 70-psig and axial position of one-inch. Axial position error of up to ± 0.25 -inches and a horizontal error of up to ± 0.15 -inches will produce essentially the same total pressure reading.

Axial and horizontal pressure scans corresponding to a nozzle inlet pressure of 80 psig are presented in Figures 3-5 and 3-6. The results at this nozzle pressure condition are very similar to those at 70 psig. The axial variation in total pressure increases from approximately 6 psig at 0.2-inches to 10 psig at 1.0-inches. Again, the pressure at one-inch is in good agreement with the small probe data presented in Figures 2-12 and 2-15. Static pressure variations are very similar to results obtained at 70 psig. The pressure profiles presented in Figure 3-6 show a little greater variation near the centerline than the results at 70 psig; however, there still exists a region of relatively uniform pressure within approximately ± 0.15 -inches of the jet axis.

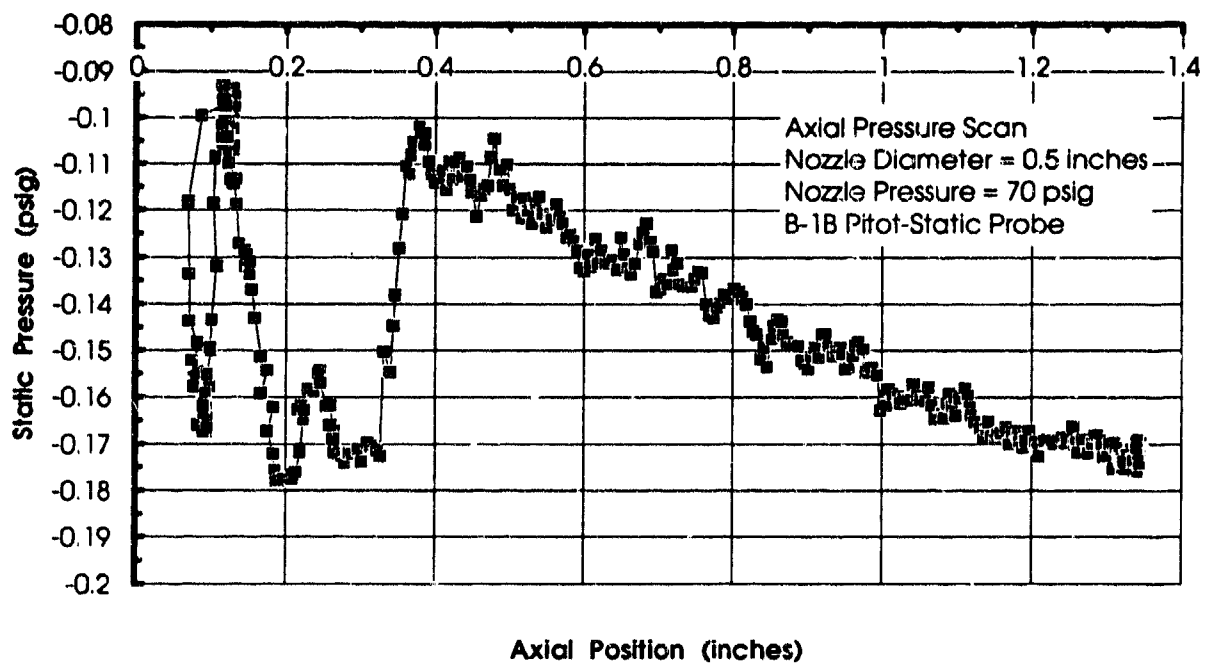
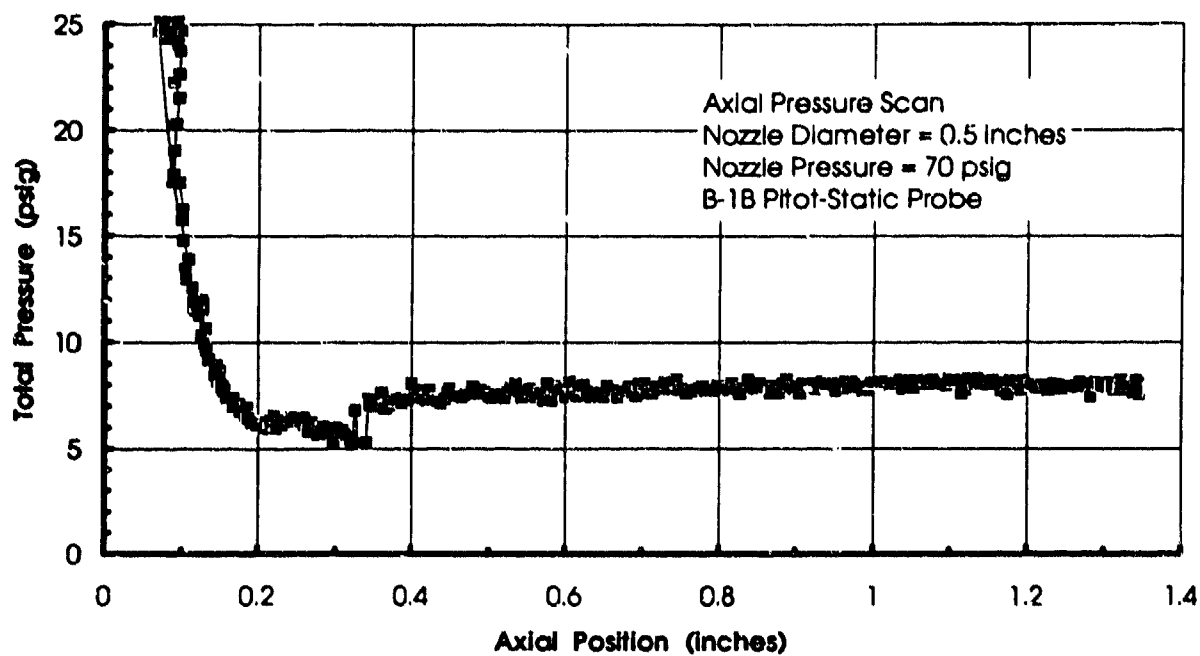


Figure 3-3. Axial pressure scan with B-1B ADS probe - $P_n = 70$ psig.

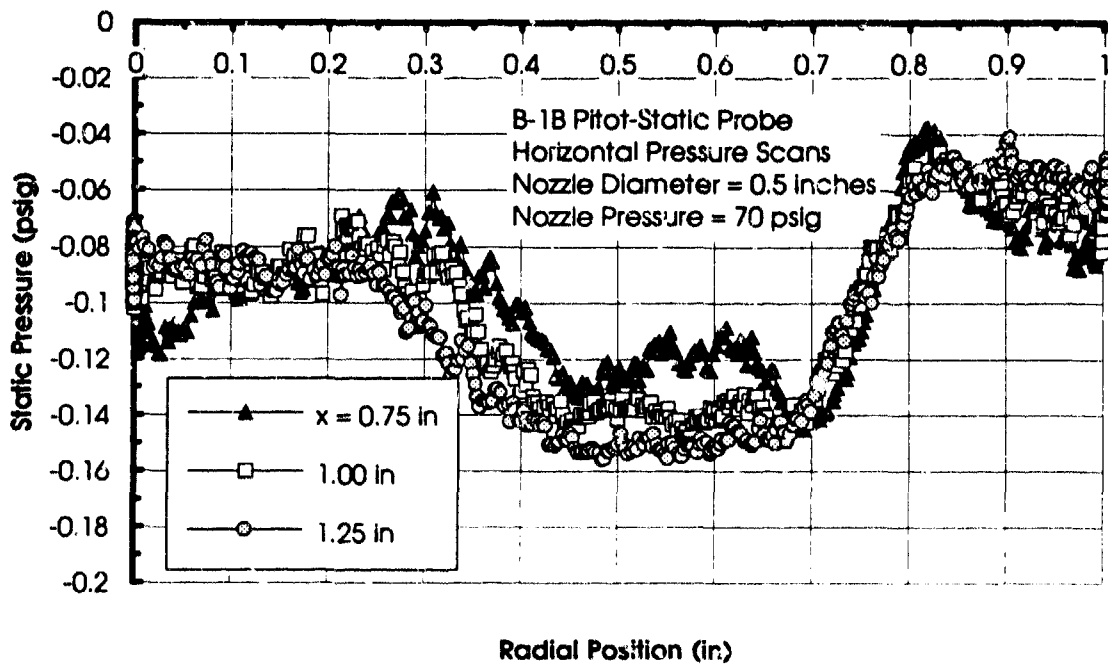
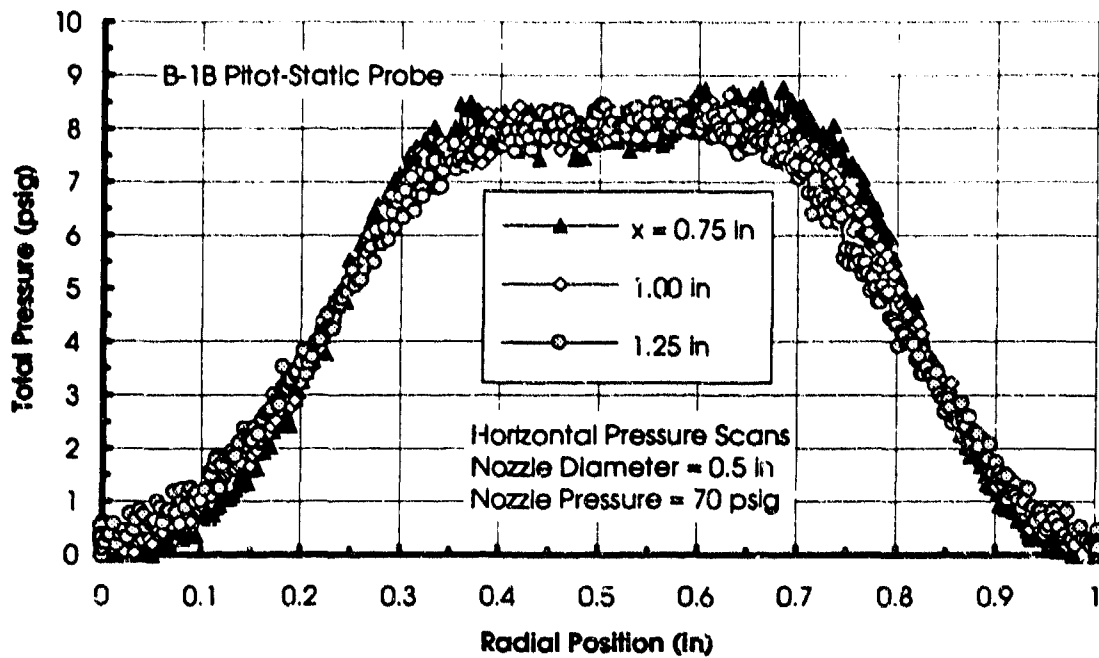


Figure 3-4. Horizontal pressure scans with B-1B ADS probe - $P_n = 70$ psig.

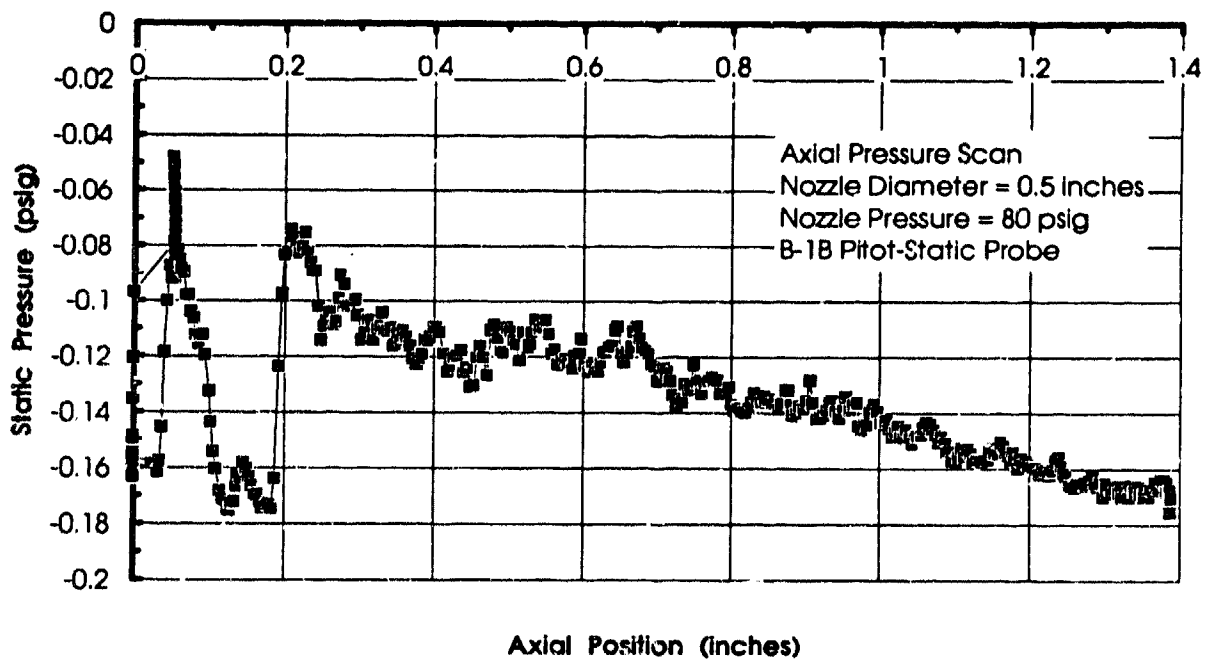
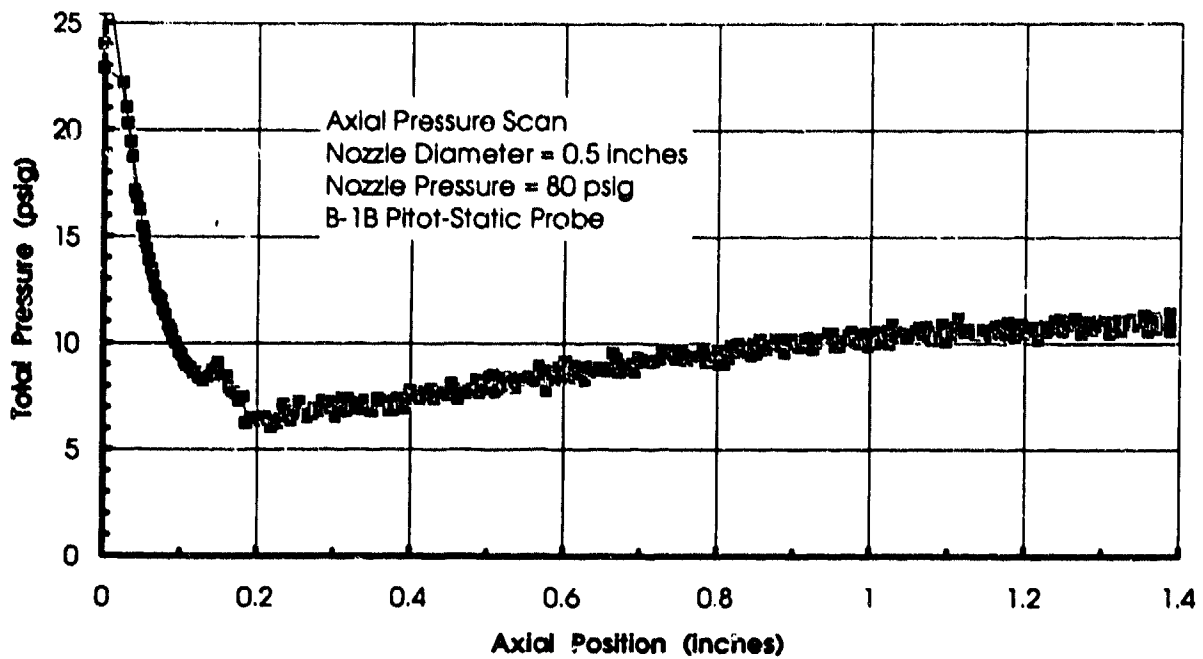


Figure 3-5. Axial pressure scan with B-1B ADS probe - $P_n = 80$ psig.

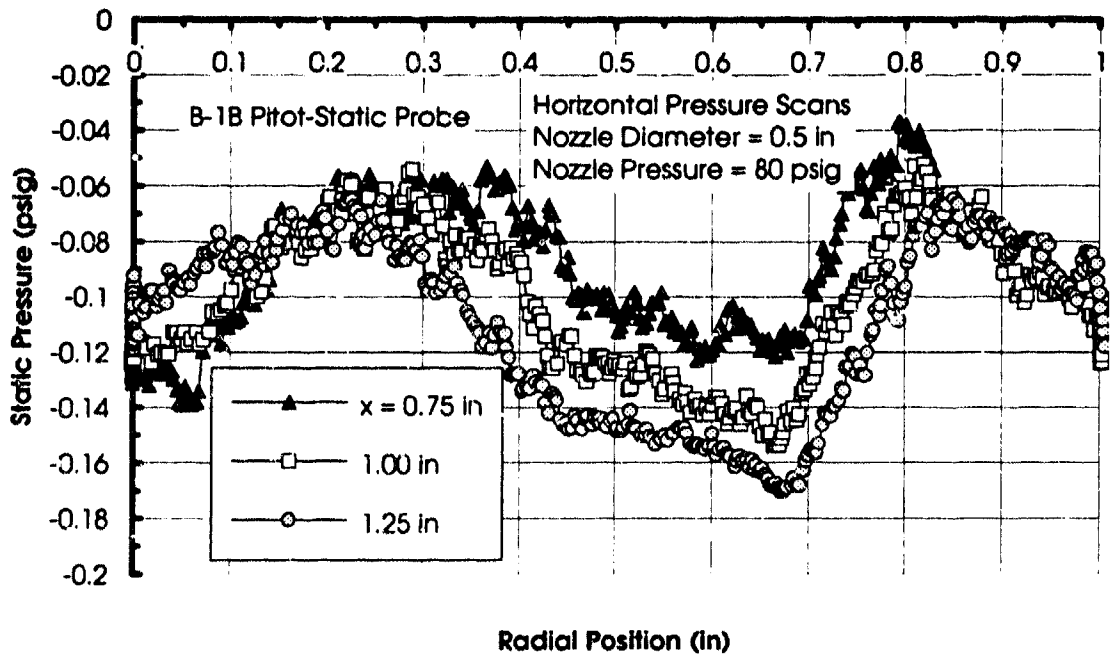
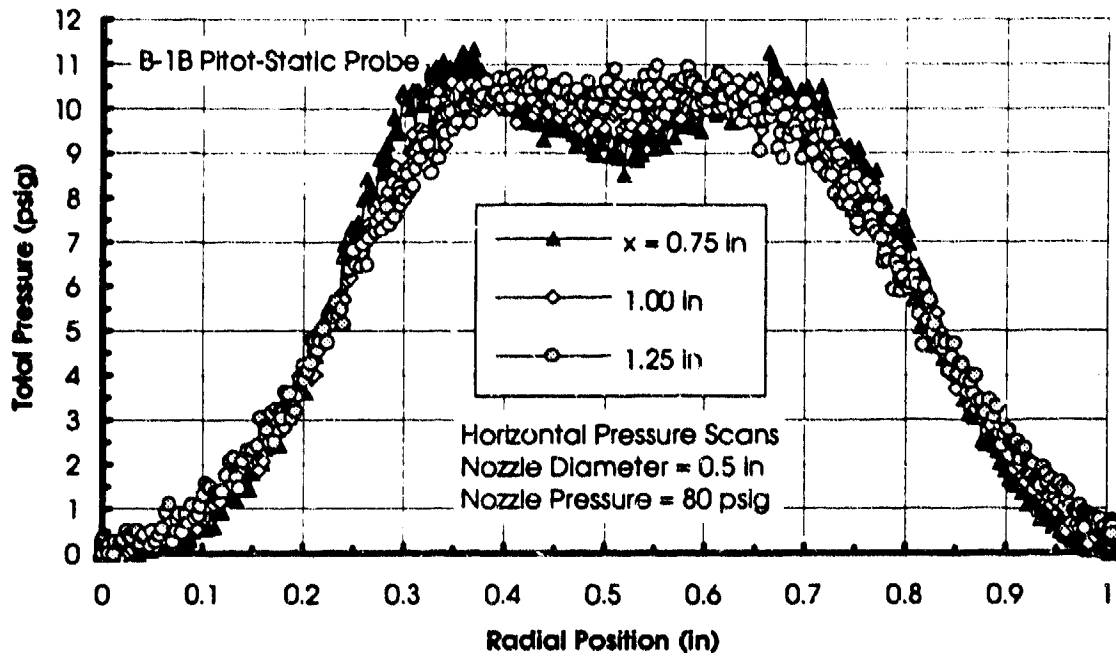


Figure 3-6. Horizontal pressure scans with B-1B ADS probe - $P_n = 80$ psig.

Axial and radial pressure scans were not conducted with the B-1B probe at the lower velocity condition (nozzle inlet pressure of 40 psig) due to limited time and resources. Pre-dust exposure measurements associated with the three dust exposures (Runs 1315 through 1317) were used to assess the baseline pressure readings for the B-1B probe. The results for these three runs were essentially identical with a total pressure of 2.70 ± 0.15 psig and a static pressure of -0.010 ± 0.005 psig. In fact, there was no noticeable effect when the particles were turned on. Pressure data obtained with the small pitot static probe at the 40 psig operating condition were presented above in Figures 2-12 and 2-13. The pressure measurements obtained with the B-1B probe were in good agreement with the centerline total pressure in Figure 2-12. The pressure scans taken with the small probe and shown in Figure 2-13, however, were approximately 0.4 psig lower than either the small probe data in Figure 2-12 or the B-1B data obtained in Runs 1315 through 1317.

In order to evaluate the effect on water injection on the jet flowfield and resulting pitot-static pressure measurements, separate exposures of the B-1B probe to water only environments were conducted as part of the data runs. A total of three water only calibration exposures were conducted. These were run numbers 1259, 1295 and 1296 and are listed in Table 3-2. Run #1259 was conducted with the lower water flow rate (8.1 ml/min) at a nozzle operating pressure of 70 psig. This nozzle pressure corresponds to the conditions used for the Blend #15 and the $<38 \mu\text{m}$ crushed silica runs. Figure 3-7 presents the total and static pressure measurements for Run #1259. The gas flow was established with dry GN_2 and the water flow was initiated at 81-sec into the run and continued for approximately 10 minutes. As seen in the figure, the total pressure which varied between 9 and 9.5 psig with gas flow only dropped to between 8 and 9 psig with the initiation of water flow. After 5 minutes, the mean total pressure was approximately 8 psig with a significant and periodic variation which was due to pulsations from the water injection pump. This pattern was consistent and continued through the completion of the run at 670 seconds. The static pressure which was consistent with the dry flow calibration values also showed the same periodic variations as the total pressure from approximately 3 minutes to the completion of the run. Thus, the lower water flow rate does not have a significant effect on the B-1B probe response other than introducing more noise into the signal. Mean pressure values are approximately the same as shown in Figures 3-3 and 3-4 for a position on the jet axis centerline at 1-inch from the nozzle exit.

The pressure response measured with the B-1B probe at the higher water flow rate (184.8 ml/min) was evaluated in Run #1295 and #1296. These runs were at a nozzle operating pressure of 80 psig which corresponds to the condition used for the 53-74 μm crushed silica. Run #1295 was run without probe heating while Run #1296 was with probe heating. Since there was no significant difference in the pressure measurements between the two runs, only the results for Run

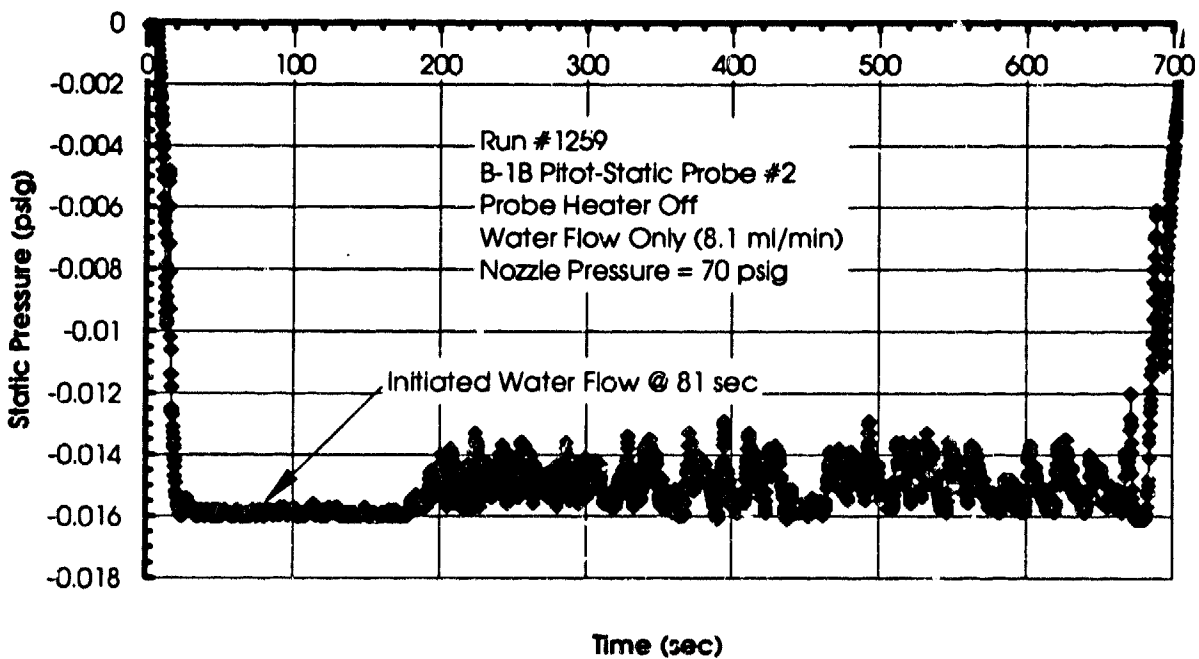
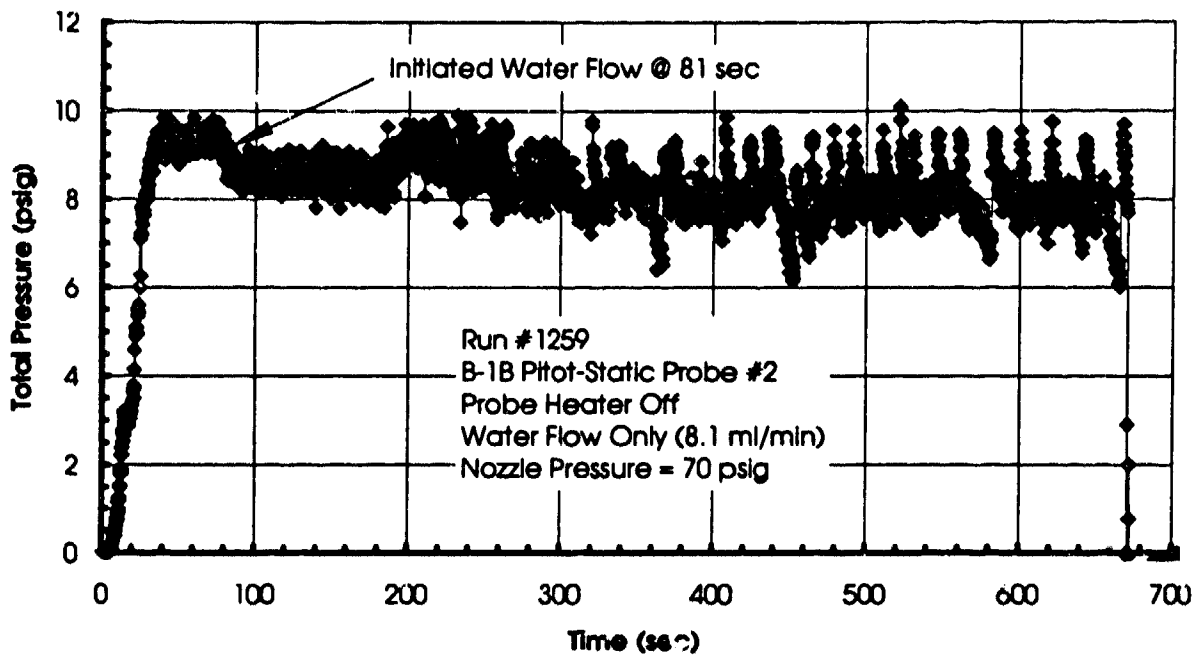


Figure 3-7. B-1B ADS probe baseline pressure response - low water flow.

#1296 are included here. Figure 3-8 presents the pressure histories for Run #1296. As shown in the figure, the total pressure trace indicates a significant drop from 10 psig to approximately 7.5 psig when the water flow was initiated. The total pressure remained constant at that level throughout the 5-minute exposure. The static pressure was also constant throughout exposure with water injection; however, that appears to be due to reaching the minimum range of the pressure transducer. This was also observed during the initial portion of the static pressure history in Figure 3-7.

Therefore, the total pressure response with the high water flow rate is reduced from the dry air calibration values. The reduction in jet gas velocity due to droplet drag effects is the likely cause. A jet of water was seen flowing from the probe drain hole. There were no indications of water being transmitted beyond the probe since none of the inline filters showed an increase in weight; this is based on pre- and post-test measurements.

3.4 DRY PARTICLE FLOW RESULTS.

The initial phase of the B-1B ADS evaluation involved the response of the pitot-static probe to dry particle flows where the transport gas was dry GN₂ and no water injection was used. These exposures consisted of the nominal velocity condition (Run #1226 through #1256) plus three runs at a reduced velocity (Run #1315 through #1317). The specific particle mass flow rates and exposure durations are presented in Table 3-2. Two dust flow rates (either 5 or 10 gm/min) were used in conjunction with exposure times of 5 and 10 minutes. Thus, the total amount of dust expended during the exposures was either 50 or 100 grams. All of the nominal velocity runs were conducted using probe #2 (right side configuration) with no probe heating or water injection while probe #3 (left side configuration) was used for the low speed exposures.

Results of the ADS probe evaluation in dry particle flow conditions consist of two data sources. These are the pressure responses measured during the exposure and the pre- and post-test weight data obtained from the probe and inline particle filters. The pressure results included the total pressure, static pressure and the average of the two angle-of-attack (AOA) pressure inputs. Pressures were recorded during the complete test including clear GN₂ startup flow, particle flow initiation and shut down. The weight data and visual inspection of the components provided particle collection results for the probe and the various pressure measurement lines.

3.4.1 Pressure Response Data.

A review of the recorded pressure histories and the post-test observations indicated that there was no significant degradation in the performance of the ADS probe in the dry flow

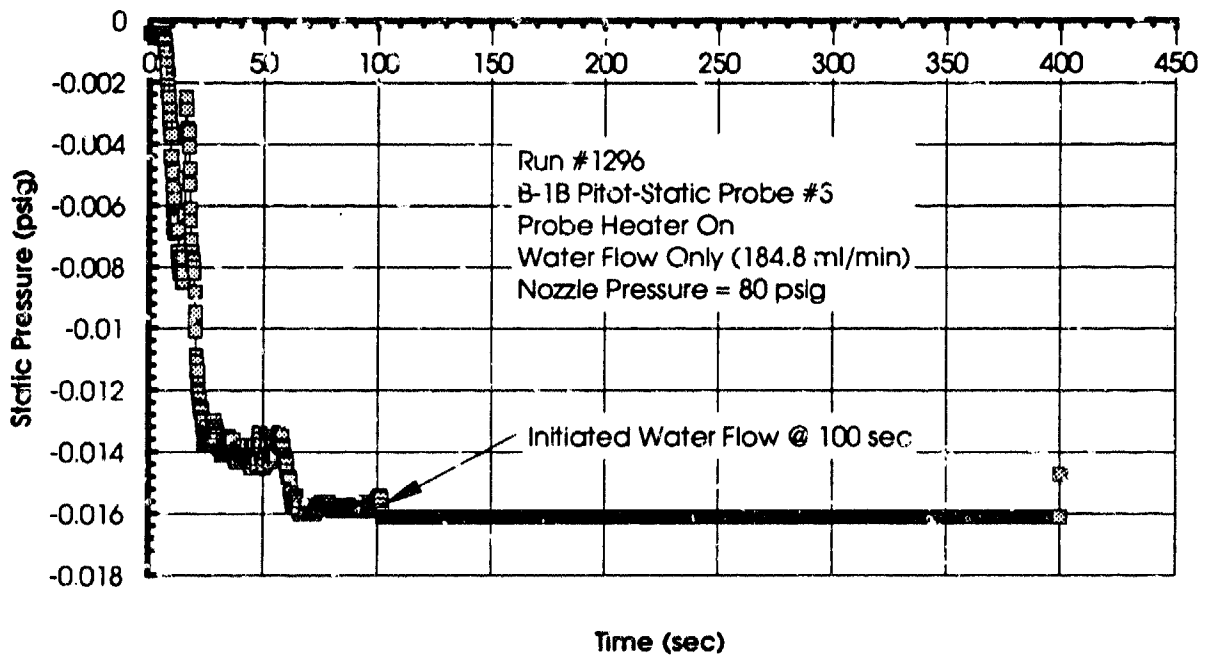
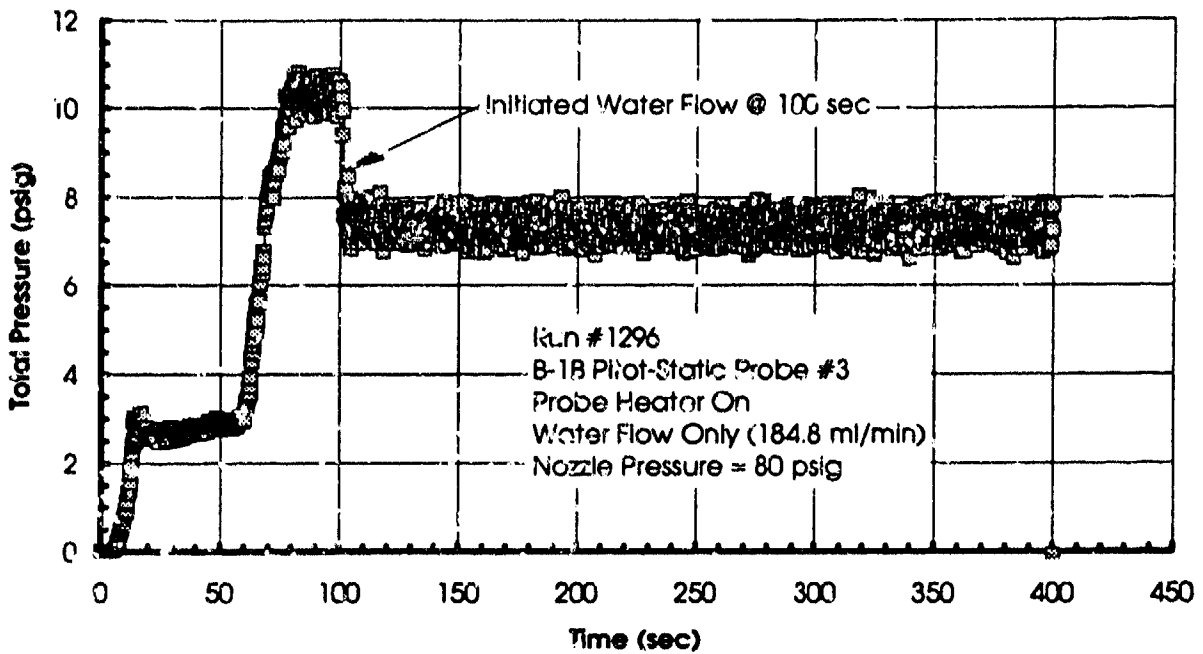


Figure 3-8. B-1B ADS probe baseline pressure response - high water flow.

environments. There was no loss in pressure which would indicate significant blockage or bridging within the probe. Typical pressure histories for the nominal velocity condition of 288 m/s are presented in Figures 3-9 through 3-11 for the three particle type/sizes. Figure 3-12 presents pressure histories for the low velocity (186 m/s) test condition which was conducted with the <38 μm crushed silica. All four runs were for a particle flow rate of 5 gm/min. However, based on an examination of the 10 gm/min flow rate data, no differences were found in pressure response between the two particle flow rates. Each of the four figures shows total, static and AOA pressure histories.

The pressure histories for the Blend #15 and the <38 μm crushed silica which are presented in Figures 3-9 and 3-10, respectively, show excellent agreement with calibration results for the 70 psig nozzle inlet pressure. Total pressure values were approximately 8 psig throughout the exposure while the mean static pressure was in the -0.015 to -0.020 range. The pressure histories for the 53-74 μm crushed silica run presented in Figure 3-11 correspond to a 80 psig nozzle inlet pressure and were also in good agreement with the calibrations results presented in Figures 3-5 and 3-6. Total pressure values were approximately 10.5 psig and mean static pressure was in the same range as the results for the 70 psig nozzle pressure. The AOA pressure for all three runs was approximately 0.01 psig.

Except for the AOA pressure in Figure 3-9, the resolution of the static and, particularly, the AOA pressure data was poor. This was due to a lack of high sensitivity transducers in the early stages of testing. Higher sensitivity transducers became available as the test series progressed. Since the first priority was accurate total pressure measurements, the specific values of the static and AOA pressures were not as important. Since static and AOA pressures were not consistent with total pressure (or each other) due to probe size and jet flow characteristics, the primary interest in these secondary pressure measurements was to monitor variations which may correlate with particle ingestion effects and indicate probe performance degradation.

The pressure response of the #3 B-1B ADS probe at the lower velocity test condition presented in Figure 3-12 shows no degradation in pressure with dust particle flow. The total pressure is essentially constant over the duration of the exposure with no difference seen between the start up (clear GN_2) flow and the initiation of the particle flow. The static pressure shows some variation with the particle flow; however, it is relatively small. The AOA pressure is slightly negative at this lower nozzle pressure and hence lower velocity test condition. Since Run #1315 was conducted late in the test program, 0 to 2-in H_2C (0.074 psig) pressure transducers were used for both the static and the AOA pressure measurements. Pressure response results similar to these were also obtained for the 10 gm/min particle flow rate tests conducted in Run #1316 and #1317.

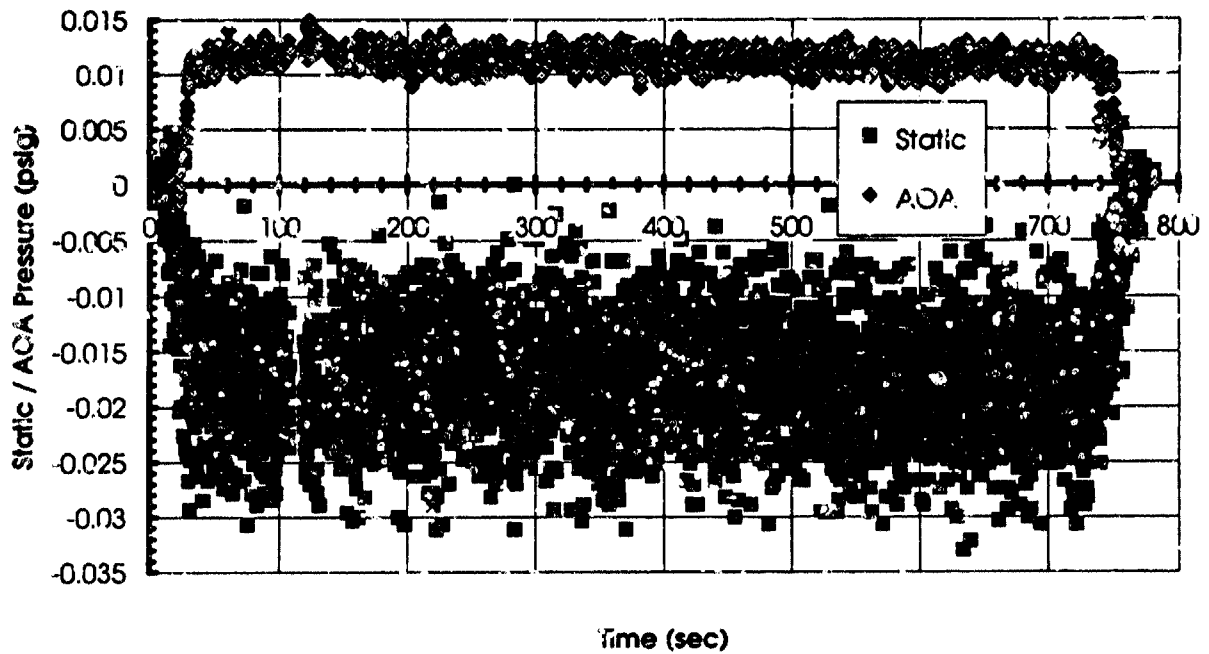
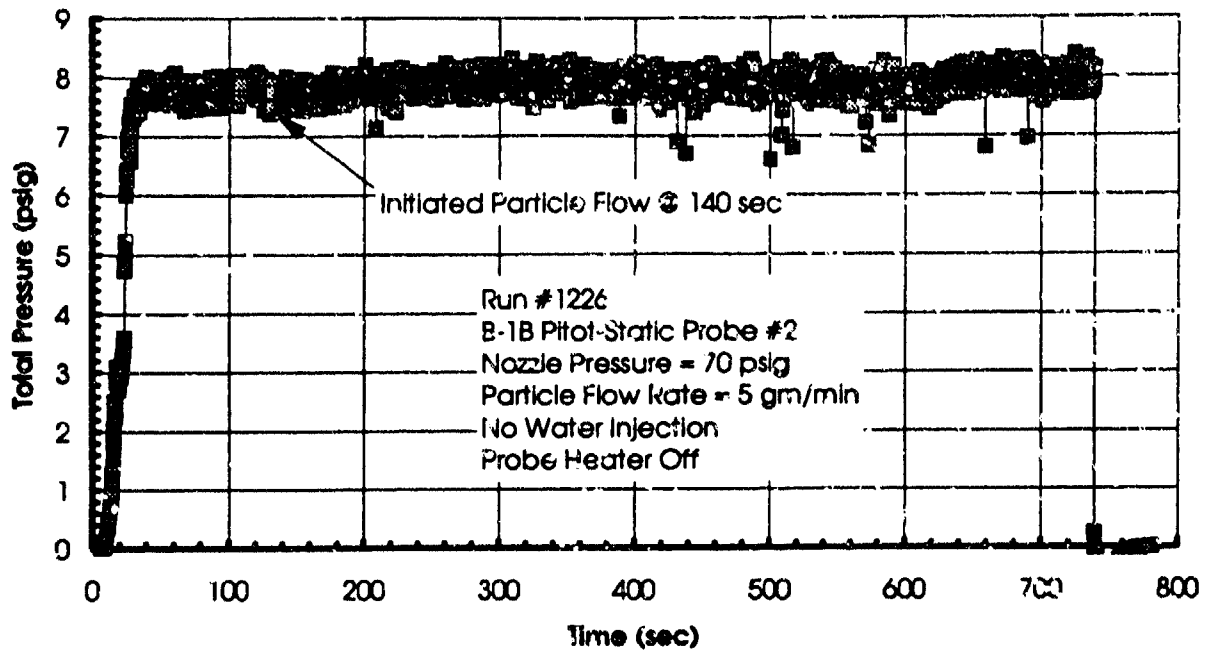


Figure 3-9. B-1B ADS pressure response with dry flow - Blend #15.

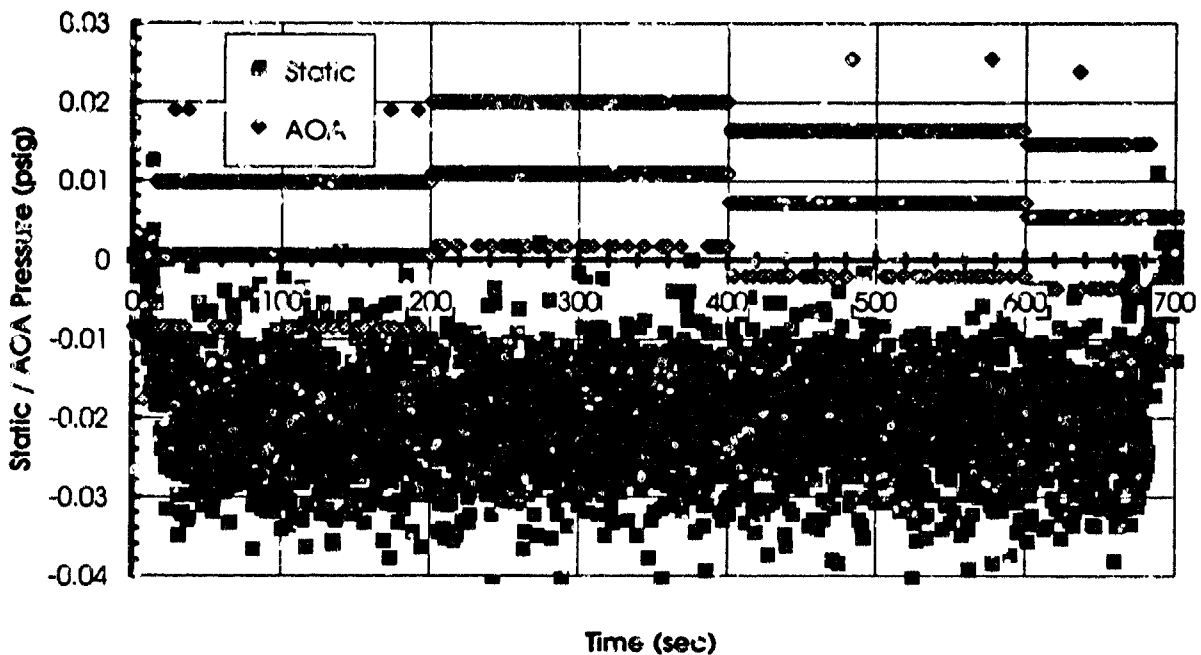
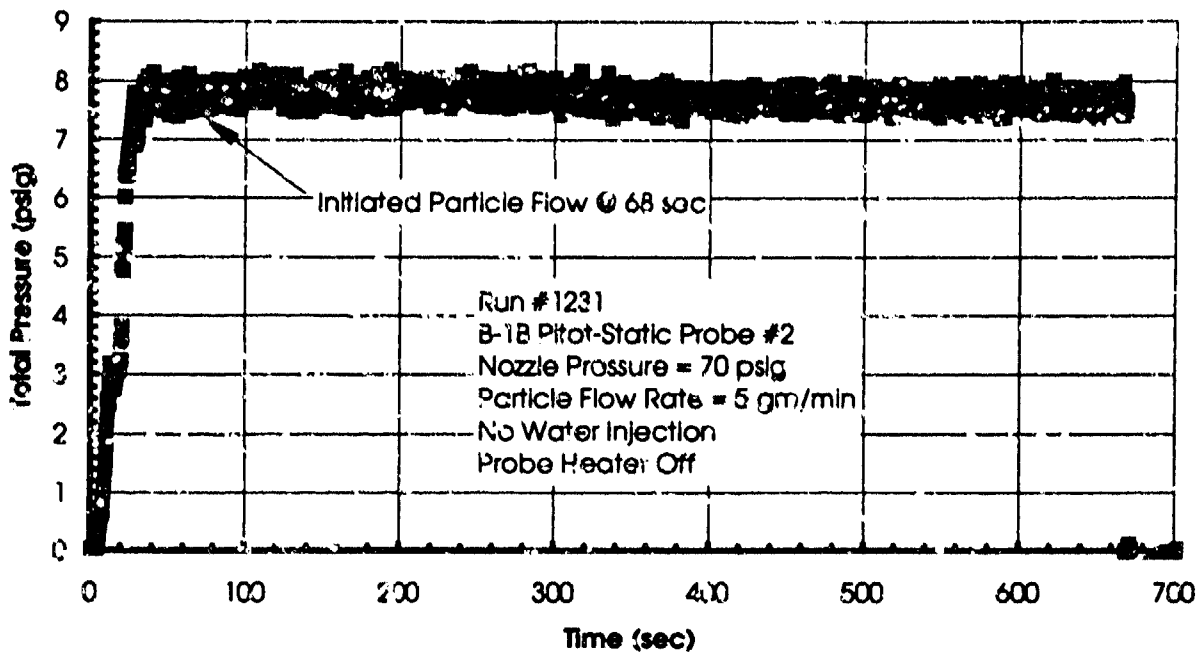


Figure 3-10. B-1B ADS pressure response with dry flow - crushed silica (<38 microns).

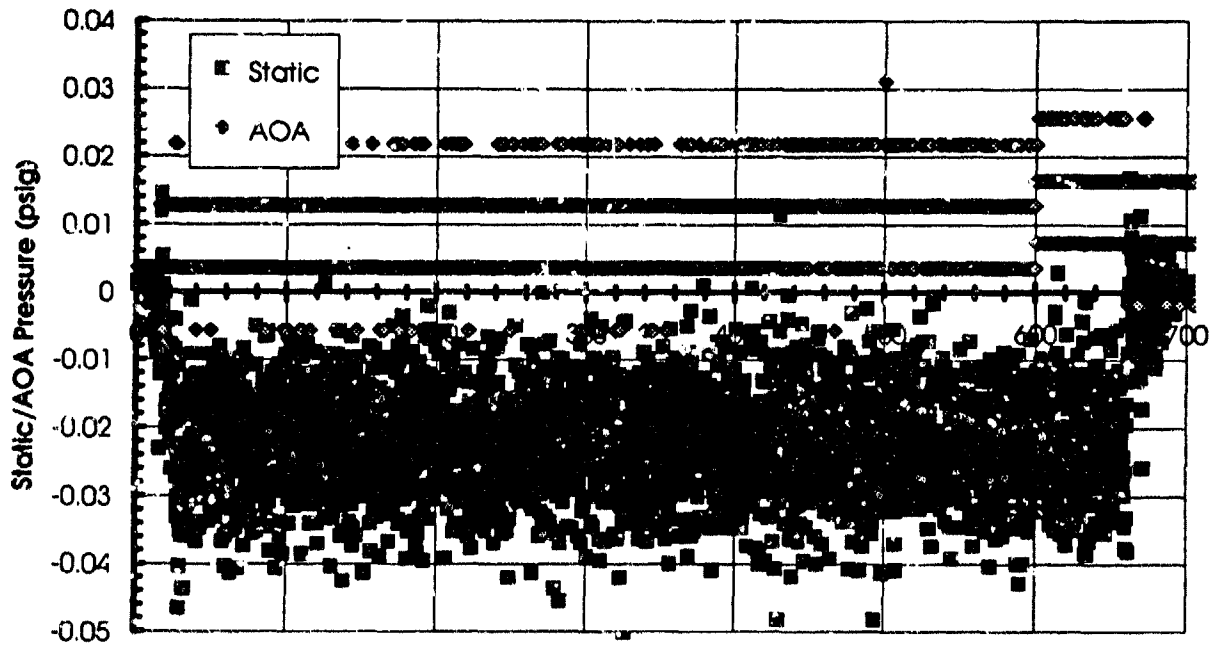
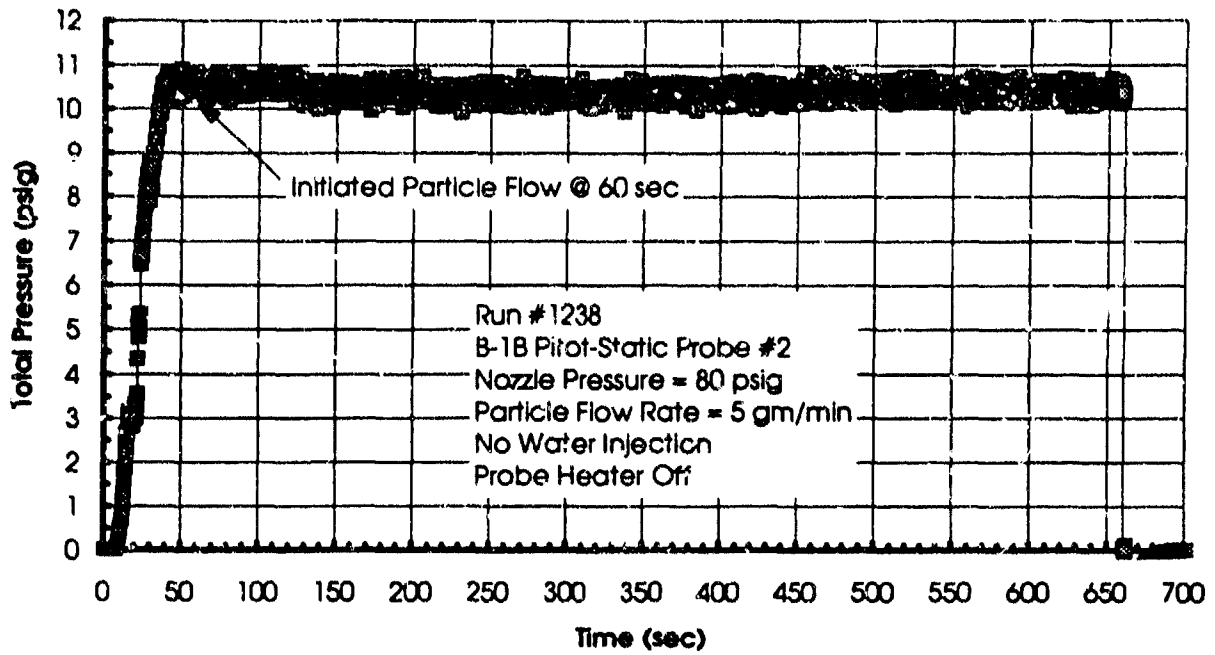


Figure 3-11. B-1B ADS pressure response with dry flow - crushed silica (52-74 microns).

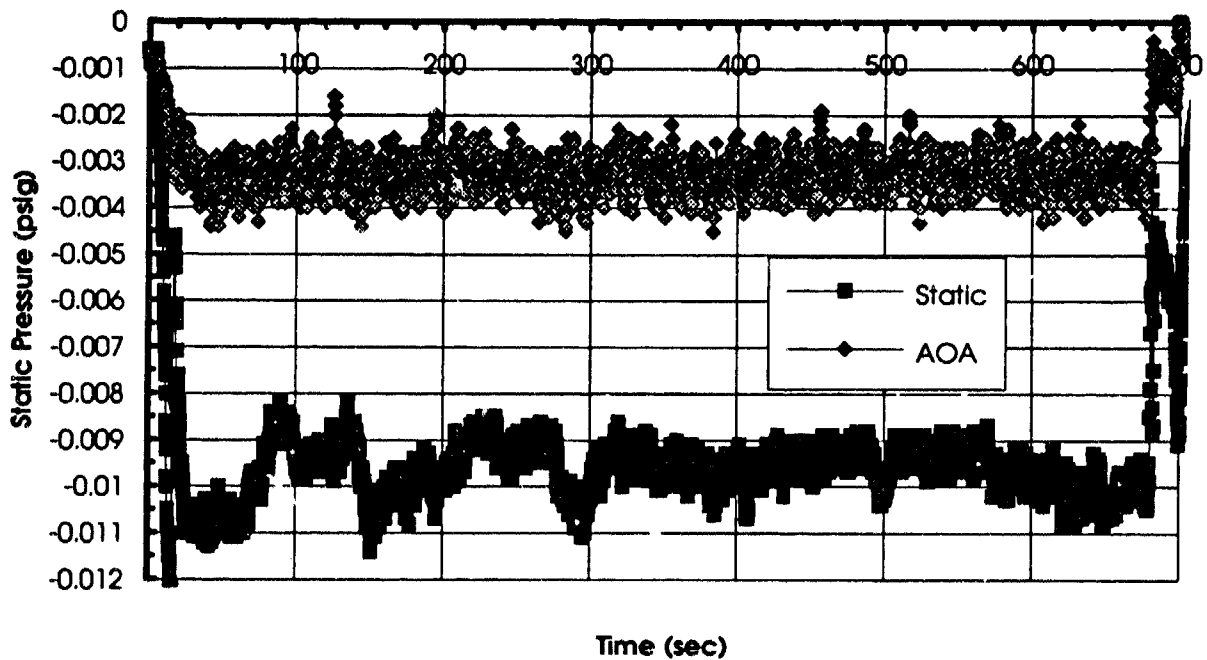
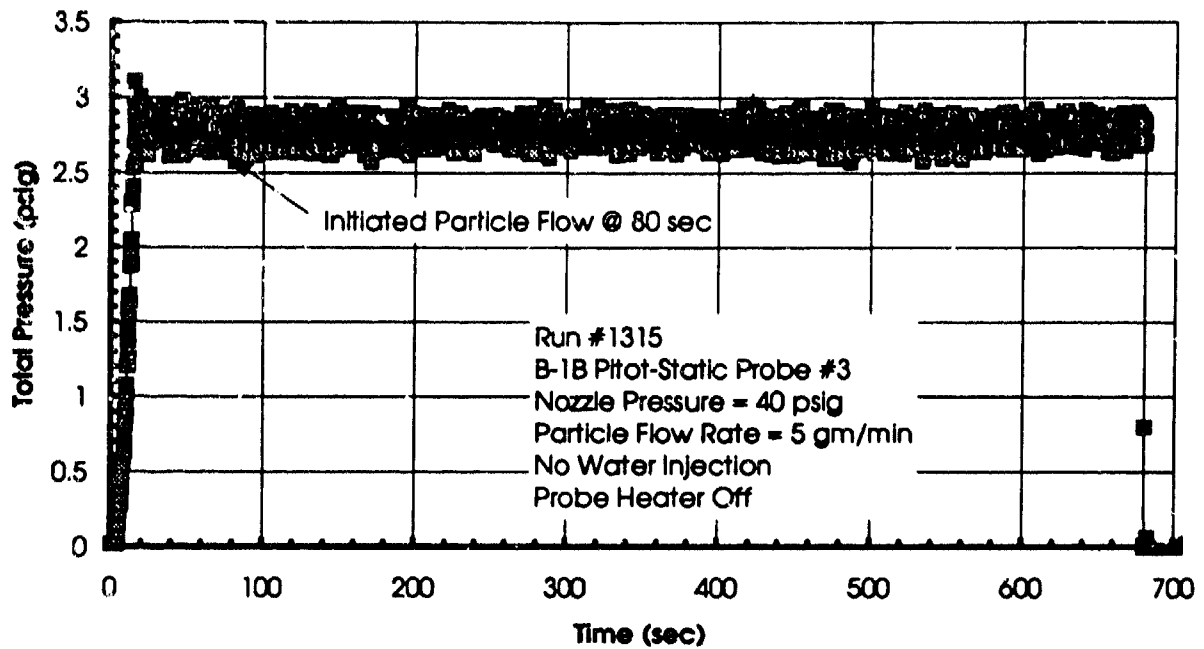


Figure 3-12. B-1B ADS pressure response with low velocity - crushed silica (<38 microns).

3.4.2 Dust Ingestion Data,

The B-1B pitot-static probe and the inline particle filters were weighted before and after each exposure in order to determine the mass of dust particles collected during the run. Three identical dust filters were used for these evaluations. These were mounted on the total, static and AOA pressure transmission lines just ahead of the transducers. A fuel filter, shown in Figure 3-13, consisting of metal canisters with a paper filter element was used to collect dust particles. These particular filters (Fram Part # G-15) were inexpensive, readily available and had been used successfully in a previous dust flow experiment conducted in a large wind tunnel (Reference 5).

The dry particle flow pre- and post-test weight data for the B-1B pitot-static probe and the inline particle filters are presented in Table 3-3. The weight data are in grams and are listed by facility run number. In addition to the pre- and post-test weights of each component, the change in weight (post-test minus pre-test) is also included in Table 3-3. Data for the total, static and AOA line filters are identified as P-T, P-S and AOA filter weight, respectively.

The key features of the weight data presented in Table 3-3 are (1) the significant variation in run-to-run weight change experienced by the probe and total pressure filter and (2) the total lack of any significant weight gain associated with the static and AOA filters. In nearly all cases, the static and AOA filters experienced a very slight decrease in weight which may represent

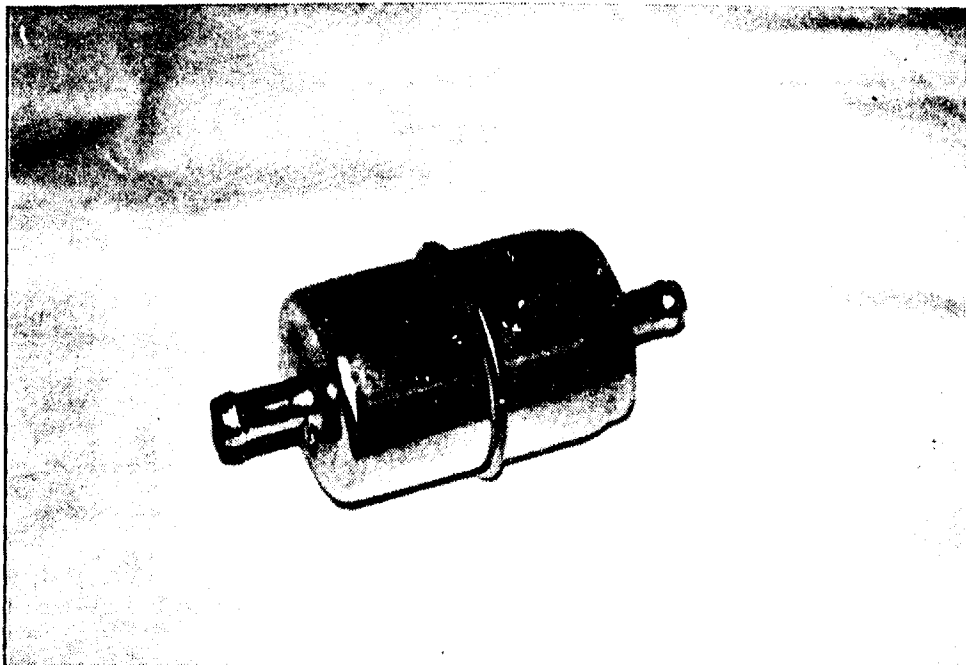


Figure 3-13. Inline filters use for particle collection.

moisture loss from the filter paper due to exposure to the dry GN₂ transport gas. The pitot-static probe gained weight for all runs where the probe was exposed to a particle flow. The five runs where the probe was pre-filled with dust and exposed to a clear GN₂ flow resulted in a loss in net probe weight due to the removal of particles during the run. In these five runs, a significant portion of the particle mass was flushed into the total pressure line and ended up in the filter. This is confirmed by the large increase in weight experienced by the total pressure filter in these runs. For the runs where the probe was exposed to a particle flow, the total pressure filter gained weight in all cases except for the low velocity condition (Run #1315 and #1317). This weight gain ranged from approximately 0.2 to 2 gms depending on exposure conditions. For the low velocity runs, none of the filters collected any significant amount of dust.

Thus, the only effects of dry dusty flow on the B-1B ADS appears to be the ingestion of dust into both the probe and the pressure line leading to the total pressure transducer. Dust collection in the probe did not appear to affect the pressure output performance of the probe. The effect of dust particles in the total pressure line is not known. These particles will likely collect in the pressure transducer. Since the necessary hardware and technical support for reading the B-1B pressure transducer output could not be obtained for this evaluation, effects of dust particles on the B-1B transducer will have to be assessed separately. The transducers used in these laboratory evaluations were not affected by dust particles since they were protected by the inline filters. Thus, dust ingestion effects must be considered as a potential hazard to the ADS system until their effects on the B-1B pressure transducer can be assessed.

Dust ingestion effects are summarized in Figures 3-14 and 3-15. Figure 3-14 presents a correlation of the total particle mass collected in the system (i.e. probe and line filters) versus the total mass of dust expended during the exposure (particle flow rate x exposure time). As shown in the figure, the total mass collected in the probe and filters is essentially a linear function of the total particle mass expended. The rate at which mass is collected appears to vary with particle type/size and/or nozzle operating conditions (since the 53-74 crushed silica utilized 80 psig nozzle pressure). Also, the efficiency at which the ADS probe collects particles is surprising. For example, approximately 28% of the total <38 μm crushed silica expended during a run was collected in the ADS system. The linear equations corresponding to the curvefits are included in the plot.

The effect of particle velocity on dust ingestion is examined in Figure 3-15. This figure presents a plot of collected mass versus total expended mass for the <38 μm crushed silica particles at both the nominal 288 m/s and the lower 186 m/s. As seen in the figure, the total mass collected at the lower velocity condition is approximately half that of the higher velocity although the same amount of particle mass was expended. The equations describing the linear fits are also included.

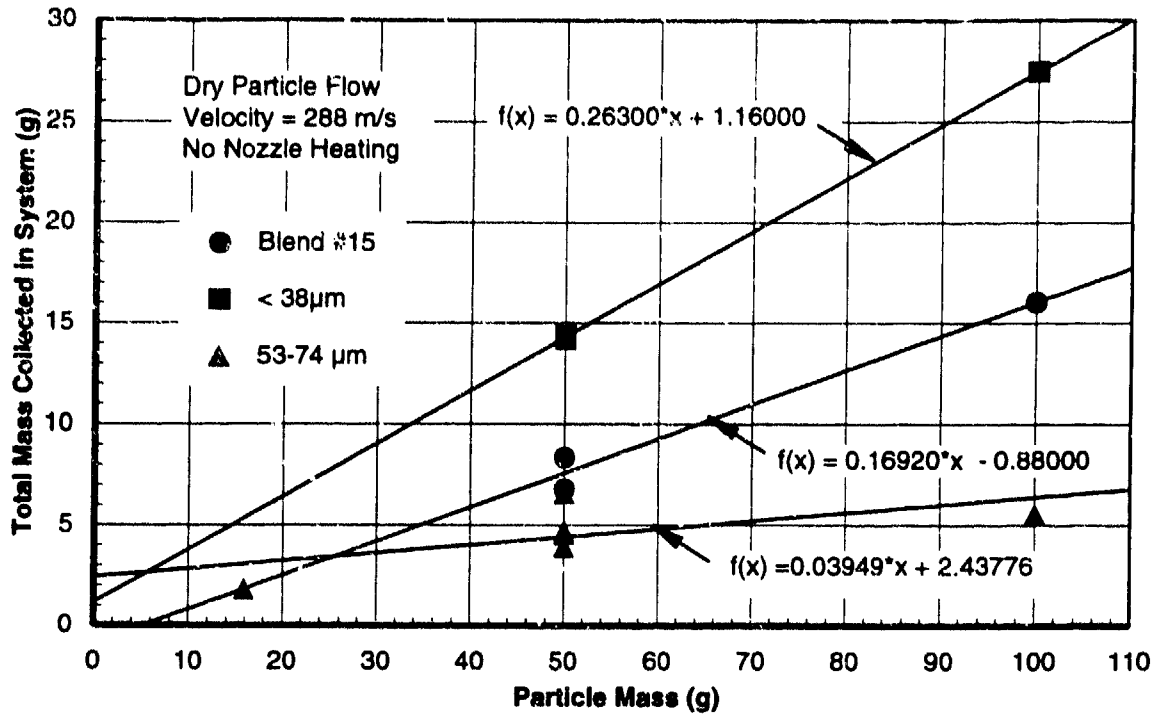


Figure 3-14. Total ingested dust mass correlations - dry flow.

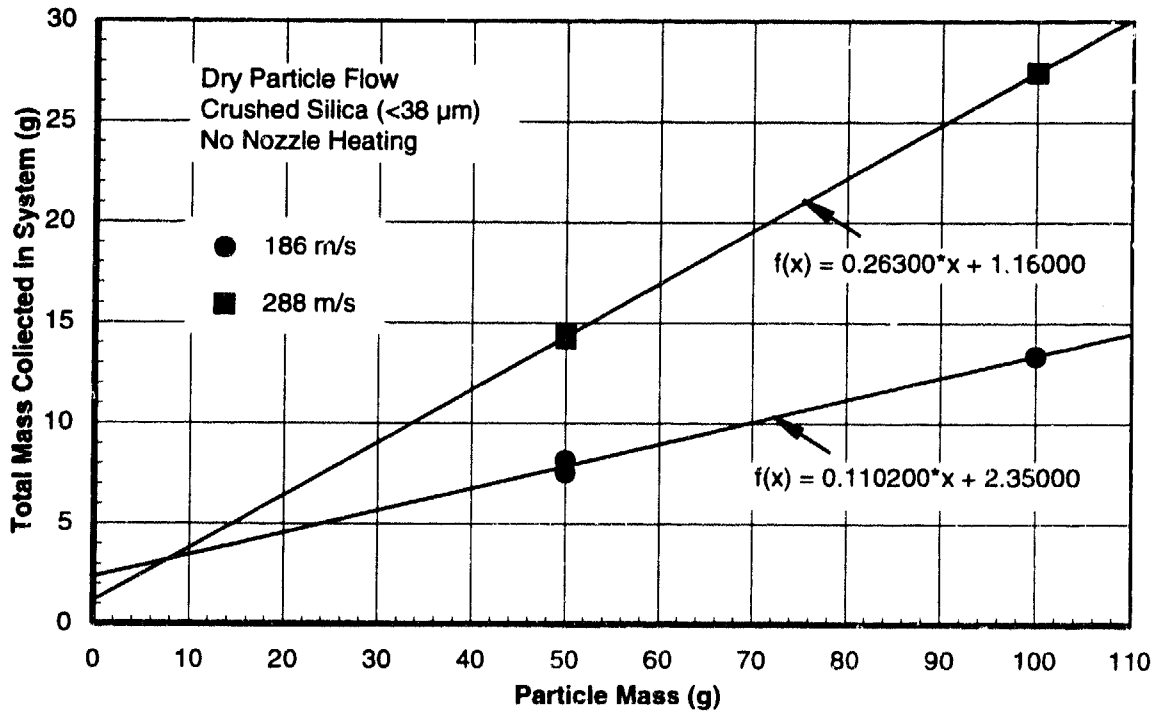


Figure 3-15. Effect of particle velocity on mass ingestion.

3.5 WET PARTICLE FLOW RESULTS.

The primary testing effort associated with this evaluation of the B-1B air data sensor involved particle flows with water injection. These wet particle flows were designed to simulate natural moisture/rain that is expected to be present in the dust environments. The same basic variation in particle type/size, flow rate and exposure duration used in the dry flow evaluations were repeated with two levels of water injection. Additional runs were also added to assess probe heating effects and to investigate a lower particle flow rate (i.e. 2.5 gm/min). All wet flow testing was conducted at the nominal particle velocity of 288 m/s. For the initial series of exposures, a nominal water flow rate of 8 ml/min was used while the remaining series of exposures were conducted with a much higher water flow rate of approximately 185 ml/min. The specific particle mass flow rates, water flow rates and exposure durations are presented in Table 3-2.

The test configuration used for the wet flow evaluations was modified slightly from that used for the dry particle flows. The probe position and orientation were the same; however, a sheet metal shroud was designed and installed around the aft portion of the probe. The purpose of the shroud was to collect most of the water/dust spray created by the expanding jet. The facility dust collector was connected to the shroud in order to provide a flow and remove any particles that did not deposit on the shroud surfaces. The recirculation of the flow surrounding the jet boundary resulted in a fine spray of water and dust being deposited on the nozzle and LDV optics. The latter were covered for protection which precluded making real time particle velocity measurements.

A photograph of the ADS probe mounted in the test facility is presented in Figure 3-16. The photograph was taken just following an exposure to a wet particle flow. The aluminum tape, which is visible in the photograph, was placed over the total pressure port immediately following the particle flow shut down. This helped prevent loss of water or dust from the probe during the jet flow shut down and subsequent probe removal. Clear plastic covering on the LDV optics and surrounding area are also visible.

Differences between the wet and dry flow exposures were dramatic. At the lower water flow rate of 8 ml/min, consistent blockage or bridging of the total pressure port of the B-1B pitot-static probe was observed in conjunction with a complete loss in total pressure output (i.e. zero psig reading). In all but one case (Run #1264), once the total pressure port was blocked and pressure response lost, there was no recovery. Continued exposure failed to clear the probe. However, when the water flow was increased to the 185 ml/min, no probe blockage or loss in pressure output were observed. In most of these cases, the high water flow rate appeared to flush the ingested dust out the probe drain hole with no dust or water being transmitted to the pressure

lines, filters and transducers. However, there were some cases involving the small Blend #15 particles where the drain hole became blocked. In these cases, water and dust were diverted into the total pressure line with the associated flooding of the pressure line and dust filters. No significant degradation in pressure was observed for the static and AOA outputs.

Results of the ADS probe evaluation for wet particle flow conditions consisted of two primary data sources. These were (1) pressure response measurements during the exposure and (2) pre- and post-test weight data obtained from the probe and inline particle filters. These measurements were augmented with visual inspection of the probe and pressure lines to identify any evidence of blockage or other forms of degradation. The pressure results included the same data as obtained for the dry particle flow exposures which were total pressure, static pressure and the average of the two angle-of-attack (AOA) pressure inputs. The weight data and visual post-test inspection of the components provided particle and water ingestion results for the probe and various pressure measurement lines. The pressure response data as well as the dust/water ingestion measurements are discussed in the following subsections.

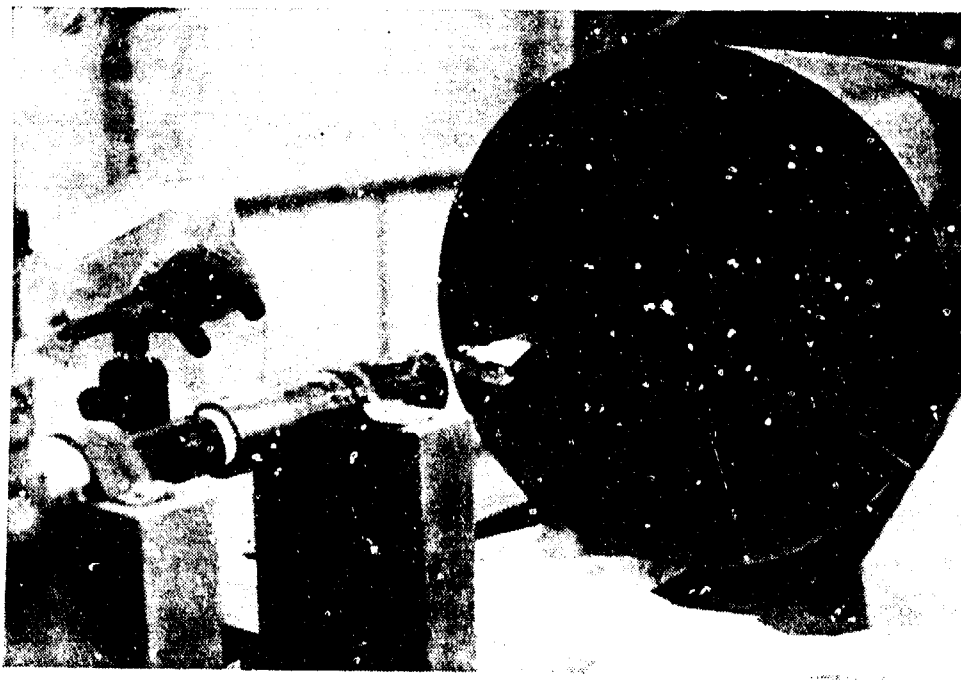


Figure 3-16. Wet flow test configuration.

3.5.1 Pressure Response Data.

A total of 35 runs were conducted with particle flow accompanied by water injection at a rate of 8 ml/min. Of these runs, 24 runs resulted in plugging or blocking of the total pressure port and a loss in total pressure output while several other runs produced only a temporary decrease in total pressure. The runs where no significant pressure degradation occurred corresponded to the lower particle flow rates and suggests that longer exposure times (if they were possible) may have produced plugging. As noted above in Section 2.5.1, it was necessary to heat the nozzle during water injection runs to prevent ice buildup in the nozzle. The initial 10 runs with water injection and dust flow were conducted without nozzle heating. These included Run #1257 and Run #1260 through #1268. Nozzle heating was utilized on the remaining 25 runs of which 19 experienced probe plugging and total pressure loss. These 19 runs included several with low particle flow rates of 2.5 g/min. The runs with nozzle heating are believed to represent the higher quality data.

Typical pressure histories for a run with blockage and pressure loss is presented in Figure 3-17. This corresponds to Run #1269 which utilized Blend #15 at a particle flow rate of 5 gm/min for an exposure time of 5 minutes. As illustrated in the figure, the measured total pressure is flat and stable for the first minute of exposure then experiences a slight decrease (from 8 to 7 psig) over the next 15-sec. This is followed by a sharp drop from approximately 7 psig to zero in about 10-sec. This sharp drop in total pressure was seen in all of the runs where plugging of the probe occurred. The static and AOA pressure generally did not show any consistent trends with particle buildup and blockage of the probe. Typically, static and AOA pressure outputs did not respond strongly as will be seen in some of the later figures. However, the AOA pressure in Figure 3-17 did show a sharp increase and then a drop in conjunction with the loss of total pressure. Similar pressure histories were obtained for runs with <38 μm and 53-74 μm crushed silica and are presented in Figures 3-18 and 3-19. Both of these runs show the total pressure output dropping sharply to zero with the blockage of the total pressure port. This occurred while the static and AOA pressure responses remained essentially unchanged.

The response characteristics for those runs which experienced complete loss of total pressure output are summarized in Table 3-4. This table lists, (1) the basic test conditions, (2) exposure time to initial (total) pressure response, (3) exposure time-to-failure and (4) the corresponding expended particle mass at failure where failure is defined as the point where the total pressure output drops to zero. The time to the initial pressure response and to failure were obtained from the recorded pressure histories such as those shown in Figures 3-17 through 3-19. The total particle mass expended at the time of failure was determined as the product of the particle flow rate and the time-to-failure.

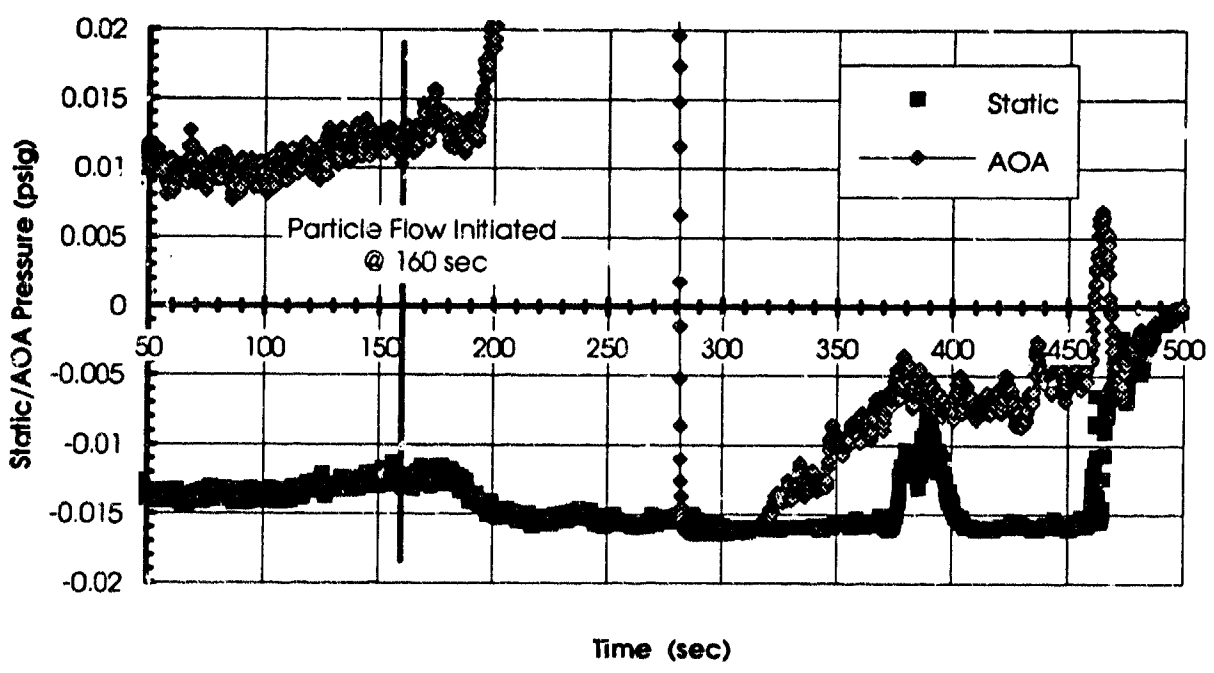
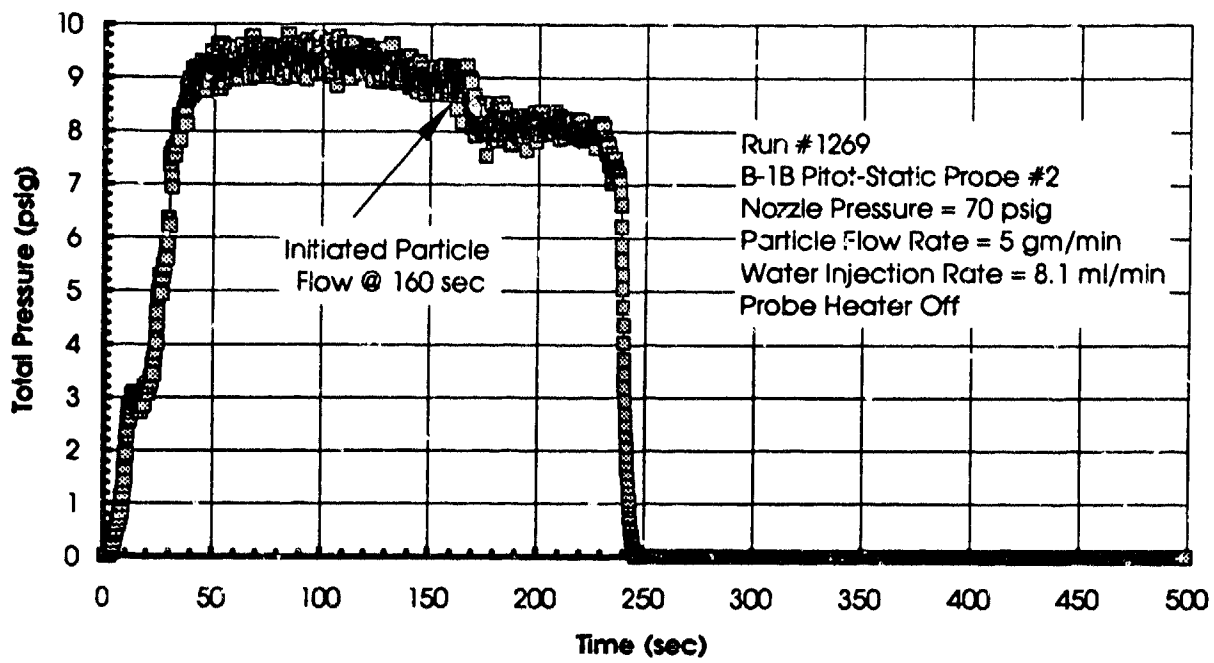


Figure 3-17. B-1B ADS pressure response with wet particle flow - Blend #15.

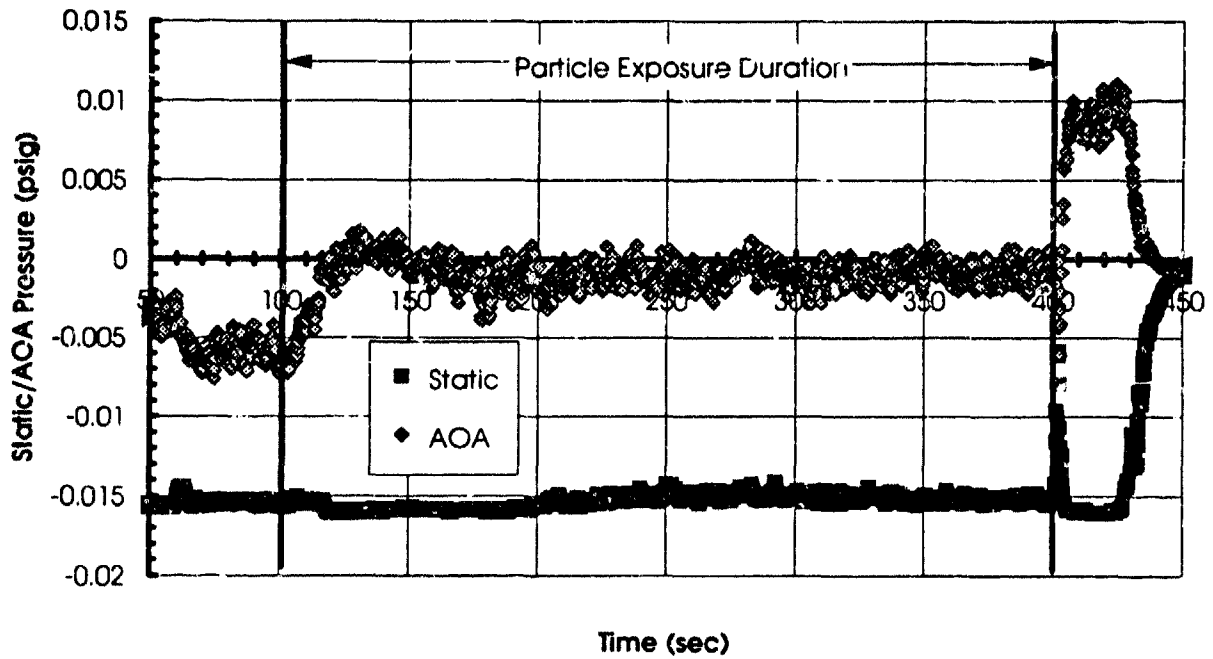
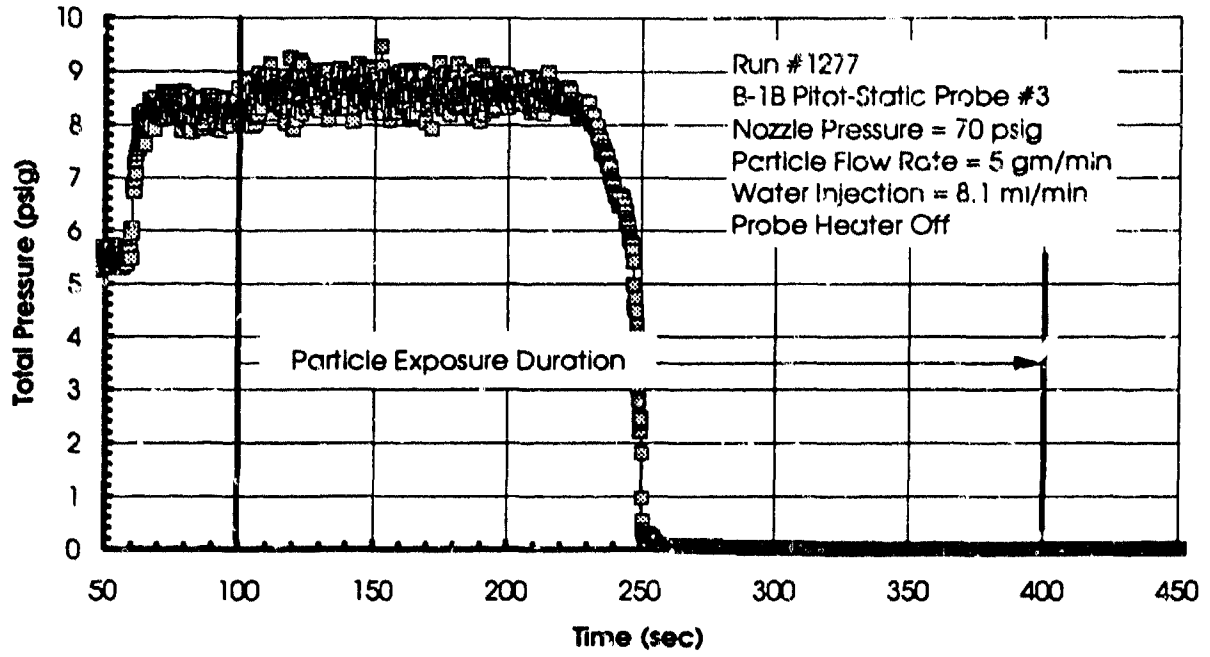


Figure 3-18. B-1B ADS pressure response with wet particle flow - <38 microns crushed silica.

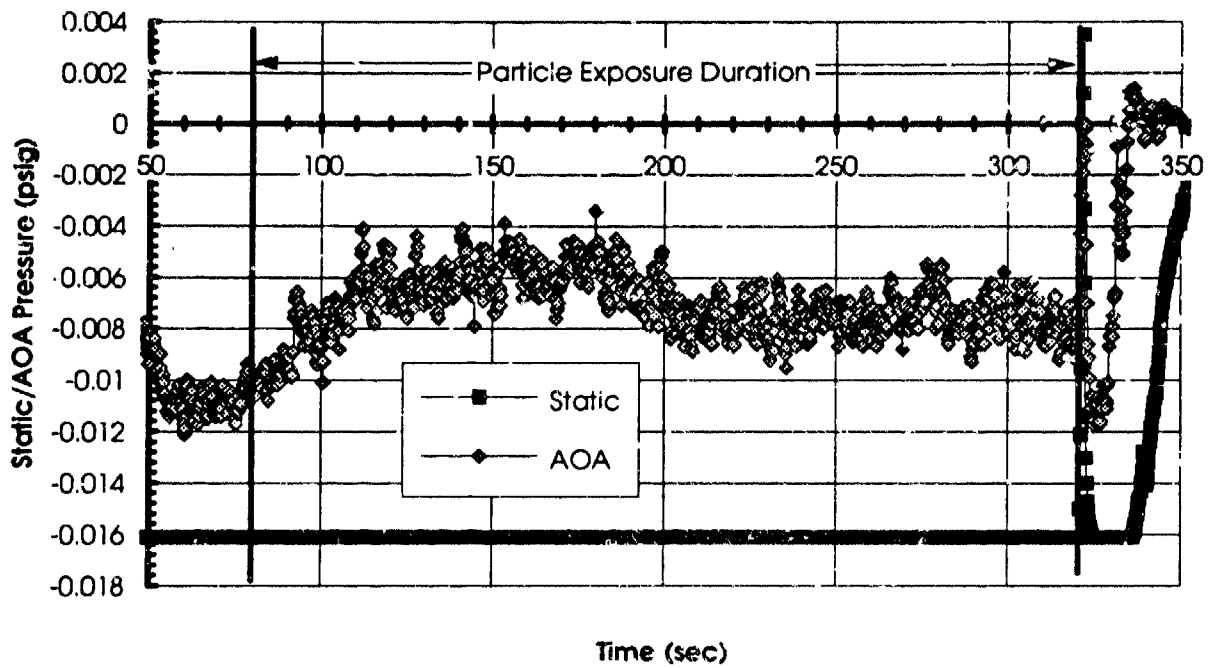
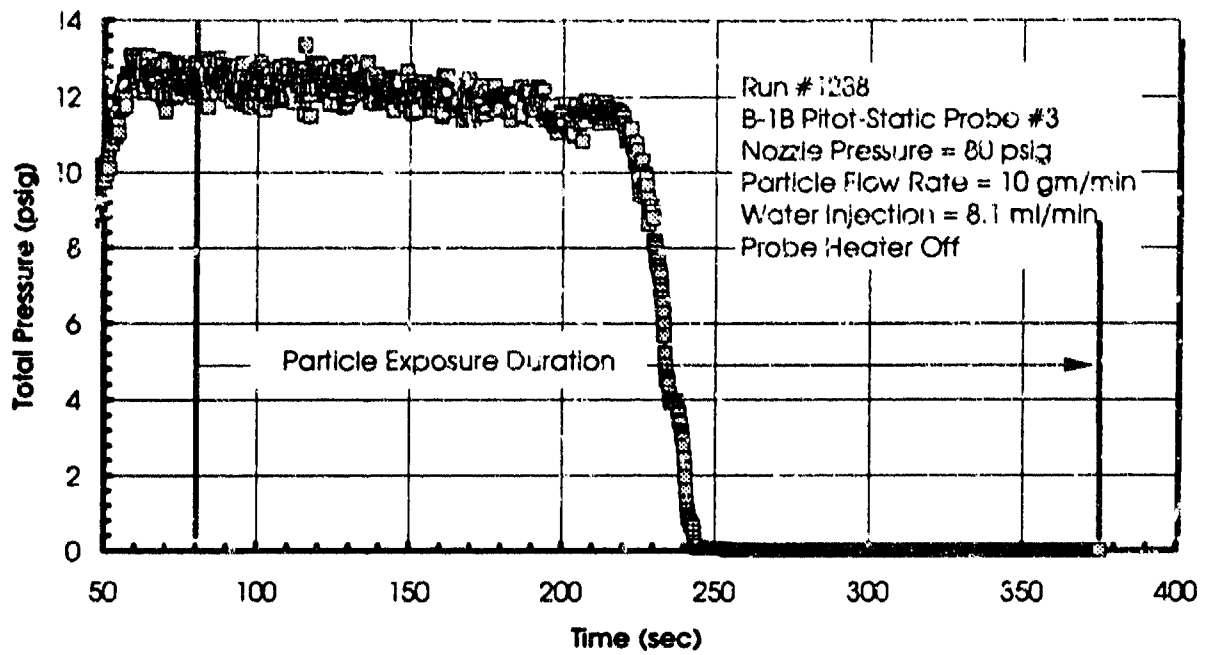


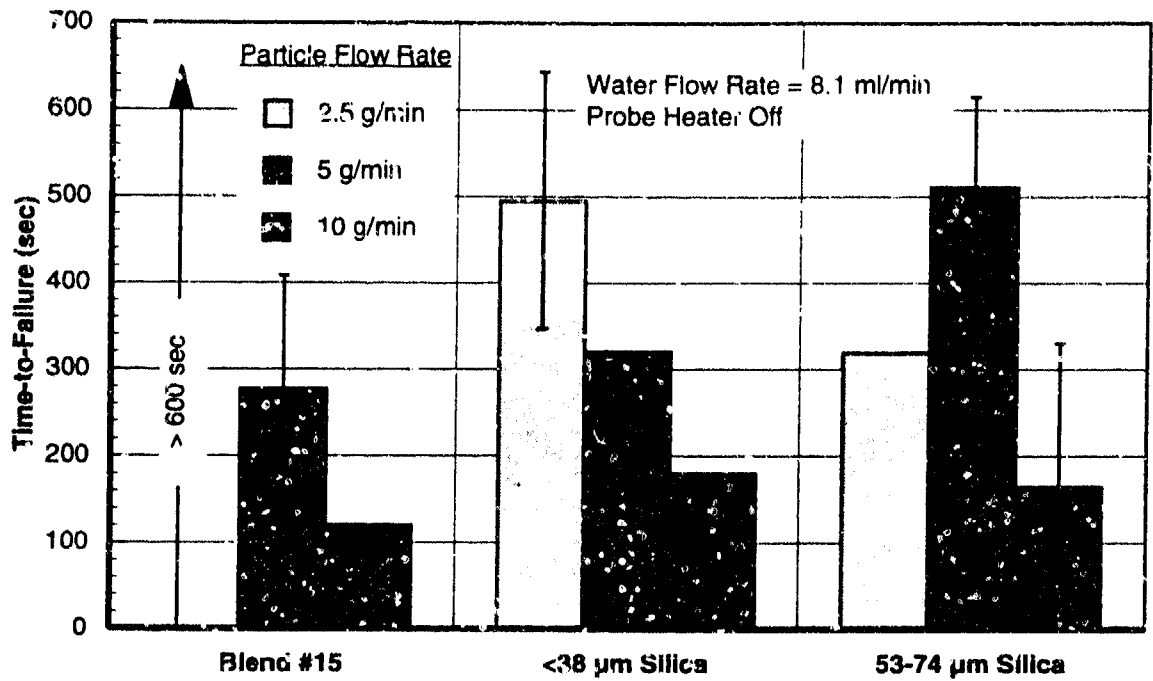
Figure 3-19. B-1B ADS pressure response with wet particle flow - 52-74 micron crushed silica.

Table 3-4. Total pressure failure response characteristics.

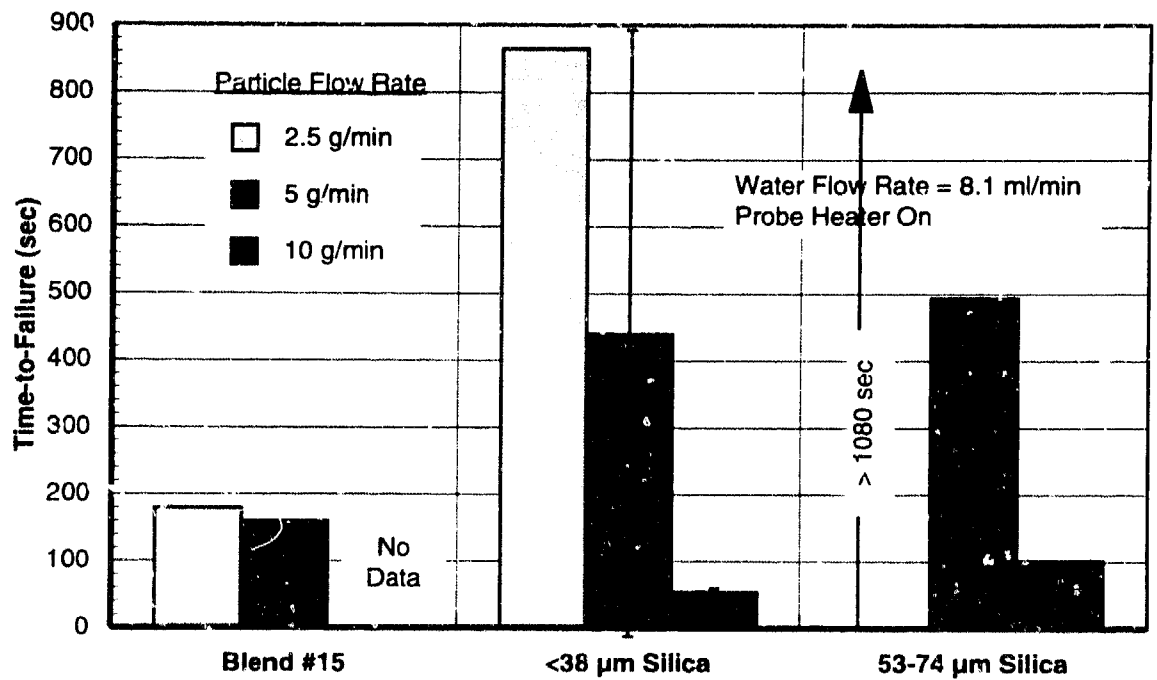
RUN NO.	PART. SIZE (μm)	PART. FLOW (g/min)	RUN TIME (min)	INITIAL P _T RESPONSE (mm:ss)	P _T TIME TO FAIL (mm:ss)	PART. MASS (gm)	NOZZLE HEAT	PROBE HEAT
1257	Blend	5.0	10.0	5:10	6:24	32.5	NO	OFF
1260	#15"	10.0	5.0	0:45	2:00	20.0	"	"
1264	"	5.0	10.0	2:00	3:00	15.0	"	ON
1266	"	5.0	10.0	3:20	4:10	20.8	"	"
1268	"	5.0	8.0	4:10	5:20	26.7	"	OFF
1269	"	5.0	5.0	1:10	1:25	7.1	YES	"
1270	"	5.0	8.0	4:10	5:20	26.7	"	ON
1273	"	5.0	5.0	1:30	2:40	13.3	"	"
1274	"	2.5	5.0	1:40	3:00	7.5	"	"
1277	<38	5.0	5.0	4:10	5:20	26.7	"	OFF
1278	"	2.5	14.0	9:50	10:00	25.0	"	"
1279	"	5.0	4.0	1:50	2:00	10.0	"	ON
1281	"	2.5	10.0	6:20	6:30	16.3	"	OFF
1282	"	5.0	14.0	11:50	12:40	63.3	"	ON
1284	"	10.0	5.0	2:30	3:00	30.0	"	OFF
1285	"	10.0	5.0	0:35	0:50	8.3	"	ON
1286	"	2.5	15.0	13:20	14:15	36.0	"	"
1288	53-74	10.0	4.0	2:20	2:45	27.5	"	OFF
1289	"	5.0	15.0	9:43	9:45	48.8	"	"
1290	"	5.0	10.0	7:15	7:18	36.5	"	"
1291	"	2.5	8.0	5:17	5:19	13.3	"	"
1292	"	10.0	3.0	0:52	1:42	17.0	"	ON
1293	"	5.0	10.0	7:50	8:14	41.2	"	"

Since it is difficult to identify trends from the tabular data, the exposure time-to-failure and the expended mass at failure are presented graphically in Figures 3-20 and 3-21, respectively. Separate bar charts are used for the runs conducted with and without probe heating. In Figure 3-20, the bar charts show the time-to-failure as a function of the particle type/size and the dust flow rate. Although the data are very limited and scatter is significant (as shown by the error bars), general trends are apparent in Figure 3-20. For the runs with the probe heater in operation, the trends are of increasing time-to-failure with increasing particle size and (within a specific particle type/size) decreasing time-to-failure with increasing particle flow rate. This flow rate dependency is particularly strong for the larger (crushed silica) particles. No data were taken with Blend #15 at a flow rate of 10 g/min. As noted in Figure 3-20 (b), if failure does occur for the 53-74 crushed silica particles at a flow rate of 2.5 g/min, it will be at an exposure time greater than 1080-sec based on the results of Run #1294.

Time-to-failure results without the B-1B pitot-static probe heater operating are shown in Figure 3-20 (a). These results are in general agreement with the heated probe results in figure (b)

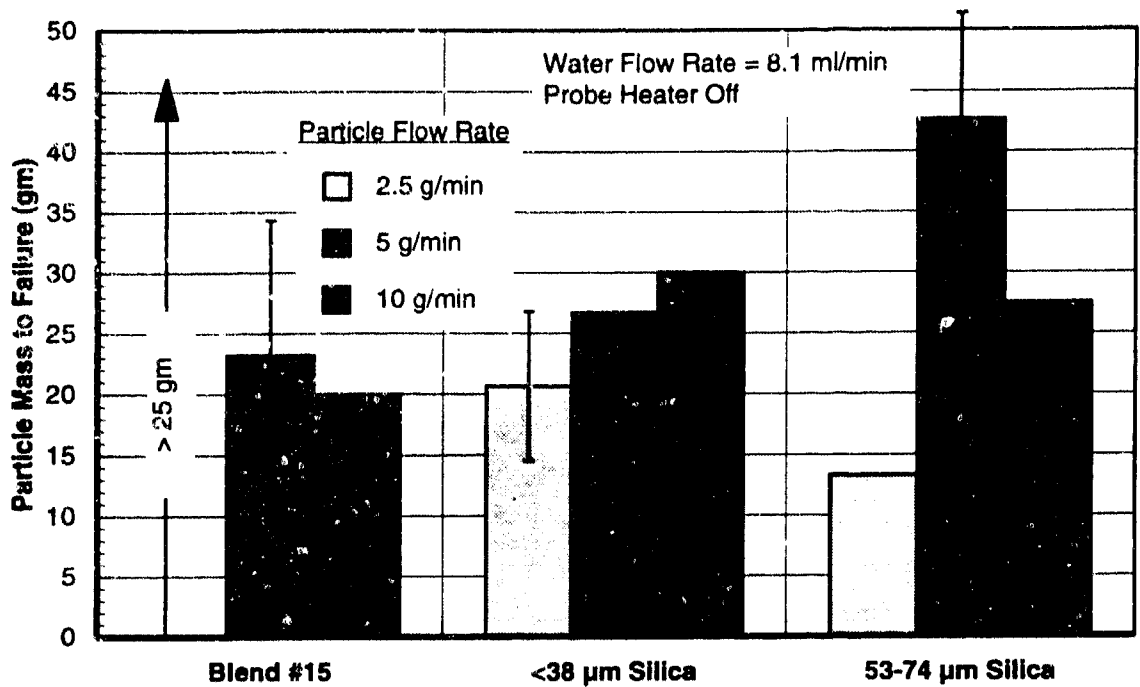


(a) Without Probe Heating

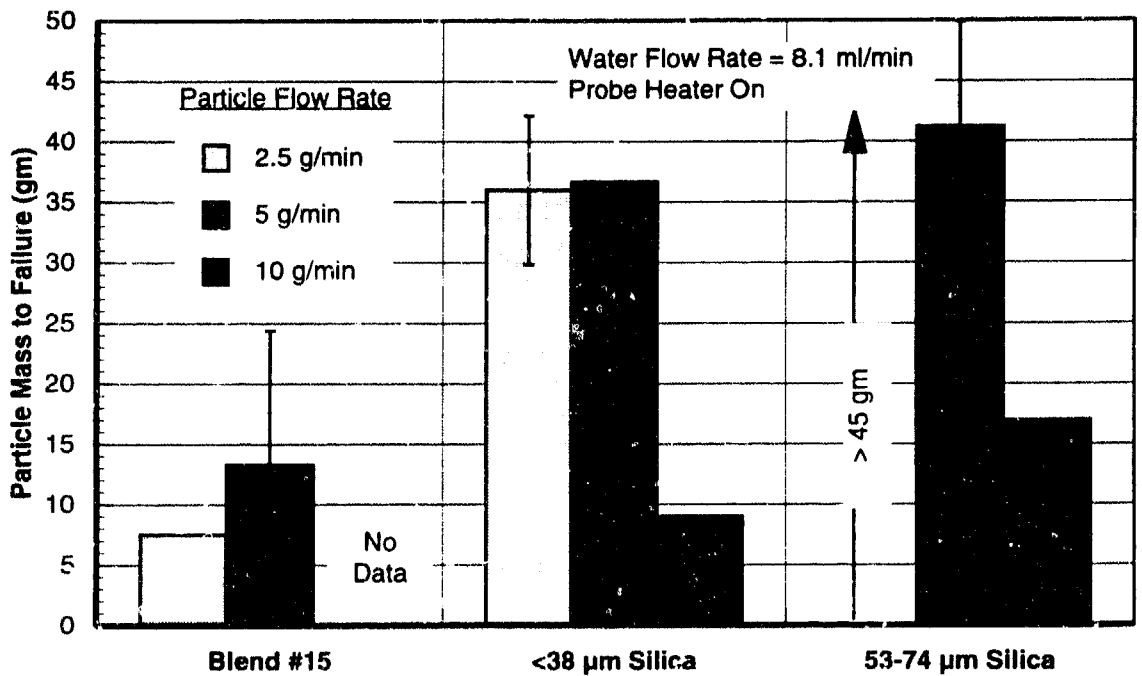


(b) With Probe Heating

Figure 3-20. Exposure time required for total pressure output loss.



(a) Without Probe Heating



(b) With Probe Heating

Figure 3-21. Expanded particle mass required for total pressure output loss.

except for the 2.5 g/min particle flow rate data which shows a decreasing time-to-failure with increasing particle size. For the smallest particles (Blend #15), total pressure loss did not occur during a 600-sec run. This trend is opposite to that of the heated probe where the time-to-failure at the 2.5 g/min flow rate occurred with the Blend #15.

The total particle mass expended during the exposure up to the time of failure is presented in Figure 3-21 as a function of the particle type/size and the dust flow rate. As would be expected, these results are similar to the time-to-failure data shown in Figure 3-20. The trends are the same although the relative amount of mass expended for the different flow rates are not the same as the relative time-to-failure values since the particle mass values were obtained as the product of the time-to-failure and the flow rate. The results for the probe heating runs indicate that much less particle mass is required to cause failure at the 10 g/min flow rate than at the either of the lower flow rates. Thus, even on a total mass expended basis, the strong rate dependency associated with total pressure output failure is evident. With the unheated probe, Figure 3-21 (a), the trends are the same as for the time-to-failure results with the 2.5 g/min data showing decreasing particle mass expended with increasing particle size which is opposite to the heated probe results.

The remainder of the wet particle flow tests (Run #1297 through 1314) were conducted with a high water flow rate of approximately 185 ml/min. These exposures included particle flow rates of 2.5, 5 and 10 g/min for each of the three particle types/sizes with and without probe heating. As note above, failure was not observed in the pressure outputs for any of these high water flow runs. While there was no apparent loss in total pressure as seen at the lower 8 ml/min water flow rates, the total pressure values measured under the high water flow conditions were somewhat lower than measured for the other conditions as noted in Section 3.3 and shown in Figure 3-8. Also, the data scatter (or noise) associated with the pressure outputs was higher than for the low water flow and dry particle flow conditions. These observation are illustrated in Figures 3-22 and 3-23 which present representative pressure data for the high water flow conditions. Figure 3-22 shows the pressure histories for Run #1298 which was conducted with 53-74 μm crushed silica at a flow rate of 5 g/min. Figure 3-23 shows similar results for Run #1310 which utilized Blend #15 at the same flow rate of 5 g/min.

3.5.2 Dust Ingestion Data.

As discussed in conjunction with the dry particle flow results in Section 3.4.2, the B-1B pitot-static probe and the inline particle filters were weighed before and after each exposure in order to determine the mass of dust particles collected during the run. Identical dust filters were used on the total, static and AOA pressure transmission lines just ahead of the transducers. The

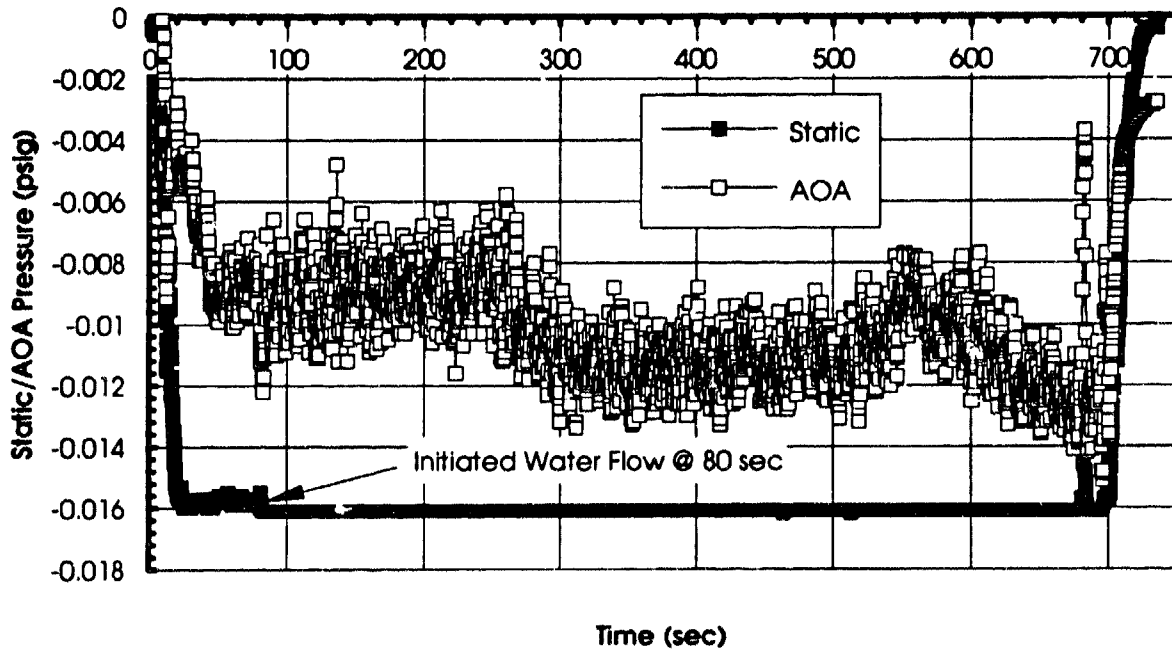
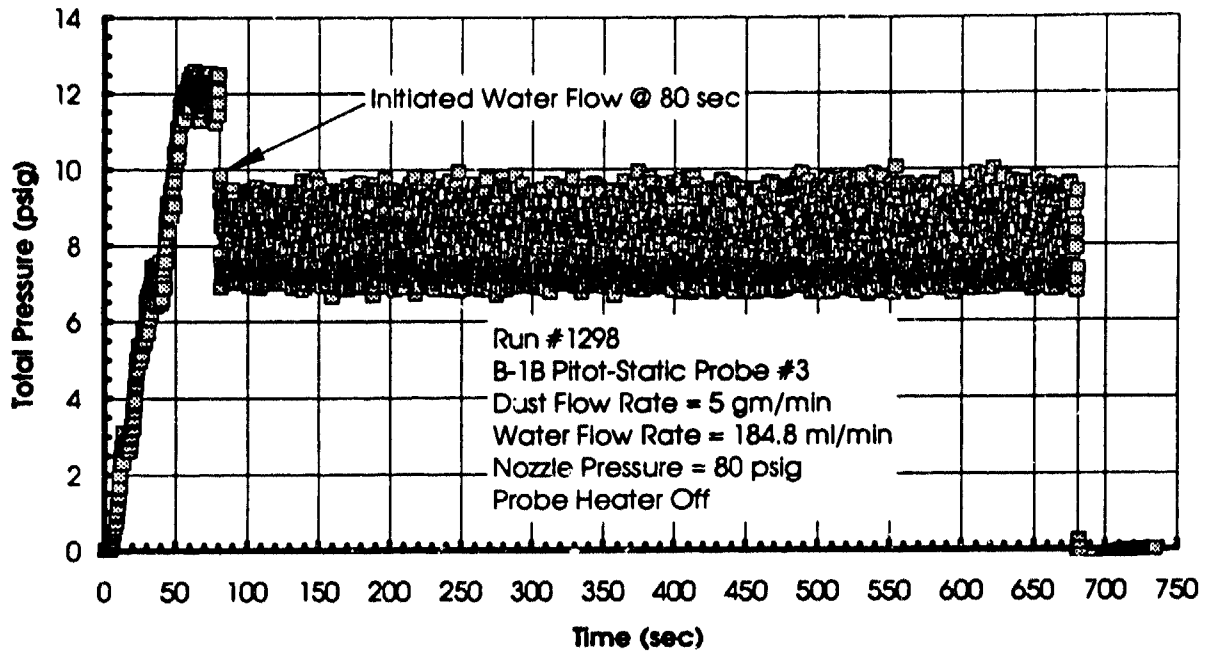


Figure 3-22. B-1B ADS pressure response with high water flow - 52-74 micron silica.

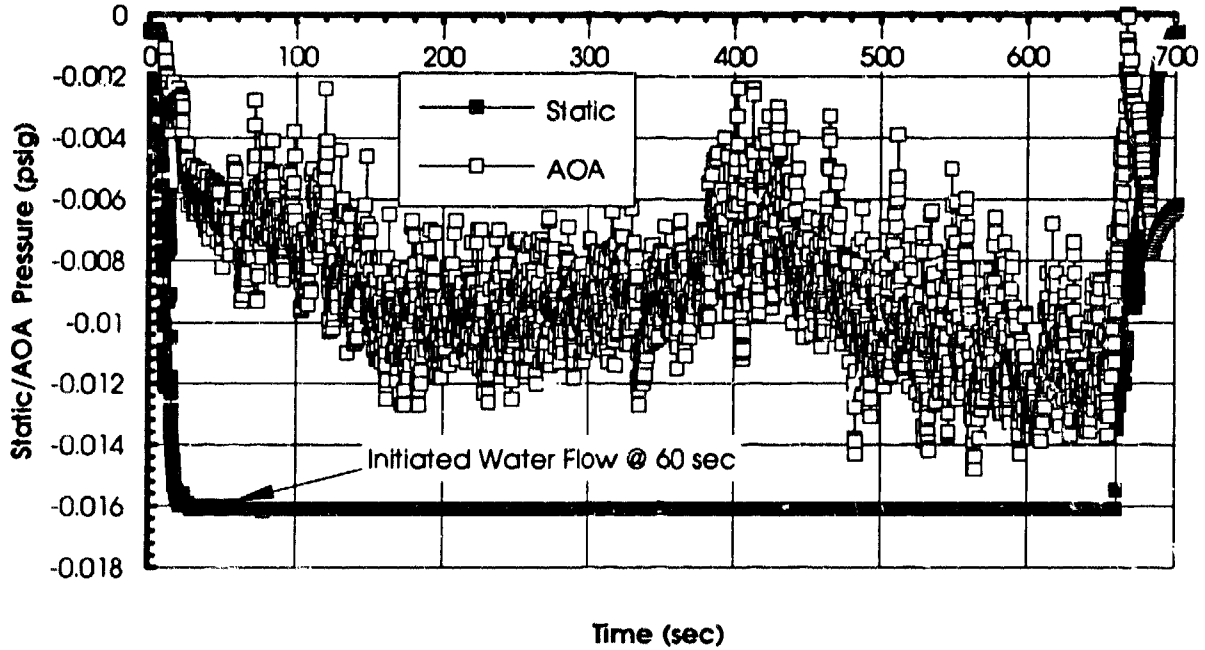
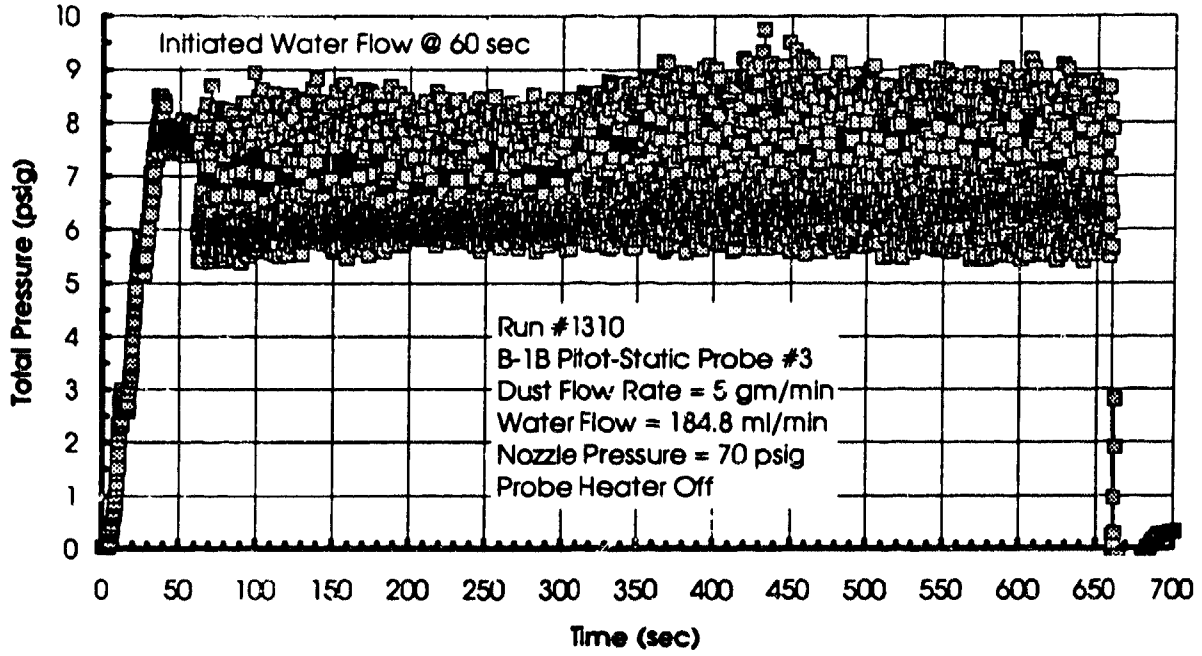


Figure 3-23. B-1B ADS pressure response with high water flow - Blend #15.

wet particle flow pre- and post-test weight data for the B-1B pitot-static probe and the inline particle filters are presented in Table 3-5. The weight data are in grams and are listed by facility run number. In addition to the pre and post-test weights of each component, the change in weight (post-test minus pre-test) is also included in Table 3-5. Data for the total, static and AOA line filters are identified as P-T, P-S and AOA filter weight, respectively.

The weight data presented in Table 3-5 indicates (1) a lack of any significant weight gain associated with the static and AOA filters, (2) lack of any significant weight gain by the total pressure filter except for the last six high water flow rate runs and (3) pitot-static probe weight gains ranging from less than one to over 30 g. The average weight change for the static and AOA filters for all of the wet flow runs was -0.0001 g indicating that the small variation in weight change shown in Table 3-5 is probably representative of the measurement accuracy. Excluding the final six runs involving Blend #15 and the high water flows, the average weight gain for the total pressure filter was also small (-0.0307 g) indicating no significant dust/water ingestion. However, for the final six runs, this average jumped to 23.43 g indicating a significant amount of water/dust ingested from the probe. The pitot-static probe showed weight gains for all runs with the larger gains corresponding to long exposures and the Blend #15 high water flow runs.

The six runs involving the small Blend #15 particles and the nominal 185 ml/min water flow rate provided a dramatically different response than the other wet flow exposures. Based on the weight data and post-test observations, it appears that the Blend #15 particles blocked (either totally or partially) the moisture drain hole in the bottom of the B-1B pitot-static probe. In fact, reduced water flow from the drain hole was observed during these runs. The partial blockage of the probe drain hole appears to have forced the water/dust slurry through the probe and into the total pressure line. For all of these final six runs, the total pressure line and filter were filled with water/dust and a significant amount of liquid poured out when the line was disconnected from the probe and filter. Thus, the actual mass of material (water plus dust) trapped in the line and filter was greater than the values shown in Table 3-5. The effect of this response on the B-1B pressure transducer is not known, but must be viewed with concern.

The dust/water ingestion data are summarized graphically in Figures 3-24 through 3-26 for the low water flow rate and in Figure 3-27 for the high water flow. Figure 3-24, 3-25 and 3-26 present correlations of the total mass (water and dust) collected in the system (i.e. probe and line filters) versus the total mass of dust expended during the exposure (particle flow rate x exposure time) for Blend #15, <38 μm and 53-74 μm crushed silica, respectively. Both the wet and dry particle flow data are included in these figures. As noted above for the dry particle flows, the total mass collected in the probe and filters is essentially a linear function of the total particle mass

Table 3-5. B-1B ADS particle collection data - wet particle flow.

RUN NO.	PROBE WEIGHT (gm)			P-T FILTER WEIGHT (gm)			P-S FILTER WEIGHT (gm)			AOA FILTER WEIGHT (gm)		
	PRE	POST	Δ	PRE	POST	Δ	PRE	POST	Δ	PRE	POST	Δ
	1257	1164.93	1168.87	3.94	65.9718	65.9990	0.0272	63.5314	63.5300	-0.0014	63.6737	63.6709
1259	1157.06	1157.65	0.59	65.6047	65.6230	0.0183	63.5215	63.5225	0.0010	63.6649	63.6639	-0.0010
1260	1157.01	1158.64	1.63	65.6065	65.6165	0.0100	63.5254	63.5240	-0.0014	63.6692	63.6665	-0.0027
1261	1157.05	1158.60	1.55	65.6189	65.6320	0.0131	63.5240	63.5246	0.0006	63.6665	63.6669	0.0004
1262	1156.84	1171.97	15.13	65.6369	65.6492	0.0123	63.5294	63.5292	-0.0002	63.6738	63.6711	-0.0027
1263	1157.22	1168.49	11.27	65.6478	65.6510	0.0032	63.5299	63.5293	-0.0006	63.6715	63.6700	-0.0015
1264	1156.22	1161.44	5.22	65.6418	65.6784	0.0366	63.5313	63.5294	-0.0019	63.6723	63.6716	-0.0007
1265	1156.86	1161.40	4.54	65.6676	65.7032	0.0356	63.5367	63.5350	-0.0017	63.6779	63.6757	-0.0022
1266	1156.86	1161.33	4.47	65.7032	65.7106	0.0074	63.5379	63.5358	-0.0021	63.6785	63.6748	-0.0037
1267	1156.99	1163.28	6.29	65.6997	65.7272	0.0275	63.5358	63.5349	-0.0009	63.6748	63.6743	-0.0005
1268	1156.92	1160.91	3.99	65.6746	65.6856	0.0110	63.5237	63.5227	-0.0010	63.6669	63.6662	-0.0007
1269	1156.88	1158.70	1.82	65.6708	65.6624	-0.0084	63.5248	63.5220	-0.0028	63.6679	63.6646	-0.0033
1270	1156.88	1159.48	2.60	65.6624	65.6837	0.0213	63.5220	63.5228	0.0008	63.6679	63.6656	-0.0023
1272	1180.30	1183.09	2.78	65.6753	65.6687	-0.0066	63.5237	63.5226	-0.0011	63.6675	63.6654	-0.0021
1273	1180.37	1182.76	2.39	65.6687	65.6807	0.0120	63.5256	63.5229	-0.0027	63.6654	63.6654	0.0000
1274	1180.37	1181.90	1.53	65.6789	65.6858	0.0069	63.5232	63.5207	-0.0025	63.6702	63.6677	-0.0025
1275	1180.37	1188.69	8.32	65.6858	65.7025	0.0167	63.5207	63.5217	0.0010	63.6677	63.6680	0.0003
1276	1180.44	1185.45	5.01	65.6751	65.7084	0.0333	63.5220	63.5215	-0.0005	63.6659	63.6657	-0.0002
1277	1180.55	1185.93	5.38	65.6882	65.6950	0.0068	63.5202	63.5170	-0.0032	63.6648	63.6611	-0.0037
1278	1180.56	1187.17	6.61	65.6924	65.7083	0.0159	63.5161	63.5148	-0.0013	63.6613	63.6593	-0.0020
1279	1180.60	1185.42	4.82	65.6845	65.6901	0.0056	63.5101	63.5083	-0.0018	63.6560	63.6530	-0.0030
1280	1180.86	1186.57	5.71	65.6922	65.7329	0.0407	63.5104	63.5086	-0.0018	63.6555	63.6532	-0.0023
1281	1180.76	1182.63	1.87	65.6997	65.7119	0.0122	63.5014	63.5043	0.0029	63.6486	63.6509	0.0023
1282	1180.77	1205.54	24.77	65.7009	65.7246	0.0237	63.5043	63.5046	0.0003	63.6509	63.6512	0.0003
1283	1181.21	1191.62	10.41	65.7144	65.7418	0.0274	63.5036	63.5040	0.0004	63.6514	63.6514	0.0000
1284	1181.22	1192.76	11.54	65.7418	65.7435	0.0017	63.5040	63.5069	0.0029	63.6514	63.6510	-0.0004
1285	1181.05	1183.51	2.46	65.6663	65.6697	0.0034	63.5145	63.5150	0.0005	63.6535	63.6551	0.0016
1286	1181.06	1195.14	14.08	65.6635	65.7070	0.0435	63.5098	63.5084	-0.0014	63.6523	63.6495	-0.0028

Table 3-5. B-1B ADS particle collection data - wet particle flow (Continued).

RUN NO.	PROBE WEIGHT (gm)			P-T FILTER WEIGHT (gm)			P-S FILTER WEIGHT (gm)			AOA FILTER WEIGHT (gm)		
	PRE	POST	Δ	PRE	POST	Δ	PRE	POST	Δ	PRE	POST	Δ
1287	1181.41	1184.00	2.59	65.6940	65.6963	0.0023	63.5013	63.5012	-0.0001	63.6450	63.6449	-0.0001
1288	1180.95	1191.04	10.09	65.6697	65.6828	0.0131	63.4973	63.4965	-0.0008	63.6429	63.6419	-0.0010
1289	1181.57	1212.10	30.53	65.6781	65.7060	0.0279	63.4937	63.4936	-0.0001	63.6411	63.6408	-0.0003
1290	1181.21	1185.85	4.64	65.6965	65.7151	0.0186	63.4952	63.4957	0.0005	63.6436	63.6439	0.0003
1291	1181.06	1184.30	3.24	65.6893	65.7096	0.0203	63.4980	63.4972	-0.0008	63.6451	63.6441	-0.0010
1292	1181.02	1187.21	6.19	65.7025	65.7111	0.0086	63.4976	63.4978	0.0002	63.6441	63.6448	0.0007
1293	1181.60	1199.77	18.17	65.6733	65.7140	0.0407	63.5122	63.5121	-0.0001	63.6541	63.6539	-0.0002
1294	1182.21	1198.70	16.49	65.7008	65.7906	0.0898	63.5097	63.5094	-0.0003	63.6515	63.6519	0.0004
1295	1181.86	1185.06	3.20	65.6588	65.6670	0.0082	63.5067	63.5073	0.0006	63.6495	63.6500	0.0005
1296	1181.93	1184.72	2.79	65.6633	65.6710	0.0077	63.5046	63.5086	0.0040	63.6476	63.6499	0.0023
1297	1181.74	1187.94	6.20	65.6663	65.6794	0.0131	63.5057	63.5083	0.0026	63.6484	63.6515	0.0031
1298	1181.53	1187.42	5.89	63.6129	63.6273	0.0144	63.5077	63.5082	0.0005	63.6483	63.6492	0.0009
1299	1181.21	1187.26	6.05	63.6248	63.6363	0.0115	63.5056	63.5056	0.0000	63.6472	63.6475	0.0003
1300	1181.01	1188.69	7.68	63.6319	63.6427	0.0108	63.5014	63.5023	0.0009	63.6454	63.6463	0.0009
1301	1180.64	1186.45	5.81	63.6371	63.6493	0.0122	63.4994	63.4997	0.0003	63.6448	63.6458	0.0010
1302	1180.46	1187.30	6.84	63.6336	63.6516	0.0180	63.5000	63.4996	-0.0004	63.6458	63.6455	-0.0003
1303	1180.35	1187.92	7.57	63.6437	63.6519	0.0082	63.5000	63.5020	0.0020	63.6462	63.6491	0.0029
1304	1180.06	1187.04	6.98	63.6475	63.6503	0.0028	63.4986	63.4989	0.0003	63.6455	63.6463	0.0008
1305	1179.74	1186.35	6.61	63.4994	63.0090	-0.4904	63.4994	63.5009	0.0015	63.6462	63.6512	0.0050
1306	1179.68	1186.66	6.98	63.6387	63.6467	0.0080	63.4969	63.4971	0.0002	63.6450	63.6457	0.0007
1307	1179.46	1185.88	6.42	63.6425	63.6536	0.0111	63.4948	63.4967	0.0019	63.6433	63.6456	0.0023
1308	1179.16	1185.04	5.88	63.6286	63.6403	0.0117	63.5068	63.5084	0.0016	63.6502	63.6514	0.0012
1309	1179.08	1206.51	27.43	63.6345	86.8923	23.2578	63.5039	63.5054	0.0015	63.6485	63.6508	0.0023
1310	1181.18	1196.68	15.50	65.7296	105.9399	40.2103	63.5087	63.5080	-0.0007	63.6519	63.6525	0.0006
1311	1181.67	1189.63	7.96	64.7382	84.9727	20.2345	63.5089	63.5090	0.0001	63.6527	63.6538	0.0011
1312	1181.15	1212.30	31.15	64.8770	86.5126	21.6356	63.5087	63.5096	0.0009	63.6529	63.6573	0.0044
1313	1181.64	1194.60	12.96	64.4350	81.2491	16.8141	63.5057	63.5065	0.0008	63.6510	63.6523	0.0013
1314	1182.22	1194.25	12.03	63.9507	82.3899	18.4392	63.5065	63.5060	-0.0005	63.6520	63.6522	0.0002

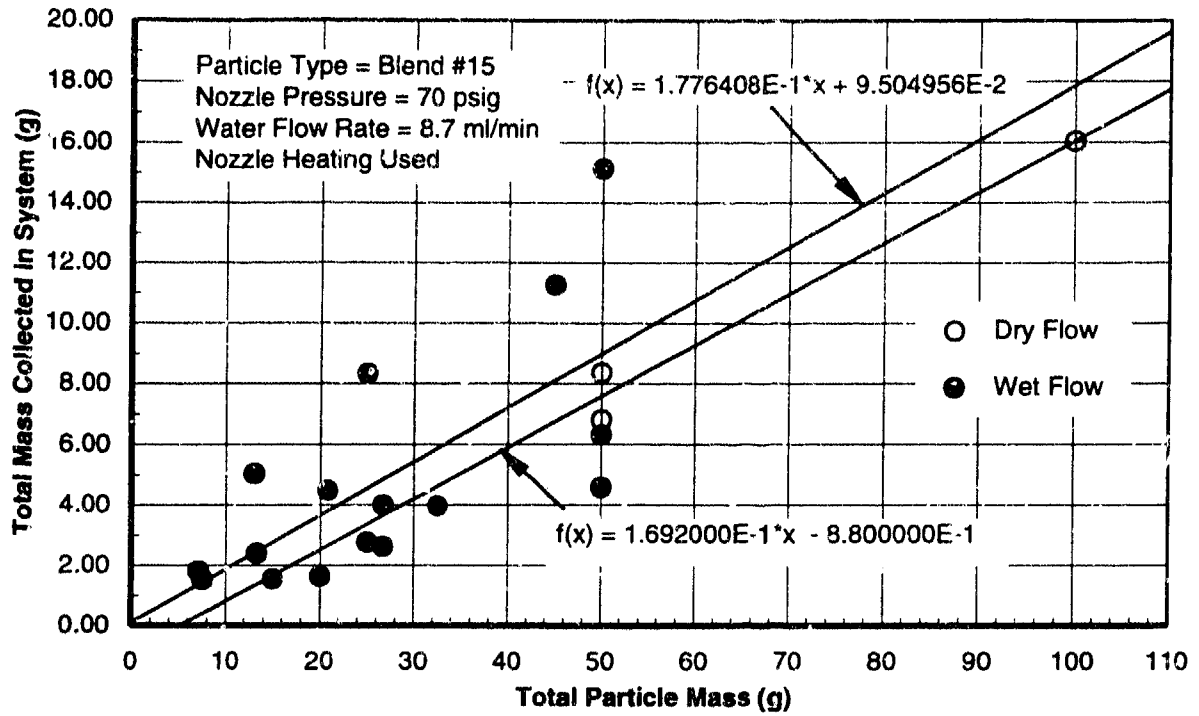


Figure 3-24. Ingested mass vs total dust mass expended - Blend #15.

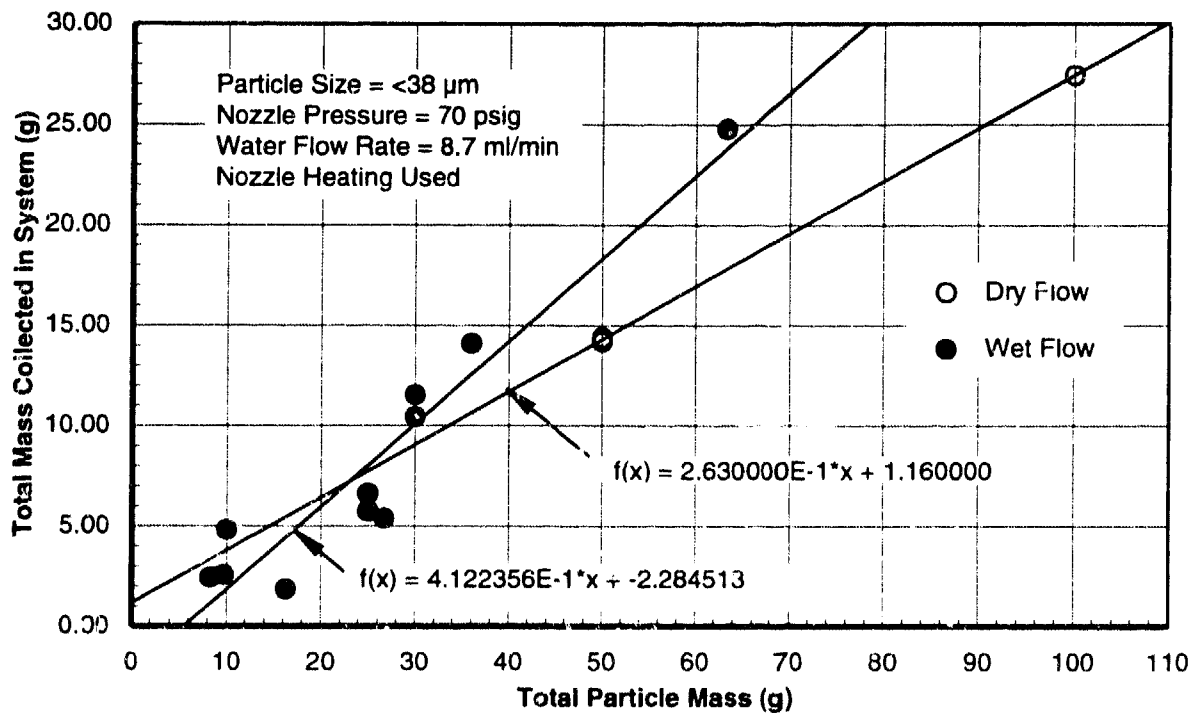


Figure 3-25. Ingested mass vs total dust mass expended - <38 μm Silica.

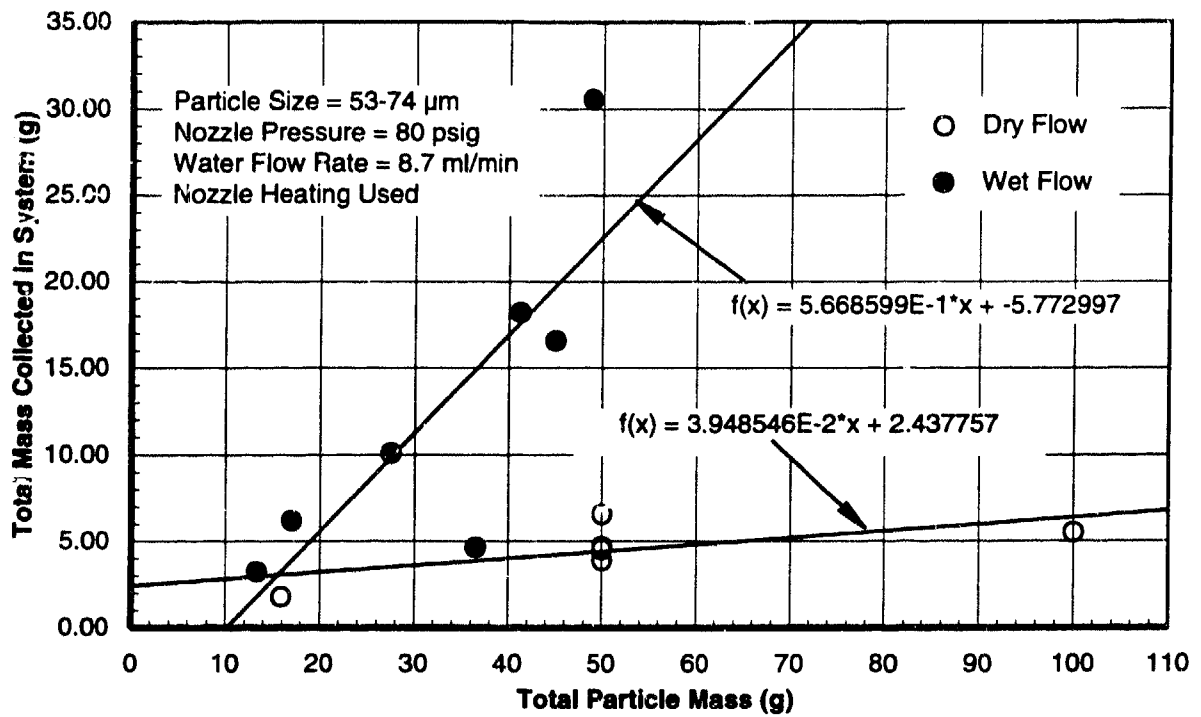


Figure 3-26. Ingested mass vs total dust mass expended -53-74 μm Silica.

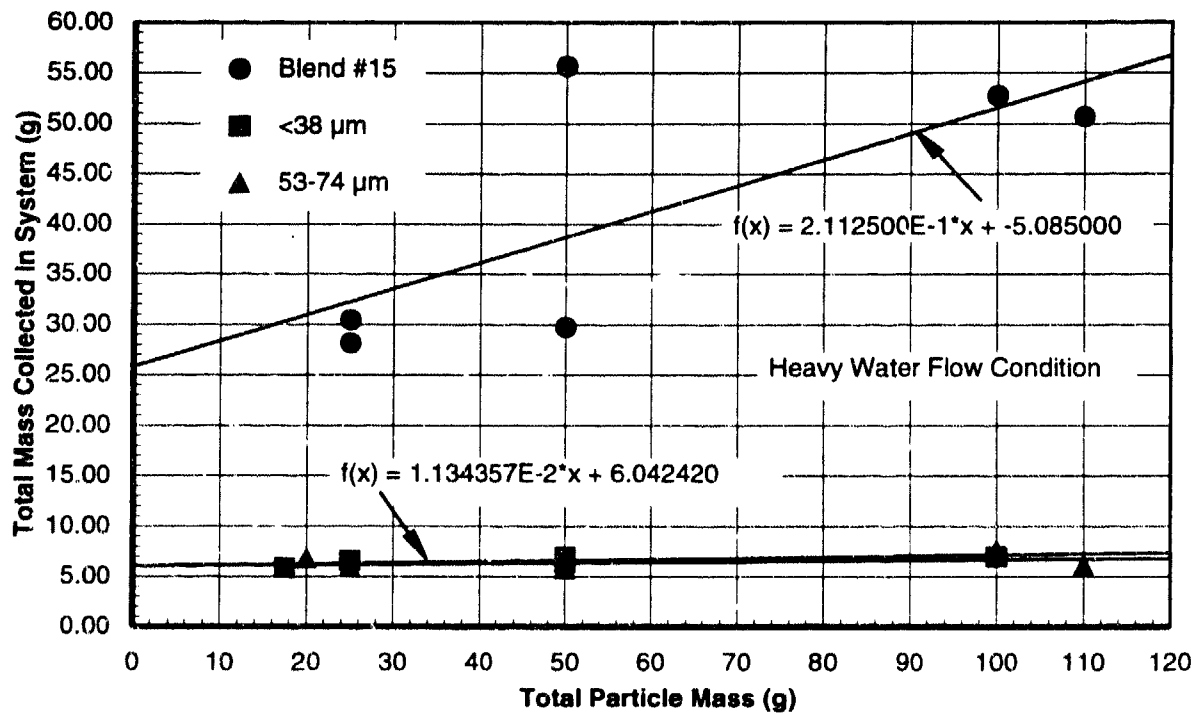


Figure 3-27. Ingested mass vs total dust mass expended - high water flow.

expended. The wet flow data, however, shows a significant amount of scatter which may reflect the presence of water in the probe. The rate at which mass is collected also appears to vary with particle type/size and test conditions. Except for the Blend #15, the mass collection rates for the wet flow runs were significantly larger than those for the dry particle runs. In fact, the differences between the wet and dry mass collection rates increased with increasing particle size. The linear curvefit equations are included in each figure.

The mass ingestion data corresponding to the high water flow runs are summarized in Figure 3-27. The total mass gain by the system is plotted for each of the three particle type/sizes. As noted in the review of the tabular data, the ingestion of water and dust for the two sizes of crushed silica particles was approximately the same and essentially independent of the expended dust or exposure duration. However, with the Blend #15, the mass ingested was much higher and appears to increase with exposure; although, the large amount scatter makes this latter observation difficult to quantify. This increase seen with Blend #15 appears to be due to blockage of the moisture drain hole and the associated ingestion of water/dust into the probe, total pressure line and filter noted above.

3.5.3 Post-test Observations.

The physical condition of the B-1B pitot-static probe was examined after each exposure to a particle flow environment. The condition of the external surfaces, pressure ports and drain hole were examined. For the dry particle flows, the only physical change observed was the slow erosion of the probe tip. Gradual roughening of the total pressure port inlet was observed initially. This was followed by recession of the outer edge of the total pressure port which prompted the replacement of the #2 probe with probe #3 beginning with Run #1272. The deposition of dust particles in the probe left no visible clues. The pressure ports appeared to be clean and open.

With the wet flow conditions, the deposition of the water/dust slurry (mud) on both the external surfaces and in the total pressure port was evident. The external probe surfaces were cleaned following the post-test inspection in order to obtain accurate weight measurements needed to determine ingested mass. Partial or total blockage of the total pressure port was visible on the runs where total pressure failure occurred. Where partial blockage of the port was visible from the front, total plugging must have occurred internally in order to reduce the pressure output to zero. No plugging or erosion of either the static or AOA pressure ports were observed.

Characteristics of the visible particle deposits in the total pressure port appeared to vary with the particle type/size. These variations are illustrated in Figures 3-28 through 3-30 which

present post-test photographs of the total pressure port of the B-1E pitot-static probe for each of the three particle type/sizes under wet flow conditions. The Blend #15 tended to form a smooth solid bridge or plug just inside the entrance of the port as shown in Figure 3-28. With the larger crushed silica particles, the material tended to be deposited deeper in the probe and in a more irregular manner. For the $<38\ \mu\text{m}$ dust as shown in Figure 3-29, the entrance to the total pressure port is not completely bridged and the deposited material is not smooth like the Blend #15 deposits. With the largest ($53\text{-}74\ \mu\text{m}$) particles as shown in Figure 3-30, the material was deposited much deeper in the probe and it was difficult in most cases to determine if the visible blockage was complete or only partial.

Examination of the probe weight change data in Table 3-5 for those runs where failure occurred in the total pressure output indicates that the probe weight gain increased with particle size. The average weight gain for the Blend #15, $<38\ \mu\text{m}$ and the $53\text{-}74\ \mu\text{m}$ crushed silica were 2.95, 8.33 and 12.14 gms, respectively. This suggests that the fine dust particles in Blend #15 readily bridged the entrance to the total pressure port without depositing a significant amount of mass in the interior of the probe. The larger crushed silica particles were able to penetrate further into the pressure port and required a greater mass of particles to form a pressure tight barrier



Figure 3-28 Post-test photograph of probe following exposure to Blend #15

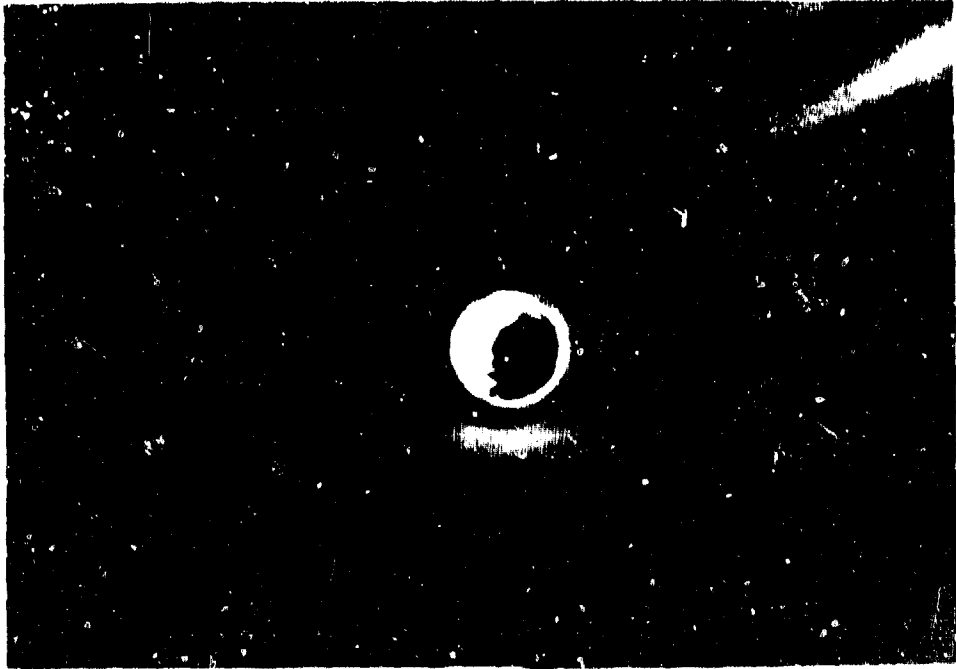


Figure 3-29 Post-test photograph of probe following exposure to $< 38 \mu\text{m}$ crushed silica



Figure 3-30 Post-test photograph of probe following exposure to 53-74 μm crushed silica

SECTION 4 SUMMARY AND RECOMMENDATIONS

4.1 SUMMARY

Potential hazards to military aircraft posed by both natural and weapon-induced dust/particle environments have been reinforced by the experiences of commercial aircraft encountering clouds of volcanic ash. Two Boeing 747 aircraft experienced the loss of air data sensors due to fouling from ash particles. For these aircraft which were flying at altitude, the loss of the air data system was not a catastrophic event. However, for a B-1B aircraft on a low altitude penetration mission, the loss of air data sensors would present serious problems both to crew safety and mission completion. Thus, since the ADS is such a critical component in the aircraft control and weapons systems, a preliminary evaluation of the B-1B ADS probe was conducted as the initial phase in a more comprehensive investigation. The vulnerability of the B-1B air data sensors to particle impact and ingestion effects was addressed as part of the DNA aircraft hazards effort. For this preliminary evaluation, the DNA Dust Erosion Facility was selected due to its capabilities, operational costs and availability.

Facility upgrades and experimental evaluations were successfully conducted during the 1992-93 time period. Successful facility modifications included (1) design and development of a large nozzle which provided a suitable gas/particle test environment, (2) the design and installation of a precision screw feeder system for accurately metering particles into the gas flow, (3) design and installation of a water injection system for simulating cloud moisture/rain and (4) installation of a computerized data acquisition system for data collection and analysis. The screw feeder and data acquisition systems have become a standard part of the erosion test facility and have been used extensively for routine erosion testing.

The evaluations of the B-1B ADS probe were directed towards verifying the effects seen in volcanic ash cloud encounters by commercial aircraft. Specifically, duplicating failure modes and establishing damage thresholds were the primary objectives of these initial evaluations. Over 70 runs were conducted where B-1B probes were exposed to high speed dust environments. These included dry gas/particles flows as well as flows with two different levels of water addition. All planned test conditions were achieved. The primary measurements included the pressure outputs from the ADS probe during dust exposures as well as pre- and post-test weight measurements. Pressure measurements were recorded with the data acquisition system and store on computer disk for later analysis and display.

The results of these evaluations identified two primary effects of dusty flows on the B-1B probe. These were (1) the loss of total pressure output due to plugging of the total pressure port and (2) ingestion of dust and water which can be transmitted to the pressure transducer. Although these effects did occur consistently, they occurred only under certain conditions which can be summarized as follows:

- (1) No effects were seen on any of the pressure outputs under dry flow conditions. Even pre-filling the probes with dust particles failed to degrade the total pressure output on subsequent exposure to a dusty flow environment.
- (2) The dry flows did result in the ingestion of dust particles into both the probe and pressure feed line leading to the transducer. This dust ingestion was only seen in conjunction with the total pressure components. No dust ingestion effects were seen with either the static or angle-of-attack (AOA) pressure components.
- (3) With the lower water flow (8 ml/min) condition, consistent plugging of the total pressure port and loss of pressure output was measured with all three particle type/sizes. The probe response was characterized by a sharp drop in measured total pressure after an incubation period of 1 to 15 minutes. This time-to-failure appeared to be a function of both particle size and particle flow rate.
- (4) No loss in static or AOA pressure outputs were recorded at the lower water flow condition. Also, no ingestion of dust or water was observed at this condition.
- (5) No plugging or loss of pressure was observed at the higher water flow rate (185 ml/min) with any of the particle type/sizes. Except for the smaller Blend #15, no significant ingestion of dust or water were seen at this higher water flow rate.
- (6) With the Blend #15 at the higher water flow rate, however, the probe drain appeared to plug resulting in ingestion of large quantities of water which filled the pressure line and dust filter leading to the pressure transducer. This occurred on all six runs at these conditions.
- (7) Use of the probe heater did not alter the results noted above. The failure modes and responses were similar between the heated and unheated probe. However, the time-to-failure data appeared to be more consistent and correlated better with particle size and flow rate for the runs using probe heating.

Thus, these initial laboratory evaluations of the B-1B ADS probe were successful in (1) creating a blockage of the total pressure port which was similar to inflight failures associated with volcanic ash cloud encounters and (2) quantifying mass ingestion of water and dust as a function of test conditions. The results have identified moisture level as a key variable in the plugging of the total pressure port and have developed preliminary data for assessing the effects of particle type/size, flow rate and velocity on both plugging and mass ingestion.

4.2 RECOMMENDATIONS.

The results of these initial evaluations have illustrated the vulnerability of the ADS probe to certain dusty flow environments. Key questions which must now be addressed are (1) what are the threshold and limiting conditions (in terms of the key parameters) associated with ADS degradation, (2) how do these vulnerability thresholds relate to operational environments and (3) how does this degradation in the air data system affect aircraft and mission performance. The first item can be address through additional testing in the DNA dust erosion facility while the latter issues require a broader investigation.

It is recommended that the next step be directed towards the validation and refinement of the results obtained in this initial evaluation. Specifically, the effects of dust mass flow rate and moisture level on ADS probe plugging and mass ingestion must be better defined. This could be accomplished through minor refinements to the test facility and additional tests with both lower dust and water flow rates. Lower particle flow rates are possible with the current screw feeder system with minimum particle flow rates being approximately 0.25 g/min. This would represent over an order of magnitude lower dust flow rates than used in the initial tests. The water injection system, however, will require some modifications in order to achieve steady flows at less than the current minimum condition of 8 ml/min. Options here include acquiring a smaller piston for the current metering pump or replacing the metering pump with a gas pressurized expulsion system. Whichever approach is used, a water flow rate capability of less than 1 ml/min will be required.

In order to better relate the laboratory results to the operational flight environments, a more detailed and extensive mapping of the dust particle flux in the plane normal to the jet axis is required. This would involve streamlining the LDV (particle velocity and data rate) measurements so as to improve overall data rate. This may also include use of the LVDT position sensor in conjunction with the computerized data acquisition system to automatically record the LDV measurement coordinates. This would allow a more accurate estimate of the equivalent particle concentration and flow rate to be determined at the total pressure port of the ADS probe.

Also, since the ADS pressure transducer is a key component in the system and will likely be exposed to dust particles and moisture, it is important that the vulnerability of the transducer be evaluated. The preferred approach would be to utilize the B-1B ADS transducer with the pitot-static probe in the evaluations conducted in the DNA dust facility. This would provide a simulation of the system up to the B-1B air data computer. If the required digital interface between the B-1B transducer and the facility data acquisition system cannot be obtained or developed, then, the B-1B transducer should be evaluated separately. This would involve the introduction of dust and

moisture to the transducer via the pressure transmission lines while the pressure inputs are maintained at realistic predetermined levels.

In conjunction with more detailed experimental evaluations, an effort is needed to assess the operational environment that the B-1B is likely to encounter. This would include developing a map of the operational parameters such as dust concentration, moisture content, particle type/size, altitude and aircraft speed. A comparison of the laboratory induced degradation thresholds with the B-1B operational conditions would provide a basis for assessing overall vulnerability. If this assessment shows a high potential for ADS damage or loss under potential operating conditions, then, a broader investigation should be initiated. This investigation should include a detailed analysis of the particle/flowfield interaction which could alter the particle concentration, speed and flow angle of the dust flow at the B-1B pitot-static probe locations. A high fidelity larger scale test series would be required to verify the degradation and failure mechanisms and thresholds developed in the small-scale testing.

SECTION 5
REFERENCES

1. Brantley, S.T., "The Eruption of Redoubt Volcano, Alaska, December 14, 1989 - August 31, 1990" (U), U.S. Geological Survey Circular 1061, 1990 (Unclassified).
2. Lloyd, A.T., "Vulcan's Blast" (U), Boeing Airliner, April-June 1990 (Unclassified).
3. Oeding, R.G., "Upgrade and Operation of the DNA Dust Erosion Test Facility" (U), Report No. DNA-TR-90-44, November 1989 (Unclassified).
4. Oeding, R.G., "Test Plan: B-1B Air Data Sensor Evaluation" (U), Report No. PDA-TR-1574-01-01, February 1993 (Unclassified).
5. Wuerer, J.E., "Dust Induced Loading Effects on a Hard Mobile Launcher" (U), Test Report, Wind Tunnel Tests, Report PDA-TR-5576-10-15, PDA Engineering, Costa Mesa, CA, July 1990 (Unclassified).

DISTRIBUTION LIST

DNA-TR-93-164

DEPARTMENT OF DEFENSE
412 TW/ LGLXP4
ATTN: P PAUGH

ASSISTANT TO THE SECRETARY OF DEFENSE
ATTN: EXECUTIVE ASSISTANT

DEPARTMENT OF ENERGY
LAWRENCE LIVERMORE NATIONAL LABORATORY
ATTN: ALLEN KUHL

DEFENSE INTELLIGENCE AGENCY
ATTN: DGI4

OTHER GOVERNMENT
CENTRAL INTELLIGENCE AGENCY
ATTN: OSWR/NED 5S09 NHB

DEFENSE NUCLEAR AGENCY
2 CY ATTN: IMTS
ATTN: NASF
ATTN: OPNA
5 CY ATTN: RAEM
ATTN: RAEM ROBERT KEHLET
2 CY ATTN: SPWE
ATTN: SPWE K DINOVA

DEPARTMENT OF DEFENSE CONTRACTORS
AEROSPACE CORP
ATTN: D LYNCH

DEFENSE TECHNICAL INFORMATION CENTER
2 CY ATTN: DTIC/OC

APPLIED RESEARCH INC
ATTN: J BOSCHMA

DEPARTMENT OF THE ARMY
CALSPAN CORP
ATTN: M DUNN

ARMY RESEARCH LABORATORIES
ATTN: SLCSM-SE

GENERAL ELECTRIC CO
ATTN: K KOCH

U S ARMY NUCLEAR & CHEMICAL AGENCY
ATTN: MONA-NU DR D BASH

HORIZONS TECHNOLOGY, INC
ATTN: E TAGGART

US ARMY CHEMICAL SCHOOL
ATTN: COMMANDING OFFICER

JAYCOR
ATTN: CYRUS P KNOWLES

USA CML & BIOLOGICAL DEFENSE AGENCY
ATTN: AMSCB-BDL J CANNALIATO

KAMAN SCIENCES CORP
ATTN: D COYNE

DEPARTMENT OF THE NAVY
KAMAN SCIENCES CORP
ATTN: J HESS

NAVAL AIR SYSTEMS COMMAND
ATTN: E ECK

KAMAN SCIENCES CORP
ATTN: DASAC

NAVAL RESEARCH LABORATORY
ATTN: CODE 7920

KAMAN SCIENCES CORPORATION
ATTN: DASAC

NAVAL SURFACE WARFARE CENTER
ATTN: CODE K42 L VALGE

LOGICON R & D ASSOCIATES
ATTN: J DRAKE
ATTN: LIBRARY
ATTN: R ROSS

STRATEGIC SYSTEMS PROGRAM
ATTN: SP0272 R G STANTON

LOGICON R & D ASSOCIATES
ATTN: E FURBEE
ATTN: J WEBSTER

STRATEGY AND POLICY DIVISION
ATTN: NIJC AFFAIRS & INTL NEGOT BR

DEPARTMENT OF THE AIR FORCE
LOGICON R & D ASSOCIATES
ATTN: G GANONG

AERONAUTICAL SYSTEMS CENTER
ATTN: ENSSS H GRIFFIS

MCDONNELL DOUGLAS CORPORATION
ATTN: L COHEN

AIR FORCE STUDIES AND ANALYSIS
ATTN: AFSAA/SAS

NORTHROP CORP
ATTN: GREG CURRY

AIR UNIVERSITY LIBRARY
ATTN: AUL-LSE

HQ USAF/XOFS
ATTN: XOFN

PACIFIC-SIERRA RESEARCH CORP
ATTN: R LUTOMIRSKI
ATTN: S FUGIMURA

OKLAHOMA CITY AIR LOGISTICS CTR
ATTN: OCALC/LPAAM S GARDNER

DNA-TR-93-164 (DL CONTINUED)

PACIFIC-SIERRA RESEARCH CORP
ATTN: M ALLERDING

PDA ENGINEERING
2 CY ATTN: R G OEDING

PHYSITRON INC
ATTN: M PRICE

S-CUBED
ATTN: C NEEDHAM

SCIENCE APPLICATIONS INTL CORP
ATTN: D BACON
ATTN: J COCKAYNE
ATTN: P VERSTEEGEN

SRI INTERNATIONAL
ATTN: E UTHE
ATTN: J PRAUSA
ATTN: M SANAI

TOYON RESEARCH CORP
ATTN: J CUNNINGHAM
ATTN: T W GEYER

W J SCHAFFER ASSOCIATES, INC
ATTN: D YOUMANS
ATTN: W BUITENHUYS

WILLIAMS INTERNATIONAL CORP
ATTN: D FISHER